

AD-A218 020

DTIC FILE COPY

2

NAVAL POSTGRADUATE SCHOOL

Monterey, California

DTIC
ELECTE
FEB 14 1990
S D D
CD



THESIS

FLOW VISUALIZATION STUDIES IN
(1) A CURVED RECTANGULAR CHANNEL
WITH 40 TO 1 ASPECT RATIO AND
(2) A STRAIGHT CHANNEL WITH BULK
FLOW UNSTEADINESS

by

Jerry Mark Longest

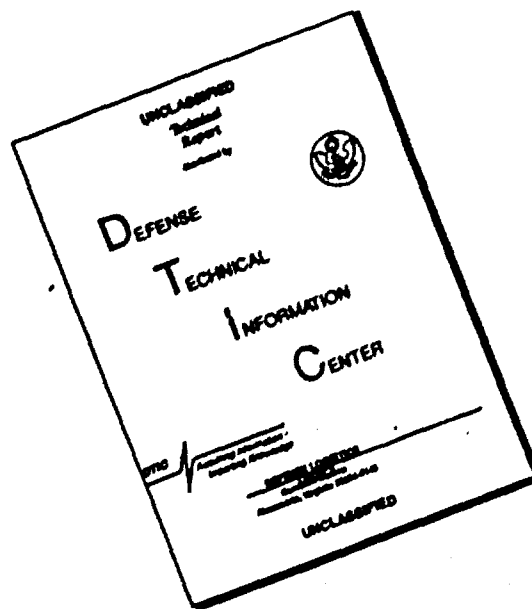
June 1989

Thesis Advisor: Phillip M. Ligrani
Co-Advisor: Chelakara S. Subramanian

Approved for public release; distribution is unlimited.

90 02 10 1

DISCLAIMER NOTICE



**THIS DOCUMENT IS BEST
QUALITY AVAILABLE. THE COPY
FURNISHED TO DTIC CONTAINED
A SIGNIFICANT NUMBER OF
PAGES WHICH DO NOT
REPRODUCE LEGIBLY.**

REPORT DOCUMENTATION PAGE

1a. REPORT SECURITY CLASSIFICATION UNCLASSIFIED			1b. RESTRICTIVE MARKINGS		
2a. SECURITY CLASSIFICATION AUTHORITY			3. DISTRIBUTION/AVAILABILITY OF REPORT Approved for public release; distribution is unlimited.		
2b. DECLASSIFICATION/DOWNGRADING SCHEDULE					
4. PERFORMING ORGANIZATION REPORT NUMBER(S)			5. MONITORING ORGANIZATION REPORT NUMBER(S)		
6a. NAME OF PERFORMING ORGANIZATION Naval Postgraduate School		6b. OFFICE SYMBOL (If applicable) Code 69	7a. NAME OF MONITORING ORGANIZATION Naval Postgraduate School		
6c. ADDRESS (City, State, and ZIP Code) Monterey, California 93943-5000			7b. ADDRESS (City, State, and ZIP Code) Monterey, California 93943-5000		
8a. NAME OF FUNDING/SPONSORING ORGANIZATION (1) U.S. Army Av. Res. & Tech. Act. (2) NPS Direct Funding AVSCOM		8b. OFFICE SYMBOL (If applicable)	9. PROCUREMENT INSTRUMENT IDENTIFICATION NUMBER (1) MIPR No. C-80019-F (2) NPS Direct Funding (ONR Review)		
8c. ADDRESS (City, State, and ZIP Code) (1) NASA-Lewis Res. Center, Cleveland, OH 44135 (2) NPS, Monterey, CA 93943-5000			10. SOURCE OF FUNDING NUMBERS		
PROGRAM ELEMENT NO.		PROJECT NO.	TASK NO.	WORK UNIT ACCESSION NO.	
11. TITLE (Include Security Classification) FLOW VISUALIZATION STUDIES IN (1) A CURVED RECTANGULAR CHANNEL WITH 40 TO 1 ASPECT RATIO AND (2) A STRAIGHT CHANNEL WITH IMPOSED BULK FLOW UNSTEADINESS					
12. PERSONAL AUTHOR(S) LONGEST, Jerry Mark					
13a. TYPE OF REPORT Master's Thesis		13b. TIME COVERED FROM _____ TO _____		14. DATE OF REPORT (Year, Month, Day) 1989, June	
15. PAGE COUNT 116					
16. SUPPLEMENTARY NOTATION The views expressed in this thesis are those of the author and do not reflect the official policy or position of the Department of Defense or the U. S. Government.					
17. COSATI CODES			18. SUBJECT TERMS (Continue on reverse if necessary and identify by block number)		
FIELD	GROUP	SUB-GROUP	Visualization, Dean Vortices, Centrifugal Instabilities, Laminar to Turbulent Transition, Laminar Flow, Turbulent Flow, Turbulent Spots, Lambda Waves and Vortices.		
19. ABSTRACT (Continue on reverse if necessary and identify by block number) Flow visualization results are presented which were obtained in a curved channel with mild curvature and 40 to 1 aspect ratio. Inside channel dimensions are 1.27 cm x 50.80 cm. For Dean numbers from 60 to 200 and angular positions from 85° to 175° measured from the start of curvature, video movies and photographic sequences of patterns in spanwise/radial planes show unsteady Dean vortex pair behavior. In particular, information is provided on mechanisms by which vortex pairs appear and disappear. Videos and still photographs of visualized flow in a straight channel with 40 to 1 aspect ratio and imposed bulk flow unsteadiness show different stages of transition, including: (1) three-dimensional Tollmien-Schlichting waves, (2) Lambda waves, (3) Lambda vortices, (4) vortex type motion, (5) turbulent spots and (6) fully turbulent flow. Instantaneous velocity traces from hot-wire probes are presented for Reynolds numbers from 1400 to 8400 and Strouhal numbers from 0.004 to 0.047. These data, without unsteadiness, show that transition occurs at a Reynolds number of approximately 3000. With imposed sinusoidal					
20. DISTRIBUTION/AVAILABILITY OF ABSTRACT <input checked="" type="checkbox"/> UNCLASSIFIED/UNLIMITED <input type="checkbox"/> SAME AS RPT <input type="checkbox"/> DTIC USERS			21. ABSTRACT SECURITY CLASSIFICATION UNCLASSIFIED		
22a. NAME OF RESPONSIBLE INDIVIDUAL Professor Ligrani			22b. TELEPHONE (Include Area Code) (408) 646-3382		22c. OFFICE SYMBOL 69Li

SECURITY CLASSIFICATION OF THIS PAGE

(19) Continued:

unsteadiness at a Strouhal number of 0.028 and 7% peak to peak amplitude (relative to mean velocity), transition occurs at a Reynolds number of approximately 2300. These.

(A-1)



Accession For	
NTIS CRA&I	<input checked="" type="checkbox"/>
DTIC TAB	<input type="checkbox"/>
Unannounced	<input type="checkbox"/>
Justification	
By	
Distribution /	
Availability Codes	
Dist	Avail and/or Special
A-1	

Approved for public release; distribution is unlimited.

**Flow Visualization Studies In (1) A Curved Rectangular
Channel with 40 to 1 Aspect Ratio and (2) A Straight
Channel with Imposed Bulk Flow Unsteadiness**

by

Jerry Mark Longest
Lieutenant, United States Navy
B. S., Purdue University, 1979


Submitted in partial fulfillment of the
requirements for the degree of

MASTER OF SCIENCE IN MECHANICAL ENGINEERING

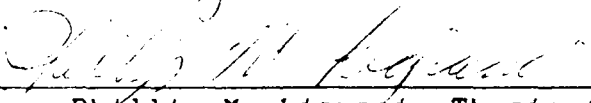
from the

NAVAL POSTGRADUATE SCHOOL
June 1989

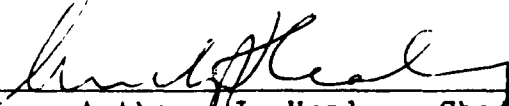
Author:



Jerry Mark Longest

Approved by:


Phillip M. Ligrani, Thesis Advisor


Chelakara S. Subramanian, Co-Advisor


Anthony J. Healey, Chairman,
Department of Mechanical Engineering


Gordon E. Schacher,
Dean of Science and Engineering

ABSTRACT

Flow visualization results are presented which were obtained in a curved channel with mild curvature and 40 to 1 aspect ratio. Inside channel dimensions are 1.27 cm x 50.80 cm. For Dean numbers from 60 to 200 and angular positions from 85° to 175° measured from the start of curvature, video movies and photographic sequences of patterns in spanwise/radial planes show unsteady Dean vortex pair behavior. In particular, information is provided on mechanisms by which vortex pairs appear and disappear.

Videos and still photographs of visualized flow in a straight channel with 40 to 1 aspect ratio and imposed bulk flow unsteadiness show different stages of transition, including: (1) three-dimensional Tollmien-Schlichting waves, (2) Lambda waves, (3) Lambda vortices, (4) vortex type motion, (5) turbulent spots and (6) fully turbulent flow. Instantaneous velocity traces from hot-wire probes are presented for Reynolds numbers from 1400 to 8400 and Strouhal numbers from 0.004 to 0.047. These data, without unsteadiness, show that transition occurs at a Reynolds number of approximately 3000. With imposed sinusoidal unsteadiness at a Strouhal number of 0.028 and 7% peak to peak amplitude (relative to the mean velocity), transition occurs at a Reynolds number of approximately 2300.

TABLE OF CONTENTS

I.	INTRODUCTION.....	1
A.	BACKGROUND.....	1
1.	Curved Channel Flow.....	1
2.	Straight Channel Flow.....	2
	with Imposed Unsteadiness	
B.	OBJECTIVES.....	3
C.	ORGANIZATION.....	3
II.	EXPERIMENTAL FACILITIES.....	4
A.	CURVED CHANNEL.....	4
B.	STRAIGHT CHANNEL.....	6
1.	Channel.....	6
2.	Unsteady Device.....	8
III.	EXPERIMENTAL PROCEDURES.....	10
A.	CURVED CHANNEL.....	10
1.	Channel Operation.....	10
2.	Smoke Generator.....	11
3.	Flow Visualization.....	12
a.	Video Procedures.....	12
(1)	Camera.....	12
(2)	Lighting.....	12
b.	Still Photography Procedures.....	13
(1)	Video Playback.....	13
(2)	Camera.....	14
(3)	Lighting.....	14

B.	STRAIGHT CHANNEL.....	15
1.	Mass Flow Rate and Mean Velocity.....	15
a.	Measurement.....	15
b.	Calibration.....	15
2.	Instantaneous Velocity Traces.....	16
a.	Hot-Wire Probe.....	16
b.	Hot-Wire Probe Operation and Calibration.....	16
c.	Instantaneous Velocity Measurement.....	17
3.	Smoke Wire System.....	17
4.	Flow Visualization.....	18
IV.	EXPERIMENTAL RESULTS.....	20
A.	FLOW VISUALIZATION IN A CURVED CHANNEL.....	20
B.	STRAIGHT CHANNEL.....	23
1.	Instantaneous Velocity Traces and Unsteady Flow Device Qualification.....	23
2.	Flow Visualization.....	27
V.	CONCLUSIONS.....	30
A.	CURVED CHANNEL.....	30
B.	STRAIGHT CHANNEL.....	30
	APPENDIX A. FIGURES.....	31
	APPENDIX B. SOFTWARE DIRECTORY.....	96
	LIST OF REFERENCES.....	99
	INITIAL DISTRIBUTION LIST.....	101

LIST OF FIGURES

Figure	Page
Figure 1. Schematic of Curved Channel Test Facility.....	31
Figure 2. Curved Channel Test Facility (side view).....	32
Figure 3. Schematic of Straight Channel Test Facility....	33
Figure 4. Straight Channel Test Facility (side view).....	34
Figure 5. Straight Channel Test Facility (front view)....	35
Figure 6. Straight Channel Test Facility..... (view of exit plenum)	36
Figure 7. Schematic of Unsteady Device.....	37
Figure 8. Unsteady Device.....	38
Figure 9. Unsteady Device and Motor.....	39
Figure 10. Unsteady Device Installed in Straight Channel..	40
Figure 11. Motor Drive System and Motor Controller.....	41
Figure 12. Schematic of the Smoke Generator.....	42
Figure 13. Radial-Spanwise Plane Flow Visualization.....	43
Figure 14. Schematic of Still Photography Set-up.....	44
Figure 15. Mass Flow Rate vs. Orifice ΔP (for $\Delta P < 2.25$ inches of water)	45
Figure 16. Velocity vs. Orifice ΔP (for $\Delta P < 2.25$ inches of water)	46
Figure 17. Reynolds Number vs. Orifice ΔP (for $\Delta P < 2.25$ inches of water)	47
Figure 18. Mass Flow Rate vs. Orifice ΔP (for $\Delta P > 2.25$ inches of water)	48
Figure 19. Velocity vs. Orifice ΔP (for $\Delta P > 2.25$ inches of water)	49

Figure 20.	Reynolds Number vs. Orifice delta P.....	50
	(for delta P > 2.25 inches of water)	
Figure 21.	Mass Flow Rate vs. Plenum delta P.....	51
Figure 22.	Velocity vs. Plenum delta P.....	52
Figure 23.	Reynolds Number vs. Plenum delta P.....	53
Figure 24.	Hot-Wire Probe.....	54
Figure 25.	Hot-Wire Probe and Unsteady Device.....	55
Figure 26.	Constant Temperature Bridge and Signal.....	56
	Conditioner with the Motor Drive and	
	Motor Controller	
Figure 27.	Data Acquisition System.....	57
Figure 28.	Smoke Wire Equipment.....	58
Figure 29.	Video Camera and Light Source Set-up for.....	59
	Straight Channel Flow Visualization	
	(a) Top View	
	(b) Side View	
Figure 30.	Flow Visualization at De=75.....	60
	and 85 Degrees from Start of Curvature	
Figure 31.	Flow Visualization at De=75.....	61
	and 95 Degrees from Start of Curvature	
Figure 32.	Flow Visualization at De=75 and 135 Degrees....	62
	from Start of Curvature (Sequence 1)	
Figure 33.	Flow Visualization at De=75 and 135 Degrees....	63
	from Start of Curvature (Sequence 2)	
Figure 34.	Flow Visualization at De=75 and 135 Degrees....	64
	from Start of Curvature (Sequence 3)	
Figure 35.	Flow Visualization at De=75 and 135 Degrees....	65
	from Start of Curvature (Sequence 4)	
Figure 36.	Flow Visualization at De=75 and 135 Degrees....	66
	from Start of Curvature (Sequence 5)	
Figure 37.	Flow Visualization at De=75 and 135 Degrees....	67
	from Start of Curvature (Sequence 6)	
Figure 38.	Flow Visualization at De=75 and 135 Degrees....	68
	from Start of Curvature (Sequence 7)	

Figure 39.	Flow Visualization at $De=75$ and 135 Degrees....	69
	from Start of Curvature (Sequence 8)	
Figure 40.	Flow Visualization at $De=75$ and 135 Degrees....	70
	from Start of Curvature (Sequence 9)	
Figure 41.	Flow Visualization at $De=75$ and 135 Degrees....	71
	from Start of Curvature (Sequence 10)	
Figure 42.	Flow Visualization at $De=100$	72
	and 95 Degrees from Start of Curvature	
Figure 43.	Flow Visualization at $De=100$	73
	and 105 Degrees from Start of Curvature	
Figure 44.	Flow Visualization at $De=100$	74
	and 145 Degrees from Start of Curvature	
Figure 45.	Flow Visualization at $De=100$	75
	and 155 Degrees from Start of Curvature	
Figure 46.	Instantaneous Velocity Traces ($Re=8444$).....	76
	(a) No Unsteadiness	
	(b) $Str=0.0040$	
	(c) $Str=0.0080$	
	(d) $Str=0.0119$	
Figure 47.	Instantaneous Velocity Traces ($Re=7578$).....	77
	(a) No Unsteadiness	
	(b) $Str=0.0044$	
	(c) $Str=0.0089$	
	(d) $Str=0.0133$	
Figure 48.	Instantaneous Velocity Traces ($Re=6729$).....	78
	(a) No Unsteadiness	
	(b) $Str=0.0050$	
	(c) $Str=0.0100$	
	(d) $Str=0.0150$	
Figure 49.	Instantaneous Velocity Traces ($Re=5943$).....	79
	(a) No Unsteadiness	
	(b) $Str=0.0057$	
	(c) $Str=0.0113$	
	(d) $Str=0.0170$	
Figure 50.	Instantaneous Velocity Traces ($Re=4954$).....	80
	(a) No Unsteadiness	
	(b) $Str=0.0068$	
	(c) $Str=0.0136$	
	(d) $Str=0.0203$	

Figure 51.	Instantaneous Velocity Traces (Re=4134).....	81
	(a) No Unsteadiness	
	(b) Str=0.0081	
	(c) Str=0.0163	
	(d) Str=0.0244	
Figure 52.	Instantaneous Velocity Traces (Re=3343).....	82
	(a) No Unsteadiness	
	(b) Str=0.0101	
	(c) Str=0.0201	
	(d) Str=0.0302	
Figure 53.	Instantaneous Velocity Traces (Re=2754).....	83
	(a) No Unsteadiness	
	(b) Str=0.0122	
	(c) Str=0.0244	
	(d) Str=0.0366	
Figure 54.	Instantaneous Velocity Traces (Re=2569).....	84
	(a) No Unsteadiness	
	(b) Str=0.0131	
	(c) Str=0.0262	
	(d) Str=0.0392	
Figure 55.	Instantaneous Velocity Traces.....	85
	(a) Re=3537 Str=0.0190	
	(b) Re=3453 Str=0.0195	
	(c) Re=3284 Str=0.0205	
	(d) Re=3158 Str=0.0213	
Figure 55.	Instantaneous Velocity Traces.....	86
	(e) Re=2990 Str=0.0225	
	(f) Re=2863 Str=0.0235	
	(g) Re=2611 Str=0.0257	
	(h) Re=2442 Str=0.0275	
Figure 55.	Instantaneous Velocity Traces.....	87
	(i) Re=2274 Str=0.0296	
	(j) Re=2063 Str=0.0326	
	(k) Re=1684 Str=0.0399	
	(l) Re=1432 Str=0.0469	
Figure 56.	Flow Visualization: Re = 2358, Str = 0.0285, ...	88
	y/d = +0.84	
Figure 57.	Flow Visualization: Re = 2527, Str = 0.0266, ...	89
	y/d = 0.00	
Figure 58.	Flow Visualization: Re = 2611, Str = 0.0257, ...	90
	y/d = +0.84	

- Figure 59. Flow Visualization: $Re = 2695$, $Str = 0.0249, \dots 91$
 $y/d = +0.84$
- Figure 60. Flow Visualization: $Re = 2190$, $Str = 0.0460, \dots 92$
 $y/d = 0.00$
- Figure 61. Flow Visualization: $Re = 2274$, $Str = 0.0443, \dots 93$
 $y/d = +0.84$
- Figure 62. Flow Visualization: $Re = 2358$, $Str = 0.0427, \dots 94$
 $y/d = +0.84$
- Figure 63. Flow Visualization: $Re = 2442$, $Str = 0.0413, \dots 95$
 $y/d = +0.84$

LIST OF SYMBOLS

$A_{c\omega}$	Cross Sectional Area of Channel
d_c	Curved Channel Height = $r_o - r_i$
d_s, d	Straight Channel Height
De	Dean Number = $(U d_c / \nu) * (\sqrt{d_c / r_i})$
ΔP	Orifice Pressure Drop
\dot{m}	Mass Flow Rate
n	Vane Rotation Frequency (revolutions per second)
Re	Reynolds Number = $U d_s / \nu$
r_i	Inside Radius of Curved Channel Curvature
r_o	Outside Radius of Curved Channel Curvature
Str	Strouhal Number = $\omega d_s / U = 2 \pi n d_s / U$
U	Velocity = $\dot{m} / \rho A_{c\omega}$
ν	Kinematic Viscosity
ρ	Density
ω	Angular Frequency

ACKNOWLEDGEMENT

The work done in the curved channel was sponsored by the Propulsion Directorate, U. S. Army Aviation Research and Technology Activity, AVSCOM, Grant No. C-80019-F. Mr. Kestutis C. Civinskas was the program monitor.

The work done in the straight channel was sponsored by the Naval Postgraduate School Direct Funding Program through the Office of Naval Research. Dr. Spiro G. Lekoudis was the program monitor.

I would like to express my sincere gratitude to all those who made this work possible. My two thesis advisors were always there for me. Professor Ligrani provided me guidance and encouragement. Professor Subramanian provided me technical assistance and helped keep things in perspective. The Mechanical Engineering shop personnel, specifically Tom McCord, Tom Christian, Charles Crow, Glenn Harrell and Jim Schofield were always there with excellent craftsmanship. The Education Media Department's Photographic Division personnel, specifically Andy Sarakon and Mitch Nichols, were outstanding in their support and quick turn-around times, without which completion of this thesis would have been impossible. Finally, to my wife Robin, who provided love, patience and encouragement to see me through this work, to you I am forever grateful.

I. INTRODUCTION

A. BACKGROUND

Flow visualization studies are conducted in two different facilities: (1) a curved rectangular channel with 40 to 1 aspect ratio and (2) a straight rectangular channel with 40 to 1 aspect ratio and imposed bulk flow unsteadiness.

1. Curved Channel Flow

The 40 to 1 aspect ratio curved channel is used to study and visualize Dean vortex flow. Other flow visualization studies in the same facility are described by Bella [Ref. 1], Niver [Ref. 2] and Baun [Ref. 3]. The flow visualization experiments undertaken here are intended to provide additional information on the time variation of the flow. Photograph sequences are obtained to show the detailed timewise development of vortex pairs.

To obtain these sequences, a video camera is used to photograph the flow in the curved channel and still photographs of the individual video frames are then taken. Using this technique, sequences of photographs are obtained spaced $1/30$ second apart. The flow is contaminated, such that it may be visualized, by burning hickory and mesquite wood chips in the same smoke generator used by Niver [Ref. 2]. The flow visualization experiments conducted are for a range of Dean numbers (De) from 60 to 200 and for a range of

angular positions from 85° to 175° measured from the start of curvature.

2. Straight Channel Flow with Imposed Unsteadiness

No experiments have been undertaken so far to study effects of periodic unsteadiness on laminar/turbulent transition in a 40 to 1 aspect ratio straight channel (Ligrani and Subramanian [Ref. 4]). Numerical simulation results are given by Singer, Ferziger and Reed [Ref. 5]. These results indicate that imposed sinusoidal flow oscillations provide a stabilizing effect at all but very low frequencies in plane channel flow at a mean Reynolds number (Re) of 5000. At moderately low frequencies, oscillations in the channel can initiate nonlinear effects which trigger transition in flow regimes where the steady flow remains laminar.

Prior to the flow visualization, the straight channel was assembled and made operational. The device used to impose periodic unsteadiness was also qualified from instantaneous velocity traces measured using a hot-wire probe. This probe was inserted into the sidewall of the channel upstream of the unsteady device. Mass flow rate is determined from the pressure difference across a 1.5 inch orifice plate inserted in the piping between the exit plenum and blower.

Flow visualization experiments are undertaken utilizing the same video techniques used for the curved

channel. Flow is visualized using the smoke wire technique described by Siedband [Ref. 6]. The flow visualization experiments conducted are for a range of Reynolds numbers from 1400 to 8400 and for a range of Strouhal numbers (Str) from 0.004 to 0.047.

B. OBJECTIVES

The objectives of this thesis are:

1. To provide photographic documentation of the timewise development of flow structure at 1/30 second intervals in a 40 to 1 aspect ratio curved channel over a range of Dean numbers and streamwise positions.
2. To provide photographic evidence of flow development in a 40 to 1 aspect ratio straight channel with imposed bulk flow unsteadiness over a range of channel Reynolds numbers and Strouhal numbers.

C. ORGANIZATION

Subsequent to this introduction, Chapter II discusses experimental facilities. Chapter III discusses experimental procedures for the curved channel and the straight channel. Here, channel operation, the smoke generator, and flow visualization techniques are described. Chapter IV details the flow visualization results obtained from the curved channel and straight channel. Chapter V gives a summary and conclusions.

II. EXPERIMENTAL FACILITIES

A. CURVED CHANNEL

The 40 to 1 aspect ratio curved channel is located in the laboratories of the Department of Mechanical Engineering of the Naval Postgraduate School. A schematic and a photograph are shown in Figs. 1 and 2, respectfully. As discussed by Ligrani and Niver [Ref. 7], the curved channel is designed and constructed especially for flow visualization. The inside dimensions and cross-sectional area of the channel are the same along its entire 6.77 m length. Side wall, longitudinal, and cross-beam supports are used to support the upper and lower walls so that the inside dimensions and their tolerances at any streamwise location are 1.27 ± 0.015 cm for the height and 50.80 ± 0.05 cm for the width. The facility was constructed by McNeal Enterprises, Inc. of Santa Clara, California.

The lip at the channel inlet is constructed of quarter circumference sections of 15.2 cm outside diameter pipe. Following this is the 25.4 cm X 50.8 cm rectangular inlet section for flow management, consisting of a honeycomb followed by three screens stretched across the cross section. Following the last screen is a 20 to 1 contraction ratio nozzle, whose contour is given by a fifth-order polynomial.

After the nozzle, flow enters the 40 to 1 aspect ratio channel. The first part is a 2.44 m long straight duct. After the straight channel, the flow enters the curved test section. The concave interior duct surface (as the flow sees it) has a radius of curvature of 60.96 cm and the convex surface has a radius of curvature of 59.69 cm. At the end of the curved portion of the channel, the air enters another 2.44 m long straight duct. At the exit are four screens and a honeycomb used to isolate the channel flow from any spatial nonuniformities in the outlet plenum. A 45.7 cm long diffuser, having a total angle of 3°, is also used to provide some pressure recovery just prior the exit plenum.

The blower/piping system attached to plenum 1 is connected to a blower (see Fig. 1), which is an ICG Industries 10P type. This blower produces 10.2 cm of water vacuum at 4.82 m³/min volumetric flow rate. Plenum 2 is used to mate the 14.0 cm diameter blower inlet to piping without significant pressure losses, and additionally helps isolate the channel from unsteadiness caused by the blower impeller. Dean numbers between 20 and 220 are obtained using this blower/piping arrangement.

Flow rate changes are made by throttling valve 1 just upstream of plenum 2 (see Fig. 1) while bypass valve 2 is kept fully open. Any flow rate or Dean number is set by referring to the pressure drop across an ASME standard 1.5 inch orifice plate.

Additional details and description of the transparent curved channel are given by Ligrani and Niver [Ref. 7] and Niver [Ref. 2].

B. STRAIGHT CHANNEL

1. Channel

The 40 to 1 aspect ratio straight channel is located in the laboratories of the Department of Mechanical Engineering of the Naval Postgraduate School. A schematic drawing is shown in Fig. 3, with photographs shown in Figs. 4-6. As discussed by Ligrani and Subramanian [Ref. 4], the channel is made of 0.635 cm thick plexiglass with a straight section 4.27 m (14 ft) in length, with inside dimensions of 1.27 cm in height and 50.80 cm in width. It is supported by ribs and cross beams along its length. Three longitudinal (in the direction of the airflow) ribs made of 1.27 cm x 1.27 cm polycarbonate are placed along the length of the channel on the sides. The side walls are removable in order to gain access to the inside of the channel. The facility was constructed by Jay-Edmund Enterprises of Sandpoint, Idaho.

The lip at the channel inlet is constructed of half circumference sections of 15.24 cm outside diameter pipe. The lip is attached to a 25.4 cm x 50.80 cm rectangular inlet section with flanges, which is 15.24 cm in length to house a honeycomb assembly. This is followed by three 1.27 cm x 50.80 cm frames with flanges, 10.16 cm in length each.

Screens are stretched across the cross section between these three frames. Following the last screen is a 20 to 1 contraction ratio nozzle, whose contour is given by a fifth order polynomial.

At the exit of the 4.27 m long test section are 10.16 cm long frames with flanges for screens, honeycomb and the unsteady device. Next, a two-dimensional diffuser 45.72 cm long with 3.0° total angle is located just upstream of the plenum chamber. The plenum chamber inside dimensions are 60.96 cm x 60.96 cm x 60.96 cm. It is made of 0.9525 cm thick acrylic except for the one removable wall which is 1.27 cm thick. In order to meter the flow, a 1.5 inch orifice plate assembly between the plenum chamber and the blower is installed. A 5 H.P. blower is employed to induct flow into the channel by depressurizing the plenum below atmospheric pressure.

The channel is designed such that transition occurs after the laminar flow is fully developed. Initial flow development length is minimized since the overall length of the test section is restricted by physical space limitations. For a channel Reynolds number of 2741, the flow becomes fully developed after 1.524 m of development length measured from the exit of the inlet nozzle (Reynolds number is based on channel width and mean velocity). For these conditions, 64.3% of the test section is then fully developed. This fully developed region is then used to study the variation of

the transition zone either as Reynolds number or flow disturbance level is varied.

2. Unsteady Device

The most important design aspect of any unsteady device is the production of controlled deterministic and periodic unsteadiness without additional flow disturbances. To achieve this in an open circuit induction channel, the unsteady device is best located just downstream of the test section. This way, wakes and other flow disturbances from the unsteady device are not convected into the test section.

The present design is shown in Fig. 7, and is based on a design described by Miller and Fejer [Ref. 8]. A photograph of the present device is shown in Fig. 8. Since the depth of the channel is only 1.27 cm, a single rotating vane is used to introduce the required unsteadiness into the flow. The vane is driven through a spur gear train by a DC stepper motor. The frequency of the imposed oscillations is controlled by varying the vane rotation rate; the amplitude of the imposed unsteadiness is altered by using different vane widths. The vane in Fig. 7 is made of a .3175 cm thick brass strip with rounded edges, and spans the entire width of the channel. The vane is supported at the ends by a .3175 cm diameter shaft and bushings that are fitted to the side walls of the frame. One end of the shaft is extended to accommodate a 48 TPI (Threads Per Inch) spur gear. This gear is driven by a driver spur gear with 12 TPI, which is mounted

on the Superior Electric, M092-FD310 Stepper Motor shaft. A photograph of the unsteady device alongside the motor is shown in Fig. 9. The unsteady device fully assembled and installed in the channel is shown in Fig. 10. Fig. 11 shows a photograph of the controller and drive system.

III. EXPERIMENTAL PROCEDURES

A. CURVED CHANNEL

The procedures used to set-up the curved channel and obtain flow visualization videos and photographs are now described.

1. Channel Operation

The first step is to choose a Dean number at which the flow visualization results are to be obtained. Once the Dean number is chosen, the pressure drop across the 1.5 inch orifice plate, used to meter the flow, is estimated using a plot of pressure drop vs. Dean number from Niver [Ref. 2: p. 32]. Valve 1 (Fig. 1) is then adjusted until this estimated pressure drop is read on the Merian SC-1213 manometer. The actual reading from the manometer is then entered into the computer program "DEAN15" contained in a Hewlett Packard HP 9000 Series computer. The true value of the Dean number is subsequently calculated by the program, taking into account ASME flow coefficients as well as the ambient temperature to calculate air density. If the Dean number is not close enough to the one desired, the procedure is repeated. With the appropriate flow rate in the curved channel, flow visualization experiments are begun.

2. Smoke Generator

The smoke generator used is described by Morrison [Ref. 9], Niver [Ref. 2] and Ligrani and Niver [Ref. 7]. A schematic is shown in Fig. 12. Smoke is produced by burning Hickory and Mesquite wood chips in a 7.6 cm diameter, 40.6 cm long vertical steel pipe. Combustion is initiated by energizing a nichrome wire heating coil at the bottom of the column of wood chips. The mixture of Hickory and Mesquite produces dense, white smoke, easily visible against the dark background paper used to line the outside of the channel convex surface. The smoke exits the steel pipe and passes into a large glass jar which is followed by a cooling system consisting of two coiled tubes surrounded by flowing water. The jar collects combustion particles and water vapor after they are separated from the smoke in the cooling system located above. The smoke then passed into a rubber hose and then to a smoke rake located at the inlet to the curved channel. This rake provides steady, laminar jets of smoke as it is directed into the channel inlet. A low pressure air stream is provided into the steel pipe for combustion and to force the smoke through the system.

With the generator, smoke is produced for as long as ten minutes. The best results are obtained when just enough smoke is produced to fill the lower half of the nozzle at the channel inlet. The smoke is dense, cool, and in sufficient

quantity to permit detailed observations of the flow structures under study.

3. Flow Visualization

a. Video Procedures

(1) Camera. The video camera used for flow visualization is the Sony DXC-M3 with Fujinon-TV-Z 1:1.7/10-140 mm DCL-914BY zoom lens connected to a Sony VO-6800 portable videocassette recorder and Sony CMA-8 camera adapter. This video camera is used because of its ability to image 30 frames per second. Camera position is shown in Fig. 13. For best results, the gain of the camera is set at 9 and filter number 1 is used. The lens is set to the macro setting for focusing. Sony KCS20BR videocassette tape is used for the flow visualization videos. The video camera is mounted on a Fairchild Camera & Instruments Corporation (Industrial Products Division) Model HS2511 tripod for stability and to maintain focus. As shown in Fig. 13, the video camera is oriented with its viewing direction at an angle of about 90° with respect to the direction of the light source. With this orientation, the camera views the flow as it moves away from the observer. Flow visualization patterns are recorded for one full minute for each experimental condition.

(2) Lighting. A General Radio Type 1531-A Strobatac strobe light is used to illuminate the flow as visual observations and photography are undertaken. If the

video camera and strobe rate are not at the same frequency, a moving line will appear on the video viewing screen. To make this line disappear, a strobe rate of approximately 3600 flashes per minute is used. The strobe is mounted near the center of curvature of the channel walls with a Rodenstock XR-Heligon collimator lens having a 75 mm focal length located just in front, as indicated by Fig. 13. The lens and strobe are adjusted so that light is in focus on a 2 mm x 46.0 mm slit located 5 cm off the channel centerline on a liner on the outside of the convex part of the curved channel surface. This dark colored liner minimizes reflections and stray light. The strobe and lens assembly is mounted so that it can be pivoted and clamped to illuminate any angular position on the curved test section. With this system, a well collimated light sheet is produced for visualization and photography in spanwise/radial planes at any one of a variety of angular positions spaced 5° apart from 0° to 185°. This strobe light orientation system is the same one used by Ligrand and Niver [Ref. 7].

b. Still Photography Procedures

(1) Video Playback. Once the flow visualization is video taped, it is played back on a Sony VO-5800 videocassette recorder connected to a Sony PVM-1910 Trinitron color video monitor. The Sony VO-5800 videocassette recorder has a scanning feature which allows viewing in a number of modes including fast/slow forward,

fast/slow reverse, or stop frame viewing. This last mode is used for the still photography. With this feature, it is possible to view individual video visualization photographs which are spaced 1/30 second apart.

(2) Camera. A Nikon F-3 SLR camera body with attached 55 mm, f2.8 lens is used for the still photography. The camera is mounted on a tripod for stability and to maintain proper focus, and positioned approximately 50.8 cm from the TV screen. The camera is focused on the stopped frame image appearing on the screen as shown in Fig. 14 which illustrates the still photography set-up.

(3) Lighting. For the still photographs the video playback equipment and still camera are set up in a room without any natural light source. All artificial light sources are turned off so that all lighting is provided from the TV screen with the brightness turned down all the way. To choose the correct camera settings for the still photography, a test roll of Kodak Tri-X pan. 400 ASA film was then taken for camera f-stop settings from 2.8 to 8 and camera speeds from 1/2 to 1/30 of a second. From these tests, the optimal camera f-stop and speed were found to be f5.6 and 1/8 second, respectively.

B. STRAIGHT CHANNEL

The procedures used to set-up and qualify the straight channel and obtain flow visualization videos and photographs are listed as follows: (1) calibrate the system for determining mass flow rate and velocity through the channel, (2) measure instantaneous velocity traces using a single hot-wire probe, (3) utilize a smoke wire and (4) perform flow visualization experiments.

1. Mass Flow Rate and Mean Velocity

a. Measurement

Mass flow rate through the channel is determined from measuring the pressure difference across a 1.5 inch orifice plate. The computer program "DEAN15" is used to calculate the mass flow rate from the measured pressure drop across the orifice plate. Flow rate is altered by adjusting the valve downstream of the orifice plate (see Fig. 3).

b. Calibration

Figs. 15-17 show plots of mass flow rate, velocity and Reynolds number versus orifice pressure drop, ΔP , for ΔP less than 2.25 inches of water. Figs. 18-20 show plots of the same quantities versus orifice ΔP for ΔP values greater than 2.25 inches of water. Figs. 21-22 show plots of mass flow rate, velocity and Reynolds number versus plenum ΔP for two runs with a 1.5 inch orifice plate and one run with a 1 inch orifice plate. The

data from these three sets of test agree, which validates the experimental procedures employed.

2. Instantaneous Velocity Traces

a. Hot-Wire Probe

A DANTEC Electronics Inc. 55 P51 probe is employed. Sensor diameter is 5.0 μm and sensor length is about 2.0 mm. For measurements, the probe is placed approximately 3.791 m from the beginning of the test section ($x/d = 298.5$, where x is measured from the nozzle exit). At this streamwise location, the probe is 8.255 cm from the left inside wall of the channel (looking downstream), as shown in Figs. 24 and 25.

b. Hot-Wire Probe Operation and Calibration

A DISA 55 M10 constant temperature bridge is used to operate the hot-wire. The connecting cable resistance is compensated using the zero ohms adjustment on the bridge when the probe is connected to a shorting plug. The probe cold resistance is then measured on the decade counter. For operation, the hot resistance is then set using an overheat ratio of 1.8.

A DANTEC Model 56 N20 signal conditioner is used to DC couple, amplify, and low-pass filter bridge voltage outputs. During measurements, the low-pass filter is set to 10 kHz, the high-pass filter is set to DC, and the gain is set to 1. A photograph of the bridge and signal conditioner

along with the vane motor drive and controller is shown in Fig. 26.

The hot-wire is calibrated in the channel. Voltages from the hot-wire bridge are measured using a 8050A digital multimeter connected to the signal conditioner. These voltages and corresponding velocities are recorded as the flow velocity is varied, and then entered into the computer program "HWCAL" to obtain calibration coefficients. These coefficients are subsequently entered into the computer program "O_SCOPE1" which determines instantaneous velocity variations and plots the results.

c. Instantaneous Velocity Measurement

The output from the signal conditioner is sent to a HP 6944 multiprogrammer/high speed data acquisition system. Data is collected by the high speed acquisition system using the HP 9000 Series computer and the computer program "HOTWIRE1". The same signal from the signal conditioner is also fed into a BK Precision Oscilloscope. The high speed acquisition system is shown in Fig. 27.

3. Smoke Wire System

A smoke wire is used to visualize flow patterns in the straight channel. The wire was located at y/d values of 0.00, +0.84 and -0.84, stretched across the channel in the transverse direction, where y is measured from the center of the channel height. The wire was located just upstream of the previous position of the hot wire probe 3.493 m from the

exit of the nozzle ($x/d = 275.5$). This was chosen to obtain flow visualization results for x/d from 295.0 to 309.3 and z/d from -17.24 to +1.65. Here, z is measured from the center plane of the channel span (right is positive looking downstream), to give the same approximate streamwise location as the hot-wire probe surveys.

For the flow visualization, the nichrome wire (smoke wire) is coated with paraffin based oil. The smoke-wire is connected to an A/C-D/C voltage adapter, which, when energized, sends current through the wire to produce a sheet of smoke which is convected downstream in the channel. Voltage is applied to the wire by means of a Calrad 45-740 (0-130 VAC) variac set at 55 VAC. Energizing the wire is accomplished by pulsing the "Momentary On" switch of the A/C-D/C voltage adapter. The smoke wire equipment used in this study is shown in the photograph of Fig. 28.

The wire penetrates the side wall of the channel through a 1.07 cm diameter hole, located 76.8 cm upstream from the end of the straight test section. Using this hole, the wire can be moved to y/d locations from +0.84 to -0.84, where y is measured from the center of the channel. Air leakage is prevented by using modeling clay or a small cork to fill in the holes around the wire.

4. Flow Visualization

The video camera used for flow visualization in the straight channel is the same one used for flow visualization

in the curved channel. The camera is positioned about 80 cm above the straight channel on a tripod. The lens macro setting was not used. The lens was focused on the straight channel in the area where the hot-wire probe had been previously placed (the hot-wire probe is not introduced into the channel during flow visualization). The same video system gain and filter settings as the curved channel videos are used for the straight channel work. Maxell KCS20BQ videocassette tape is used for the flow visualization videos.

Lighting is provided by two Berkey ColorTran Multibeam "650" Model LQF-6 650W lights placed approximately 1.015 m on either side of the channel and at the same height as the channel. The bottom of the channel is lined with black paper to provide a contrasting background for the white smoke generated from the smoke wire. To obtain the best possible videos, stray light is blocked off as much as possible from the camera's field of view. Figs. 29(a) and 29(b) show schematics of the location of the camera and lighting for the straight channel.

The photographic procedures used to obtain the still photographs are the same as used for the curved channel work. The Nikon F-2 SLR camera was positioned approximately 85.1 cm from the TV screen. Kodak Tri-X pan, 400 ASA film was used with optimal camera f-stop and speed settings of f4 and 1/4 second, respectively.

IV. EXPERIMENTAL RESULTS

A. FLOW VISUALIZATION IN A CURVED CHANNEL

Flow visualization results for the 40 to 1 aspect ratio curved channel are now presented. In each sequence of photographs in Figs. 30 through 45, time increases from top to bottom. Each separate photograph in the sequence shows the convex surface of the channel at the top and the concave surface at the bottom. The spanwise extent of each photograph is approximately 46 mm and the vertical extent of each photograph is 12.7 mm. The sequences show the flow as it is moving away from the observer.

Photographic results for a Dean number of 75 at angular positions of 95° and 95° from the start of curvature are shown in Figs. 20 and 21, respectively. The time interval between photographs in each of these sequences is 1/10 second. These results are discussed further by Hughes [Ref. 10].

Flow characteristics at a Dean number of 75 and 135° from the start of curvature are studied because a variety of Dean vortex pair phenomena are observed. These include fairly steady Dean vortex pairs (over small time intervals), as well as pairs with considerable spatial unsteadiness resulting from vortex pair appearance and vortex pair disappearance.

One mode of vortex pair disappearance is due to vortex cancellation. This occurs when a positive vortex and a negative vortex merge together, and then disappear. Except for vortex cancellation, a positive vortex does not generally merge with a negative vortex. Instead vortices of like sign generally merge together. In the flow visualization sequences, this is seen when a large vortex pair engulfs a smaller vortex pair such that one "petal" of the larger vortex pair surrounds the smaller pair. The smaller pair is then engulfed such that vortices of like sign merge together. Another alternative has also been observed wherein smaller vortex pairs are engulfed into the stem of a larger vortex pair.

Figures 22 through 41 show photo sequences for a Dean number of 75 and an angular position 135° from the start of curvature. These figures are now discussed in detail. The time interval between photographs in each sequence is $1/20$ period.

Fig. 22 shows steady Dean vortex pairs with very little variation over the total time period. Fig. 23 shows the growth of a vortex pair forming from the concave wall which then merges with a vortex pair to its left. Fig. 34 shows a vortex pair which is becoming smaller and is then engulfed into the stem of a larger vortex pair. Fig. 35 shows the growth of a vortex pair which then engulfs an adjacent vortex pair. Fig. 36 also shows a smaller vortex pair engulfed by a

portion of a larger pair. Also evident is the development of a new pair on the right-hand sides of the photographs. Fig. 37 shows a smaller vortex pair being engulfed by the "petal" of a larger vortex pair.

Fig. 38 initially shows a small vortex pair in the center which gets smaller and then starts to tilt to the left until the stem is almost horizontal. A "petal" of the larger vortex pair to the left then surrounds and engulfs the smaller vortex pair.

Fig. 39 shows complicated phenomena wherein a vortex pair or some similar symmetric structure initially appears to split. The resulting pair on the left is then surrounded and engulfed by the "petal" of a larger vortex pair. The resulting pair on the right appears to grow into a stronger vortex pair which then engulfs a weaker vortex pair to its right.

Fig. 40 shows a smaller vortex pair being engulfed into the stem of a larger vortex pair. Fig. 41 shows a vortex pair merging into the wall.

Photographic results for Dean number 100 at angular positions of 95° , 105° , 145° and 155° are shown in Figs. 42 through 45, respectfully. The time interval in Figs. 42 and 43 is 1/10 second. For Figs. 44 and 45, the time interval is 1/20 second. These results are discussed further by Hughes [Ref. 10].

B. STRAIGHT CHANNEL

Experimental results for the straight channel are presented in two parts: (1) Instantaneous Velocity Traces and Unsteady Flow Device Qualification and (2) Flow Visualization.

1. Instantaneous Velocity Traces and Unsteady Flow Device Qualification

Instantaneous velocity data are presented for velocities from 3 m/s to 10 m/s and vane speeds from 0 to 1.5 revolutions per second (rps). Data are also provided for a vane speed of 1.0 rps for velocities from 1.7 m/s to 4.2 m/s. Tables I and II list channel mean velocity (U), vane rotation frequency, Reynolds number (Re) and Strouhal number (Str) for each run.

In Table I, the first two numbers of the "Run Number" give the approximate flow velocity (in m/s) and the last two numbers give the vane rotation frequency (in rps, multiplied by 10). The "T" value in the flow velocity position of the run number is for the approximate transition point from laminar flow to turbulent flow with no imposed unsteadiness.

In Table II, the "V1" of the Run Number column indicates a vane speed of 1.0 rps. The last two numbers are used to designate separate data runs, but also give the approximate ΔP (divided by 2) across the 1.5 inch orifice plate.

TABLE I. EXPERIMENTAL CONDITIONS FOR INSTANTANEOUS VELOCITY TRACES

Run #	Velocity (m/s)	Vane Rotation Freq (rps)	Reynolds No. (Re)	Strouhal No. (Str)	Comments
RUN10_00	10.026	0.0	8444	No Unsteadiness	Turbulent
RUN10_05	10.026	0.5	8444	0.0040	Turbulent
RUN10_10	10.026	1.0	8444	0.0080	Turbulent
RUN10_15	10.026	1.5	8444	0.0119	Turbulent
RUN09_00	8.9776	0.0	7578	No Unsteadiness	Turbulent
RUN09_05	8.9776	0.5	7578	0.0044	Turbulent
RUN09_10	8.9776	1.0	7578	0.0089	Turbulent
RUN09_15	8.9776	1.5	7578	0.0133	Turbulent
RUN08_00	7.9898	0.0	6729	No Unsteadiness	Turbulent
RUN08_05	7.9898	0.5	6729	0.0050	Turbulent
RUN08_10	7.9898	1.0	6729	0.0100	Turbulent
RUN08_15	7.9898	1.5	6729	0.0150	Turbulent
RUN07_00	7.0562	0.0	5943	No Unsteadiness	Turbulent
RUN07_05	7.0562	0.5	5943	0.0057	Turbulent
RUN07_10	7.0562	1.0	5943	0.0113	Turbulent
RUN07_15	7.0562	1.5	5943	0.0170	Turbulent
RUN06_00	5.8827	0.0	4954	No Unsteadiness	Turbulent
RUN06_05	5.8827	0.5	4954	0.0068	Turbulent
RUN06_10	5.8827	1.0	4954	0.0136	Turbulent
RUN06_15	5.8827	1.5	4954	0.0203	Turbulent
RUN05_00	4.9093	0.0	4134	No Unsteadiness	Turbulent
RUN05_05	4.9093	0.5	4134	0.0081	Turbulent
RUN05_10	4.9093	1.0	4134	0.0163	Turbulent
RUN05_15	4.9093	1.5	4134	0.0244	Turbulent
RUN04_00	3.9694	0.0	3343	No Unsteadiness	Turbulent
RUN04_05	3.9694	0.5	3343	0.0101	Turbulent
RUN04_10	3.9694	1.0	3343	0.0201	Turbulent
RUN04_15	3.9694	1.5	3343	0.0302	Turbulent
RUN03_00	3.27	0.0	2754	No Unsteadiness	Laminar
RUN03_05	3.27	0.5	2754	0.0122	Intermittent
RUN03_10	3.27	1.0	2754	0.0244	Turbulent
RUN03_15	3.27	1.5	2754	0.0366	Turbulent
RUN02_00	3.05	0.0	2569	No Unsteadiness	Laminar
RUN02_05	3.05	0.5	2569	0.0131	Laminar
RUN02_10	3.05	1.0	2569	0.0262	Intermittent
RUN02_15	3.05	1.5	2569	0.0393	Turbulent

TABLE II. EXPERIMENTAL CONDITIONS FOR
INSTANTANEOUS VELOCITY TRACES

Run #	Velocity (m/s)	Vane Rotation Freq (rps)	Reynolds No. (Re)	Strouhal No. (Str)	Comments
RUNV1_13	4.2	1.0	3537	0.0190	Turbulent
RUNV1_12	4.1	1.0	3453	0.0195	Turbulent
RUNV1_11	3.9	1.0	3284	0.0205	Turbulent
RUNV1_10	3.75	1.0	3158	0.0213	Turbulent
RUNV1_09	3.55	1.0	2990	0.0225	Turbulent
RUNV1_08	3.4	1.0	2863	0.0235	Turbulent
RUNV1_07	3.1	1.0	2611	0.0257	Turbulent
RUNV1_06	2.9	1.0	2442	0.0275	Turbulent
RUNV1_05	2.7	1.0	2274	0.0296	Intermittent
RUNV1_04	2.45	1.0	2063	0.0326	Laminar
RUNV1_03	2.0	1.0	1684	0.0399	Laminar
RUNV1_02	1.7	1.0	1432	0.0469	Laminar

$$ReynoldsNumber = \frac{Ud_s}{\nu}$$

$$StrouhalNumber = \frac{\omega d_s}{U} = \frac{2\pi n d_s}{U}$$

Figs. 46 through 55 show graphs of instantaneous velocity. The same coding system used in Tables I and II for the "Run Number" is also used here. The time for each graph begins 10 seconds after the start of data collection and continues for 2.5 seconds.

Figs. 46 through 52 all show turbulent behavior for vane speeds of 0.0, 0.5, 1.0 and 1.5 rps. In Fig. 53(a), at a vane speed of 0.0 rps, the flow is laminar with some intermittency. Fig. 53(b) (0.5 rps) shows significant intermittent unsteadiness and turbulence which is occurring during the decelerating portion of each phase of the imposed oscillation. Figs. 53(c) and 53(d) (vane speeds of 1.0 and 1.5 rps, respectively) again show turbulent behavior.

Fig. 54(a) (0.0 rps) shows laminar behavior. In Fig. 54(b) (0.5 rps), a slight sinusoidal oscillation is evident with some small turbulence fluctuations. In Fig. 54(c) (1.0 rps), the flow shows significant intermittent unsteadiness and turbulence which seems to be occurring during a particular portion of the phase of the imposed oscillation. Fig. 54(d) (1.5 rps) shows turbulent behavior.

Fig. 55 shows data for a vane speed of 1.0 rps and different flow velocities. Turbulent behavior is shown in Figs. 55(a) through 55(h). Fig. 55(i) shows intermittent unsteadiness and turbulence which occurs during the decelerating portion of each imposed oscillation. Figs. 55(j) through 55(l) show sinusoidal flow oscillations with a

very small amount of turbulence. The amplitudes of these turbulent fluctuations increase with vane speed.

2. Flow Visualization

Flow visualization results for the 40 to 1 aspect ratio straight channel are now discussed. In each photograph sequence shown in Figs. 56 through 63, time increases from top to bottom. In cases where there are two sets of sequences to a page, the time begins at the top left photograph and ends at the lower right photograph. The spanwise extent of each photograph is approximately 240 mm and the longitudinal extent of each photograph is approximately 181.5 mm. The dark line at the bottom left of each photograph indicates the location of the hot-wire probe used for instantaneous velocity trace measurements. The probe was not in the flow as visualization sequences were filmed. Flow is moving from the bottom of each photograph to the top. The time interval between photographs in each sequence is 1/20 second.

Flow visualization results show a variety of transition phenomena including: (1) three-dimensional Tollmien-Schlichting waves, (2) Lambda waves, (3) Lambda vortices, (4) vortex type motion, (5) turbulent spots and (6) fully turbulent flow.

Table III lists channel mean velocity, vane rotation frequency, Reynolds number, Strouhal number and y/d for each sequence of photographs in Figs. 56 through 63.

TABLE III. FLOW VISUALIZATION
EXPERIMENTAL CONDITIONS

Figure #	Velocity (m/s)	Vane Rotation Freq (rps)	Reynolds No. (Re)	Strouhal No. (Str)	y/d
56	2.8	1.0	3537	0.0190	+0.84
57	3.0	1.0	3453	0.0195	0.00
58	3.1	1.0	3284	0.0205	+0.84
59	3.2	1.0	3158	0.0213	+0.84
60	2.6	1.5	2990	0.0225	0.00
61	2.7	1.5	2863	0.0235	+0.84
62	2.8	1.5	2611	0.0257	+0.84
63	2.9	1.5	2442	0.0275	+0.84

Figs. 56 through 59 are photographic sequences for a vane rotation frequency of 1.0 rps. Fig. 56 is for a flow velocity of 2.8 m/s at a y/d of +0.84. Wavy three-dimensional Tollmien-Schlichting waves are evident. Fig. 57 is for a flow velocity of 3.0 m/s at the center of the channel. Here two Lambda vortices are seen to convect downstream. A turbulent/laminar wave front is shown in Fig. 58 for a flow velocity of 3.1 m/s and a y/d of +0.84. Fig. 59, for a flow velocity of 3.2 m/s at a y/d of +0.84 shows turbulent flow with a wavy structure convecting downstream.

Figs. 60 through 63 are photographic sequences for a vane rotation frequency of 1.5 rps. Fig. 60, for a flow velocity of 2.6 m/s at the center height of the channel, shows Lambda waves and Lambda vortices convecting downstream. Fig. 61 is for a flow velocity of 2.7 m/s and a y/d of +0.84.

Here, wavy laminar motion is observed. Three-dimensional Tollmien-Schlichting waves are evident in Fig. 62 for a flow velocity of 2.8 m/s at a y/d of +0.84. Fig. 63, for a flow velocity of 2.9 m/s and a y/d of +0.84, shows turbulent flow including a number of turbulent spots.

V. CONCLUSIONS

A. CURVED CHANNEL

In the curved channel, video movies and photographic sequences of smoke patterns in spanwise/radial planes show unsteady Dean vortex pair behavior. In particular, information is provided on mechanisms by which vortex pairs appear and disappear.

B. STRAIGHT CHANNEL

For the range of imposed unsteadiness that was studied in the straight channel, instantaneous velocity traces show that transition occurs at a Reynolds number of approximately 3000 without unsteadiness. With imposed sinusoidal unsteadiness at a Strouhal number of 0.028 and 7% peak to peak amplitude (relative to the mean velocity), transition occurs at a Reynolds number of approximately 2300.

Flow visualization results in the straight channel show different stages of transition, including: (1) three-dimensional Tollmien-Schlichting waves, (2) Lambda waves, (3) Lambda vortices, (4) vortex type motion, (5) turbulent spots and (6) fully turbulent flow.

APPENDIX A

FIGURES

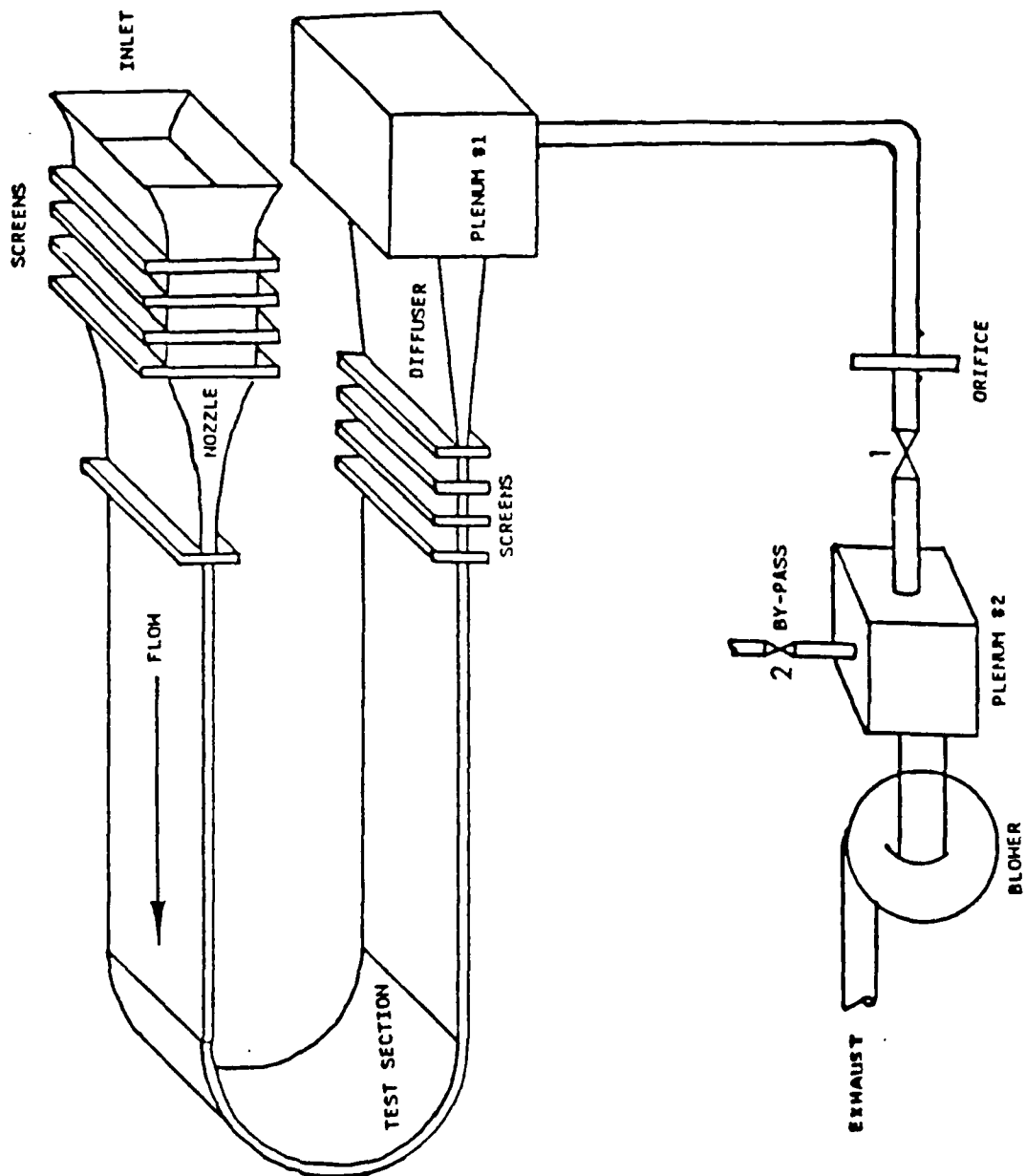


Figure 1. Schematic of Curved Channel Test Facility

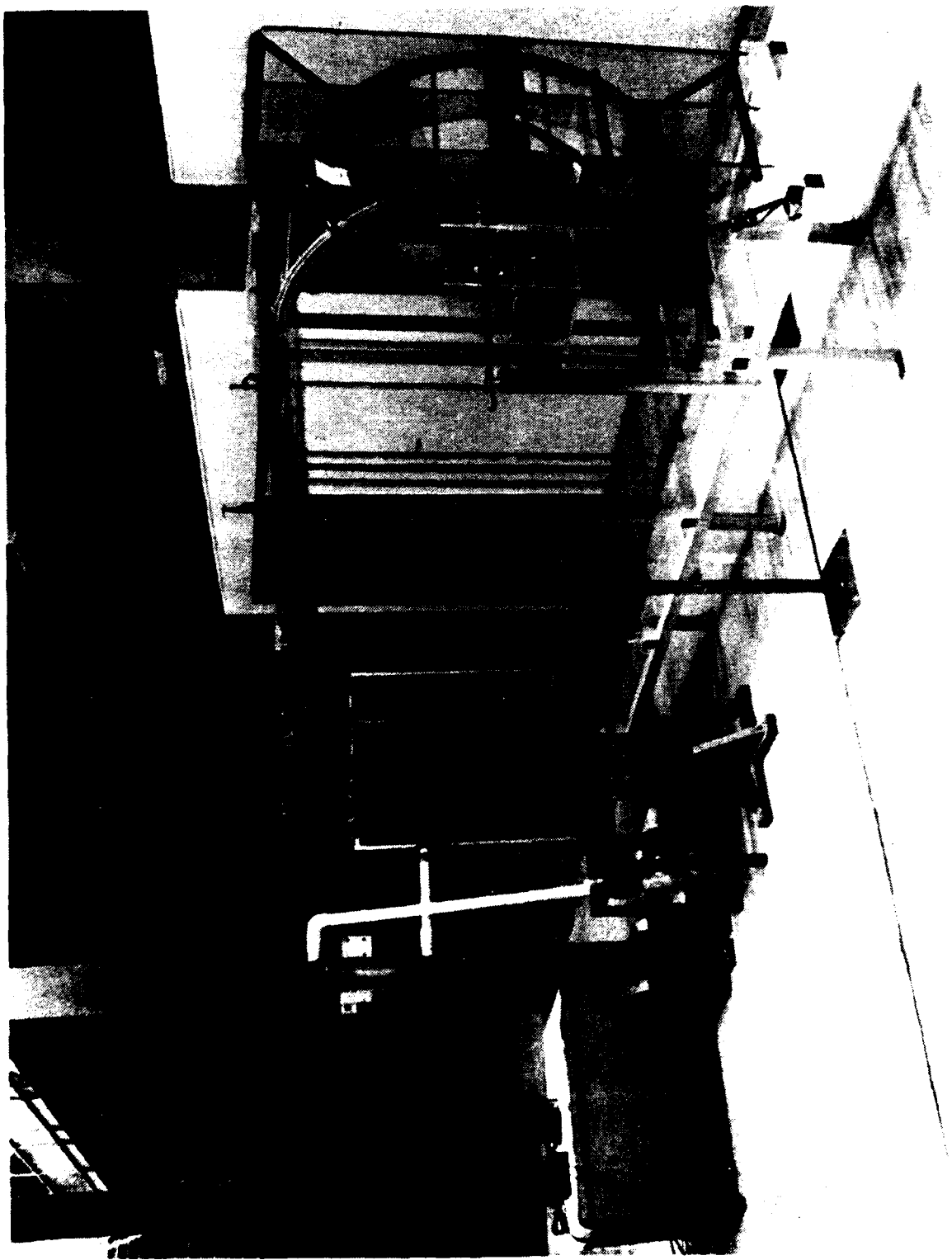


Figure 2. Curved Channel Test Facility (side view)

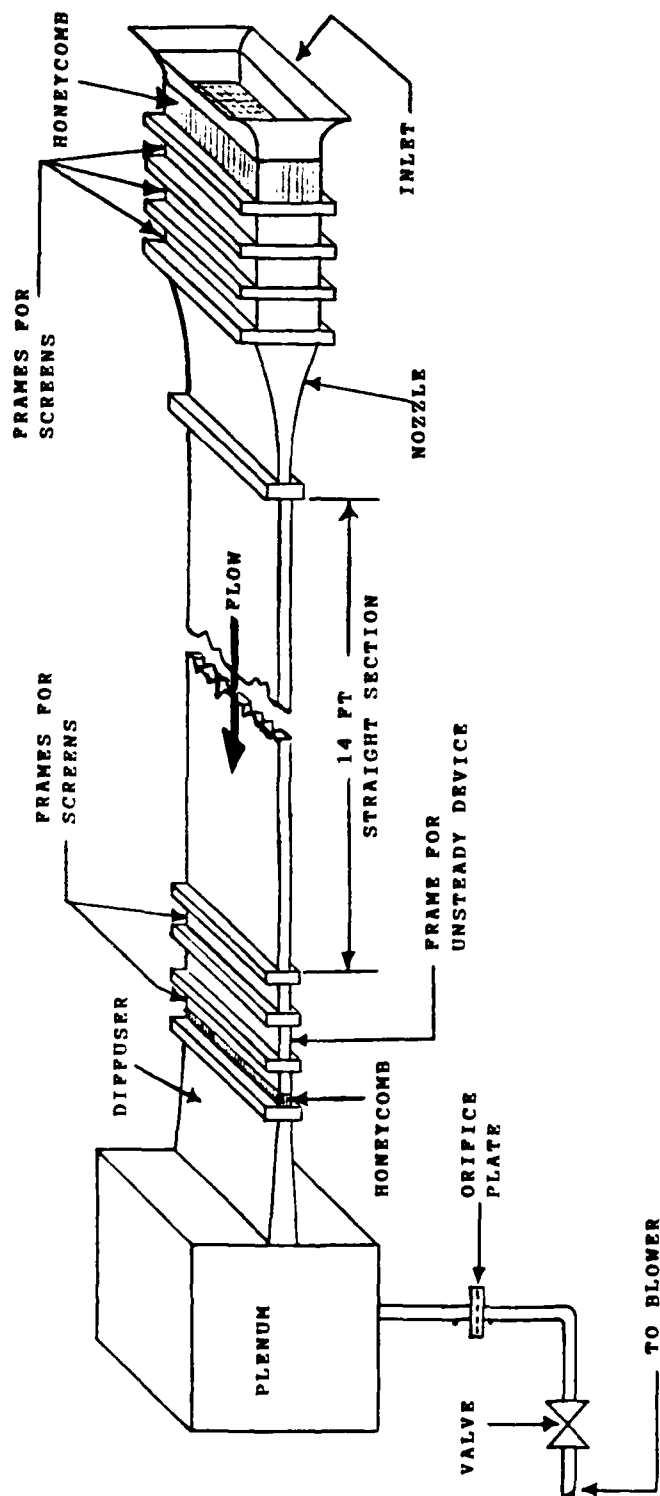


Figure 3. Schematic of Straight Channel Test Facility



Figure 4. Straight Channel Test Facility (side view)



Figure 5. Six-light Channel Test Facility, 16-17-1961

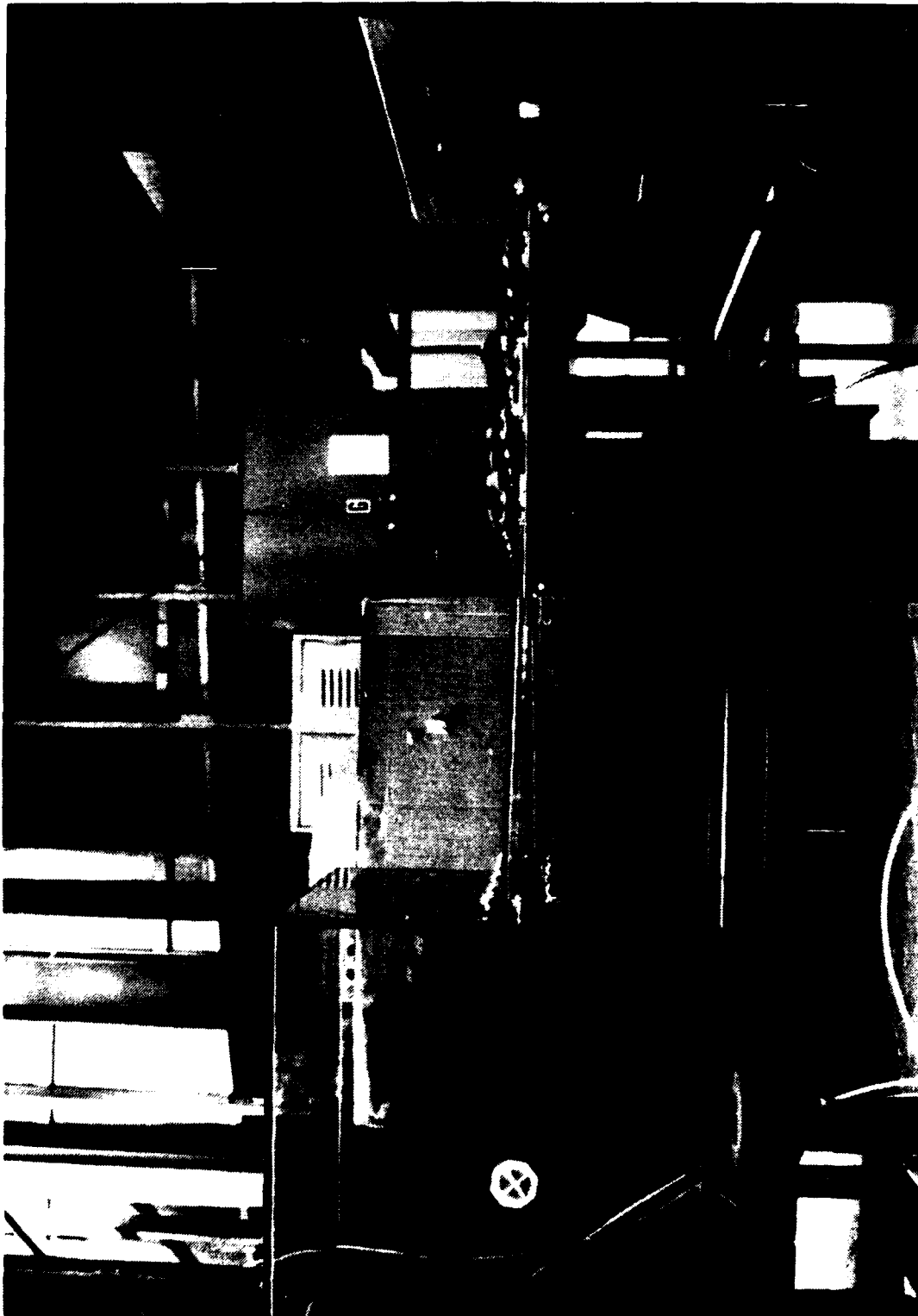


Figure C. Straight Channel Test Facility,
(view of exit plenum)

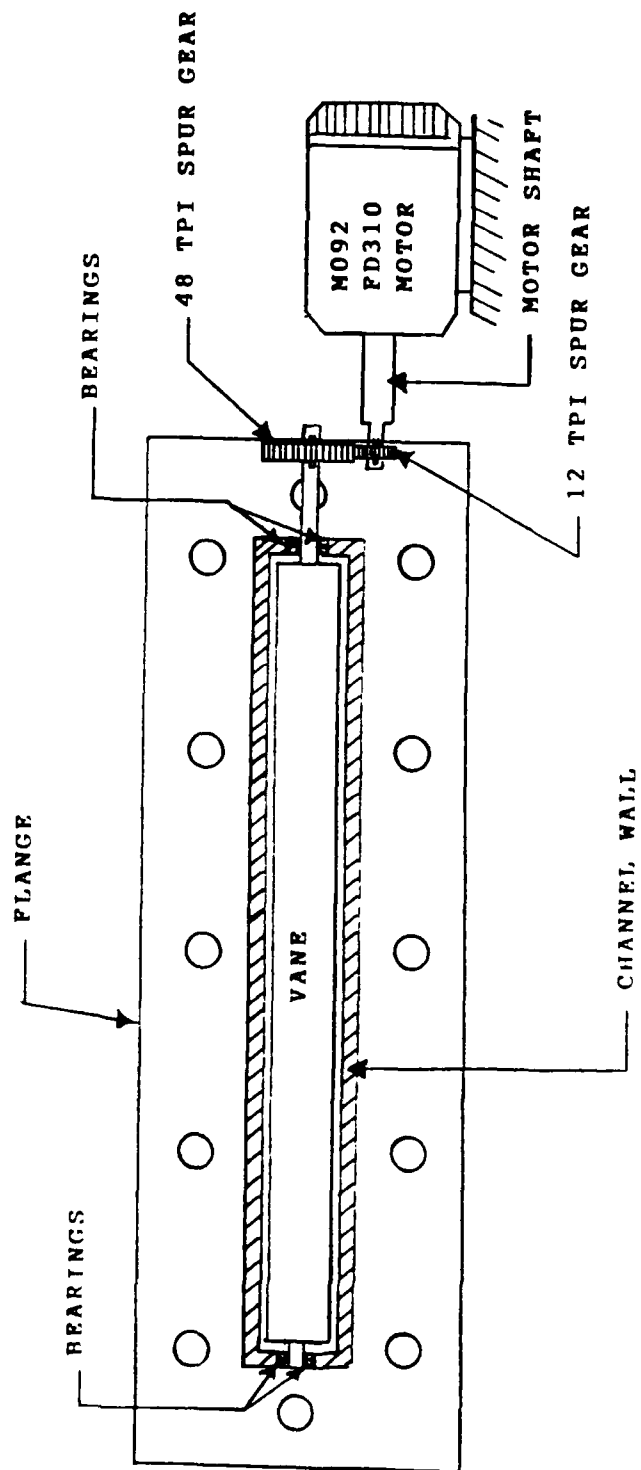


Figure 7. Schematic of Unsteady Device



Figure 2. Unsteady, Device

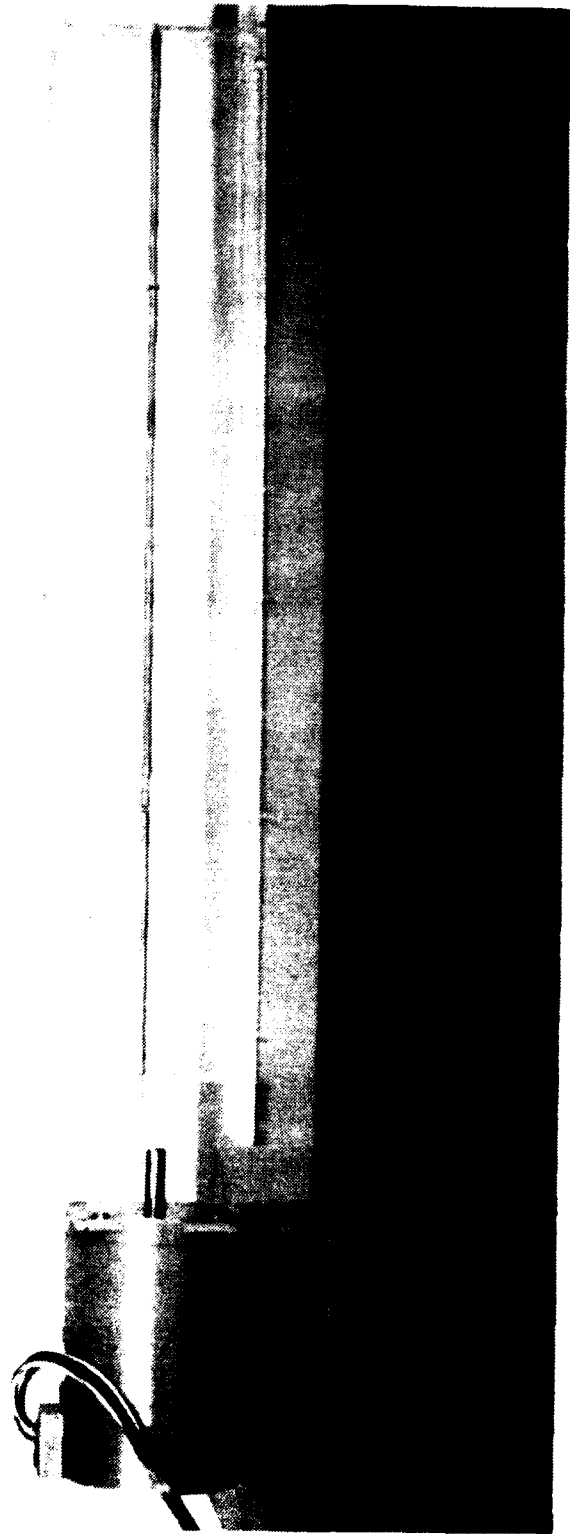


Figure 2. Unsteady Device and Motor

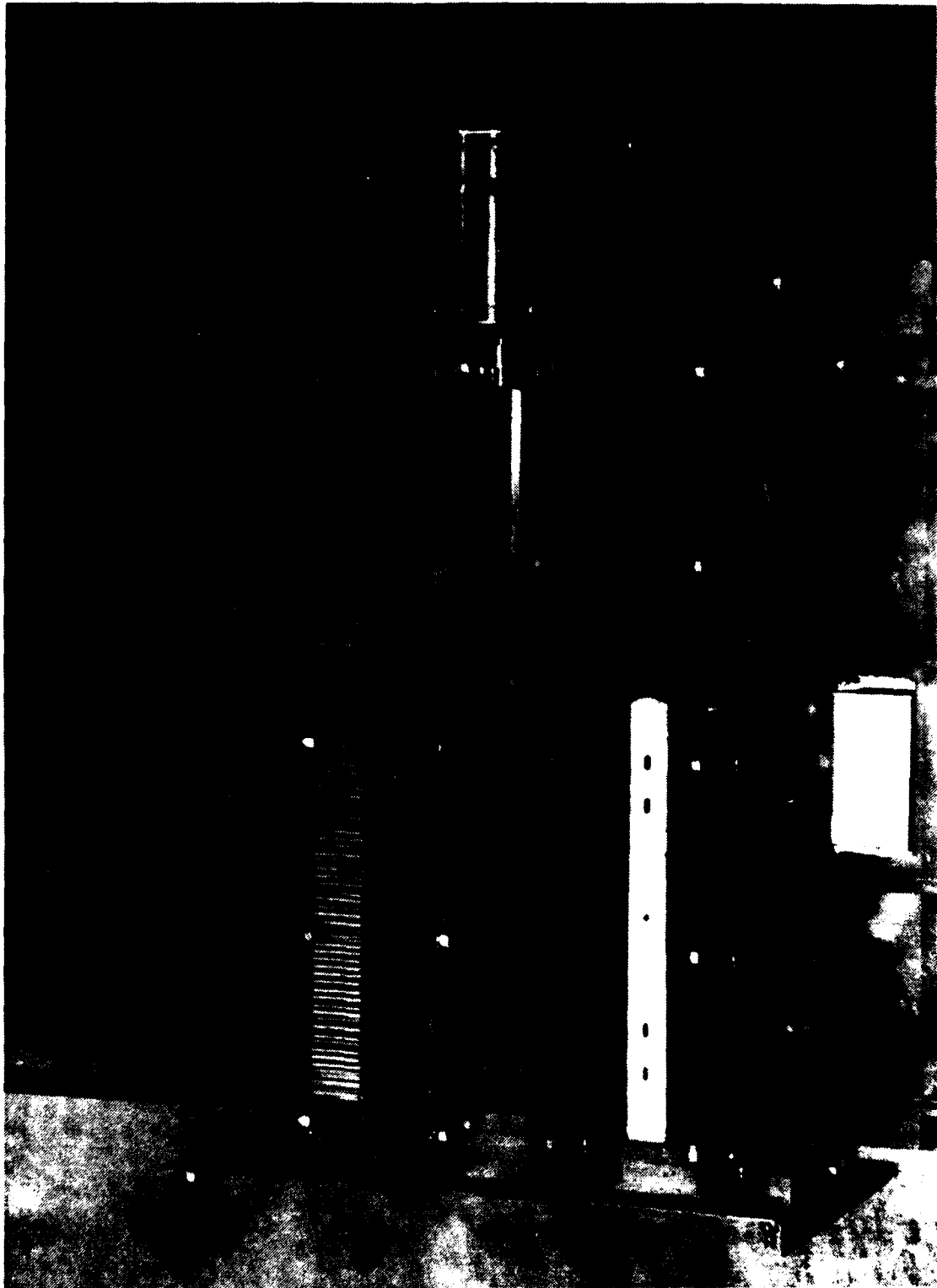


Figure 10. Unsteady Device Installed in Straight Channel

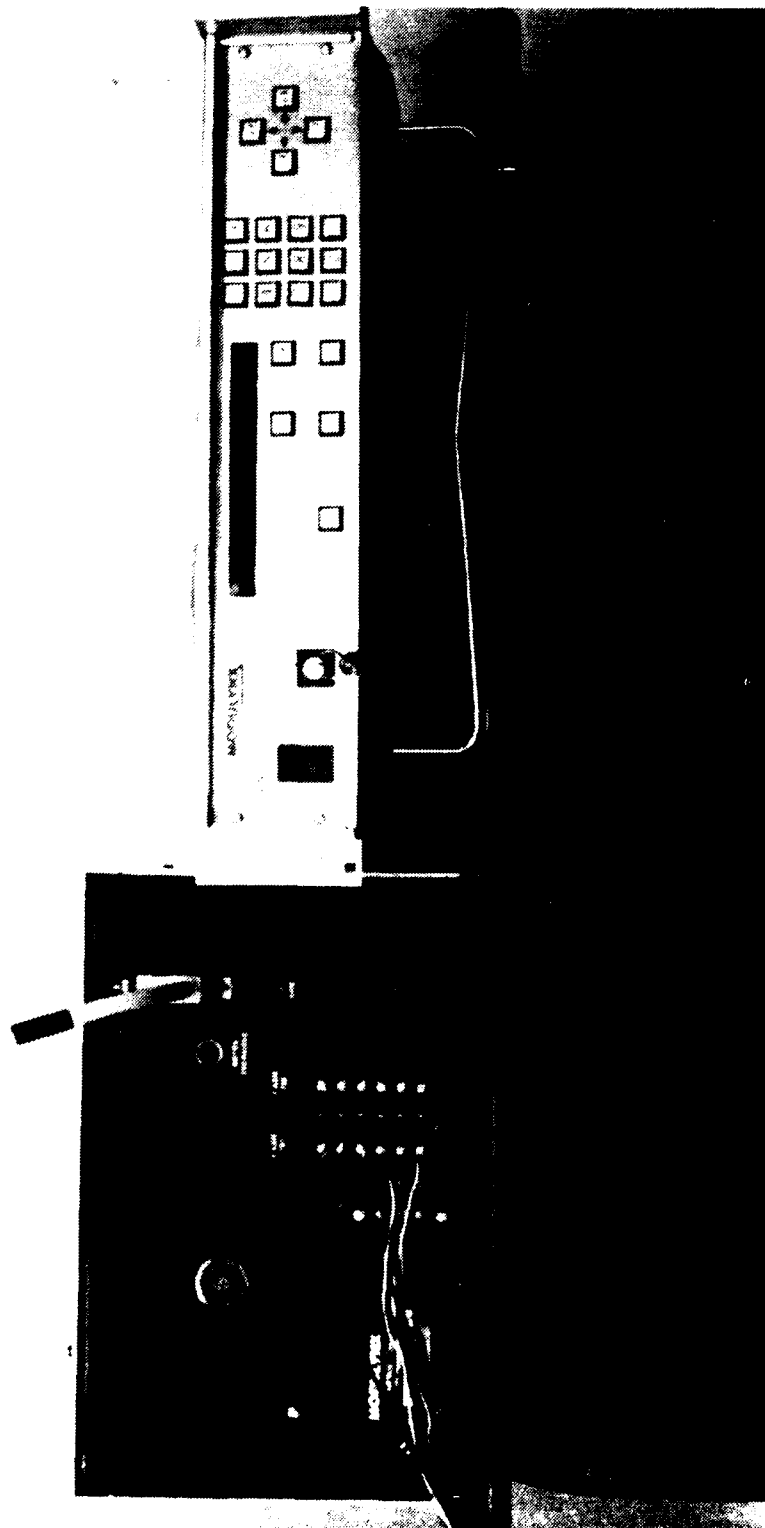


Figure 11. Motor Drive System
and Motor Controller.

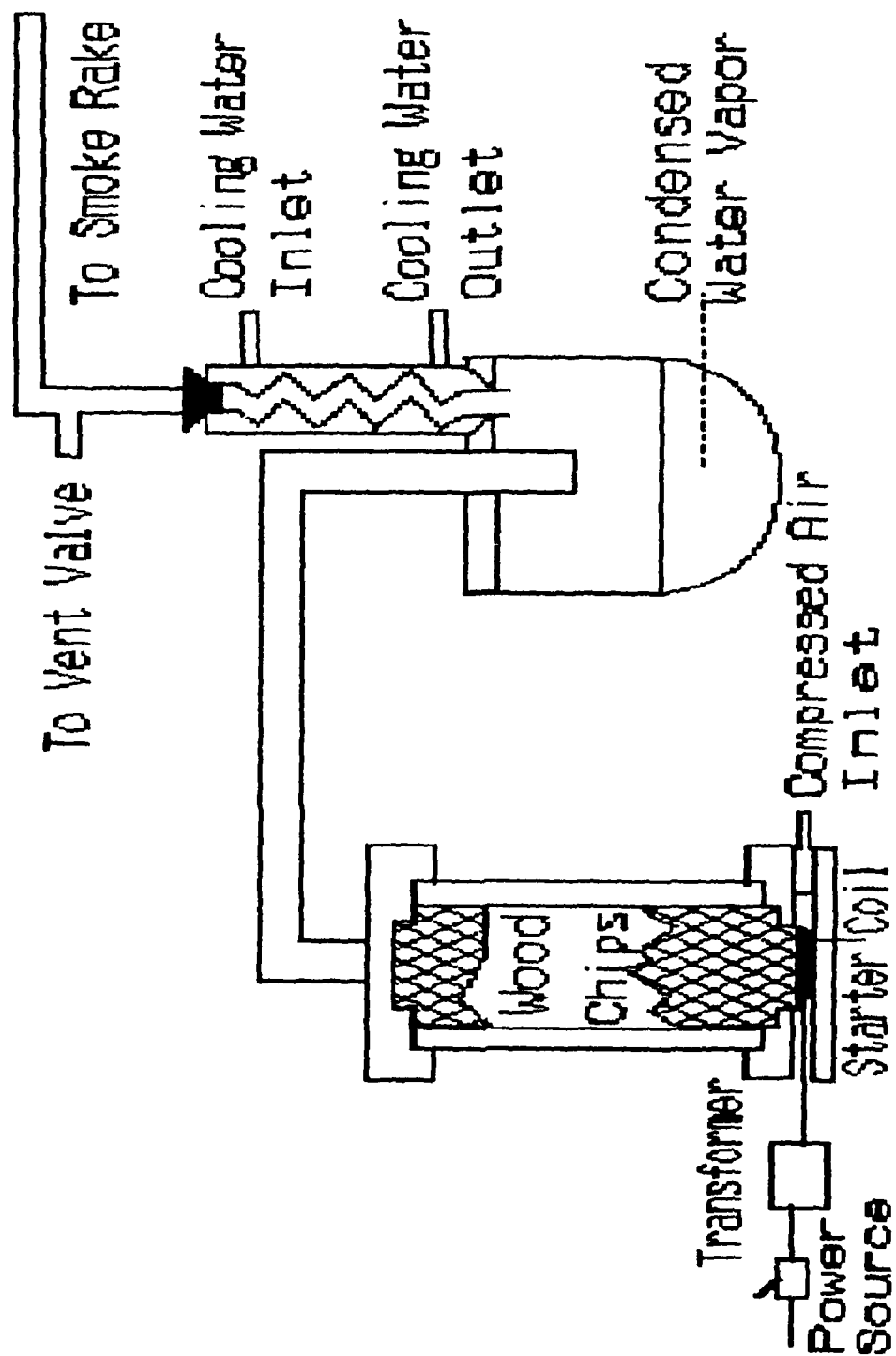


Figure 12. Schematic of the Smoke Generator

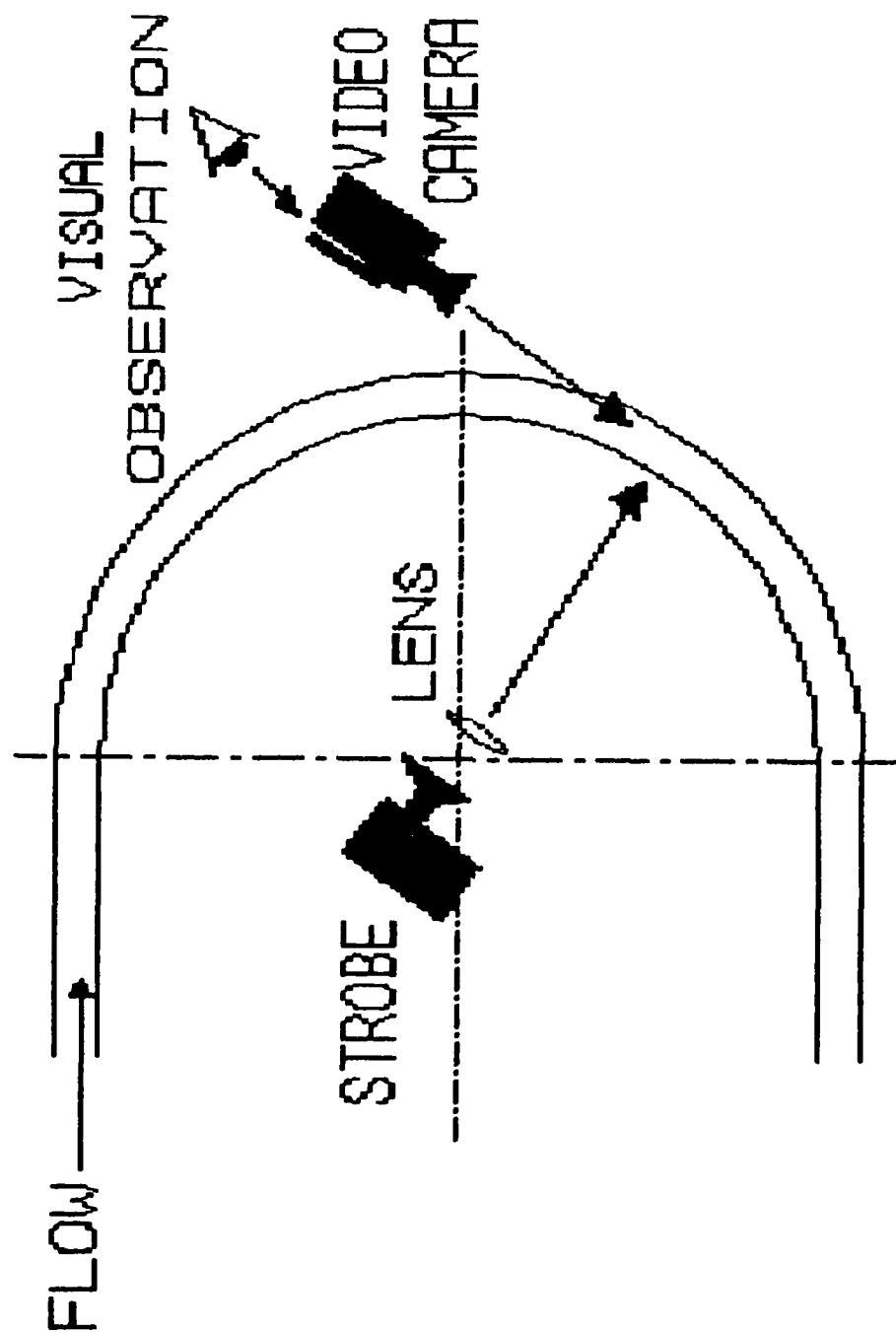


Figure 13. Radial-Spanwise Plane Flow Visualization

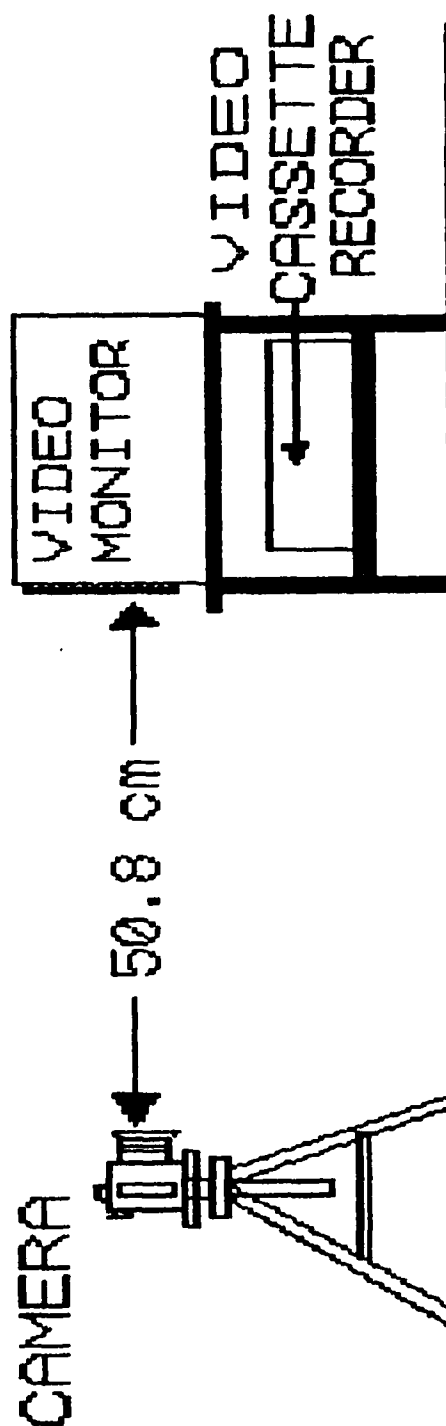


Figure 14. Schematic of Still Photography Set-up

MASS FLOW RATE

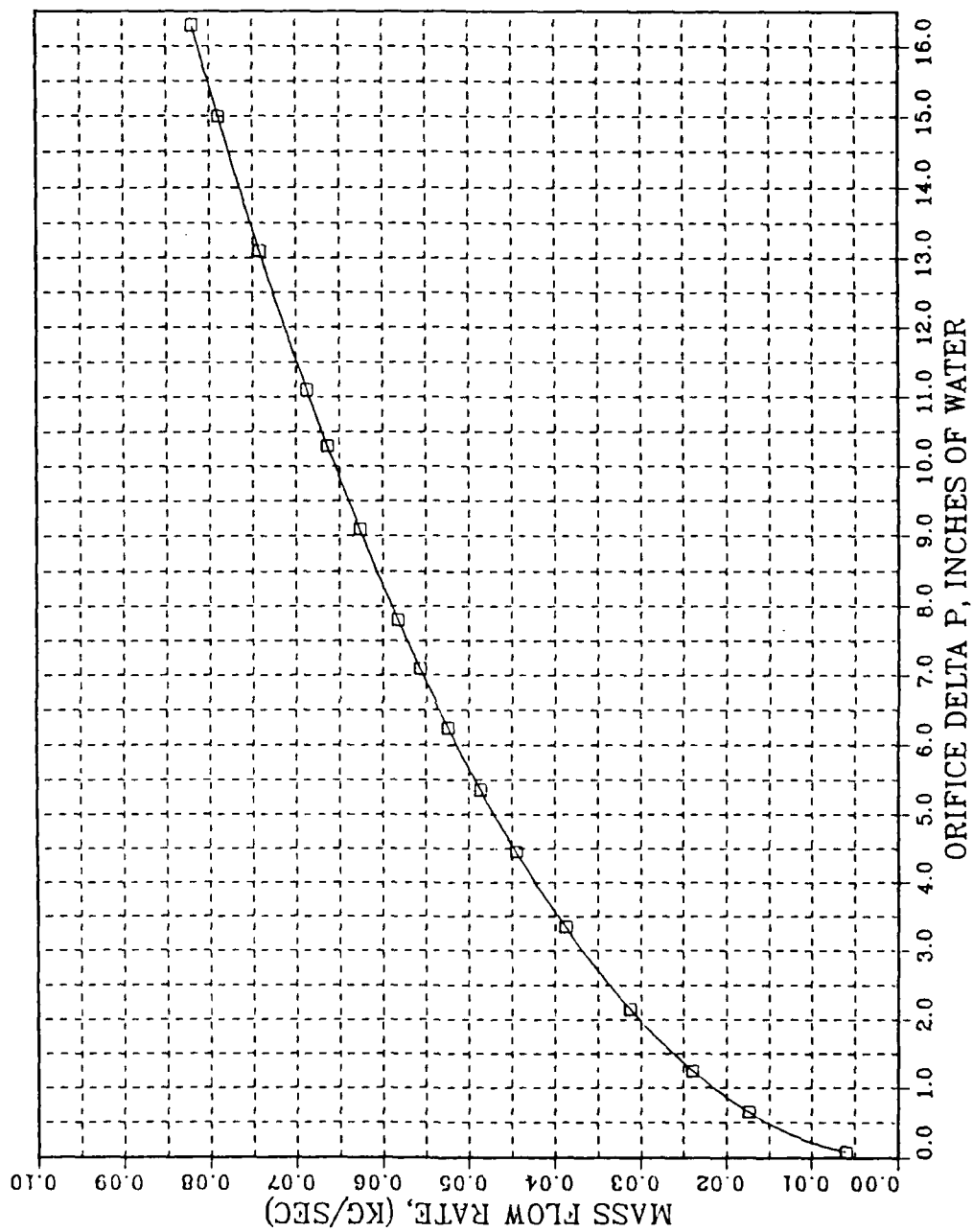


Figure 15. Mass Flow Rate vs. Orifice delta P
(for delta P < 2.25 inches of water)

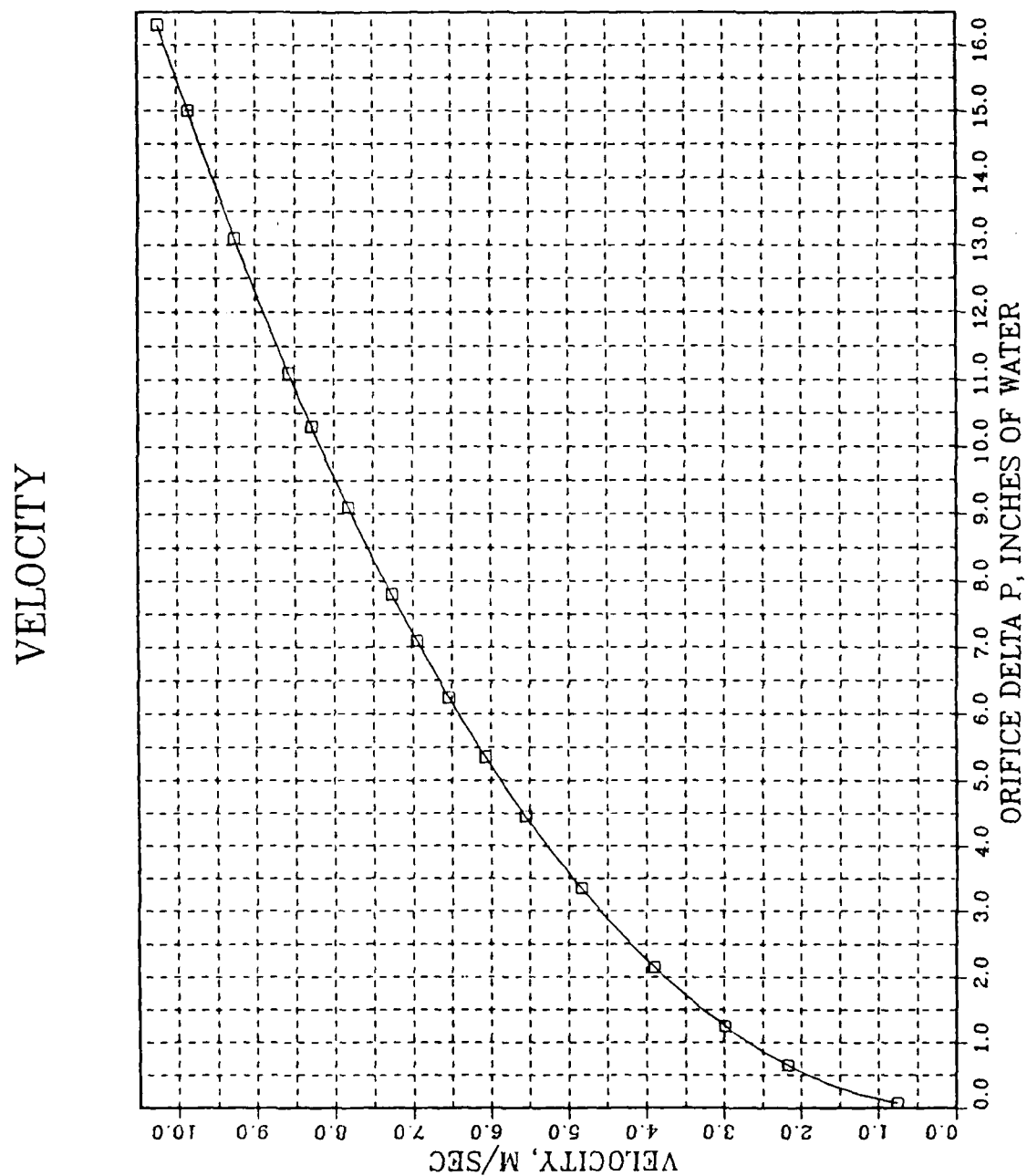


Figure 16. Velocity vs. Orifice delta P
(for delta P < 2.25 inches of water)

REYNOLDS NUMBER

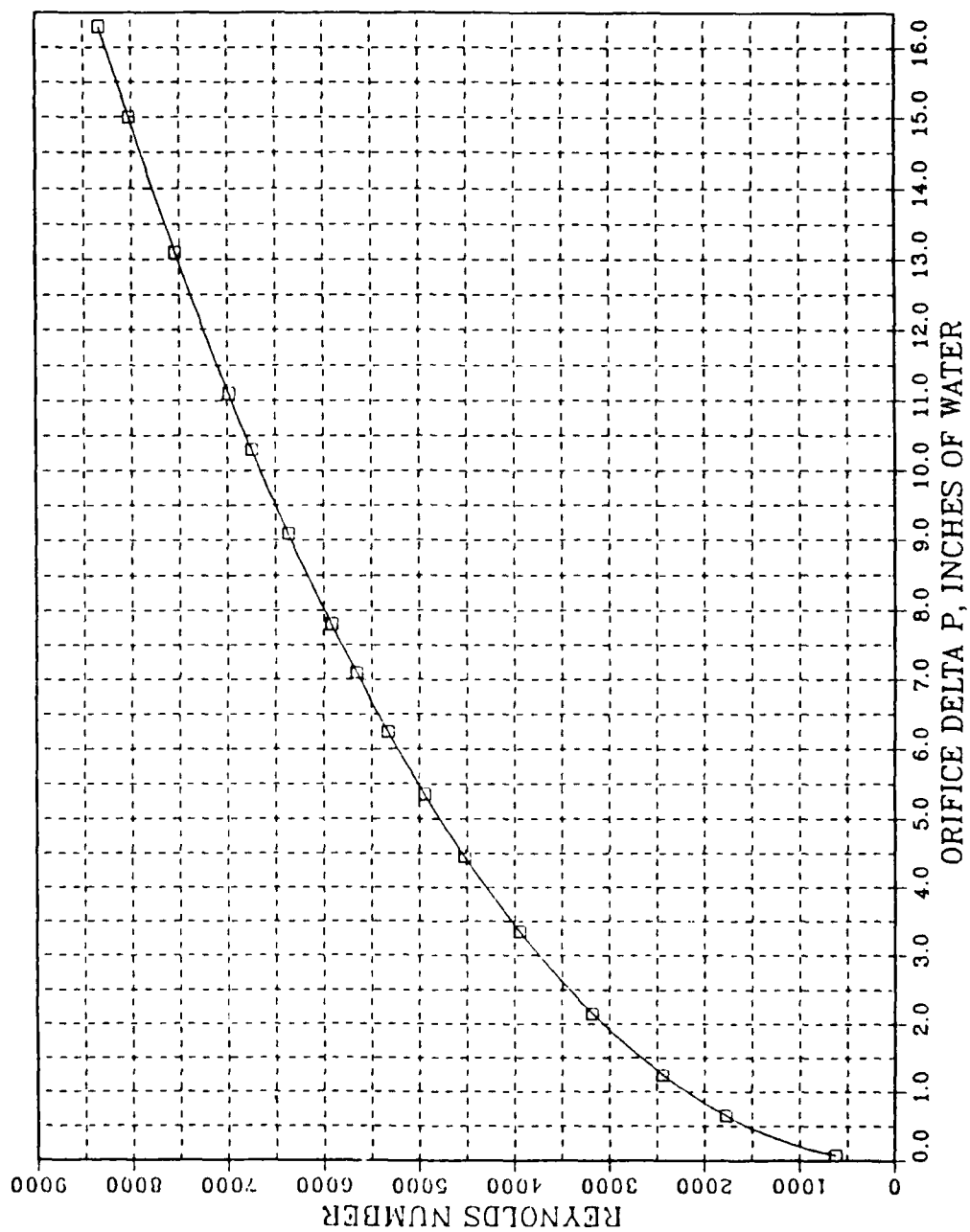


Figure 17. Reynolds Number vs. Orifice delta P
(for delta P < 2.25 inches of water)

MASS FLOW

$$y = 1.6665e-2 + 7.6213e-3x - 3.5705e-4x^2 + 8.3296e-6x^3 \quad R^2 = 1.000$$

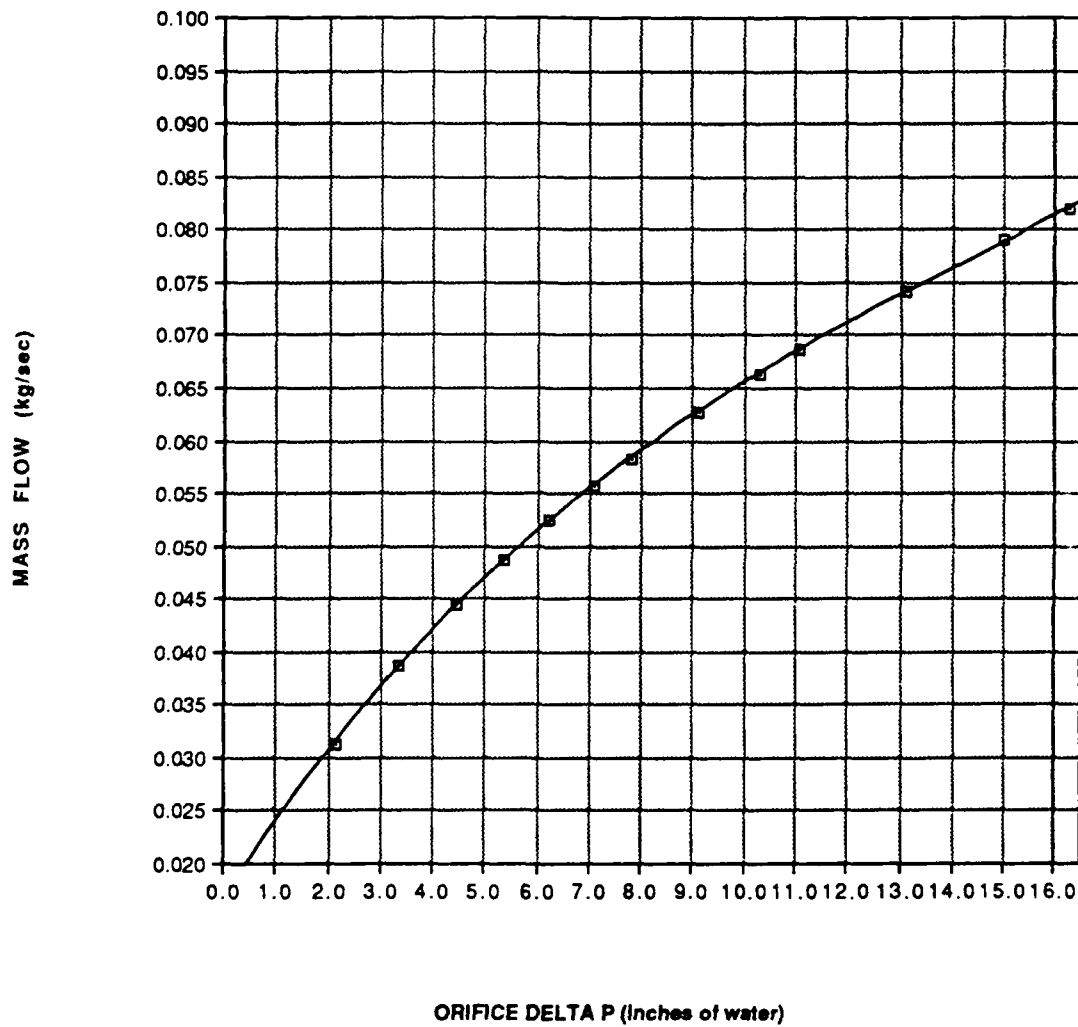


Figure 18. Mass Flow Rate vs. Orifice delta P
(for delta P > 2.25 inches of water)

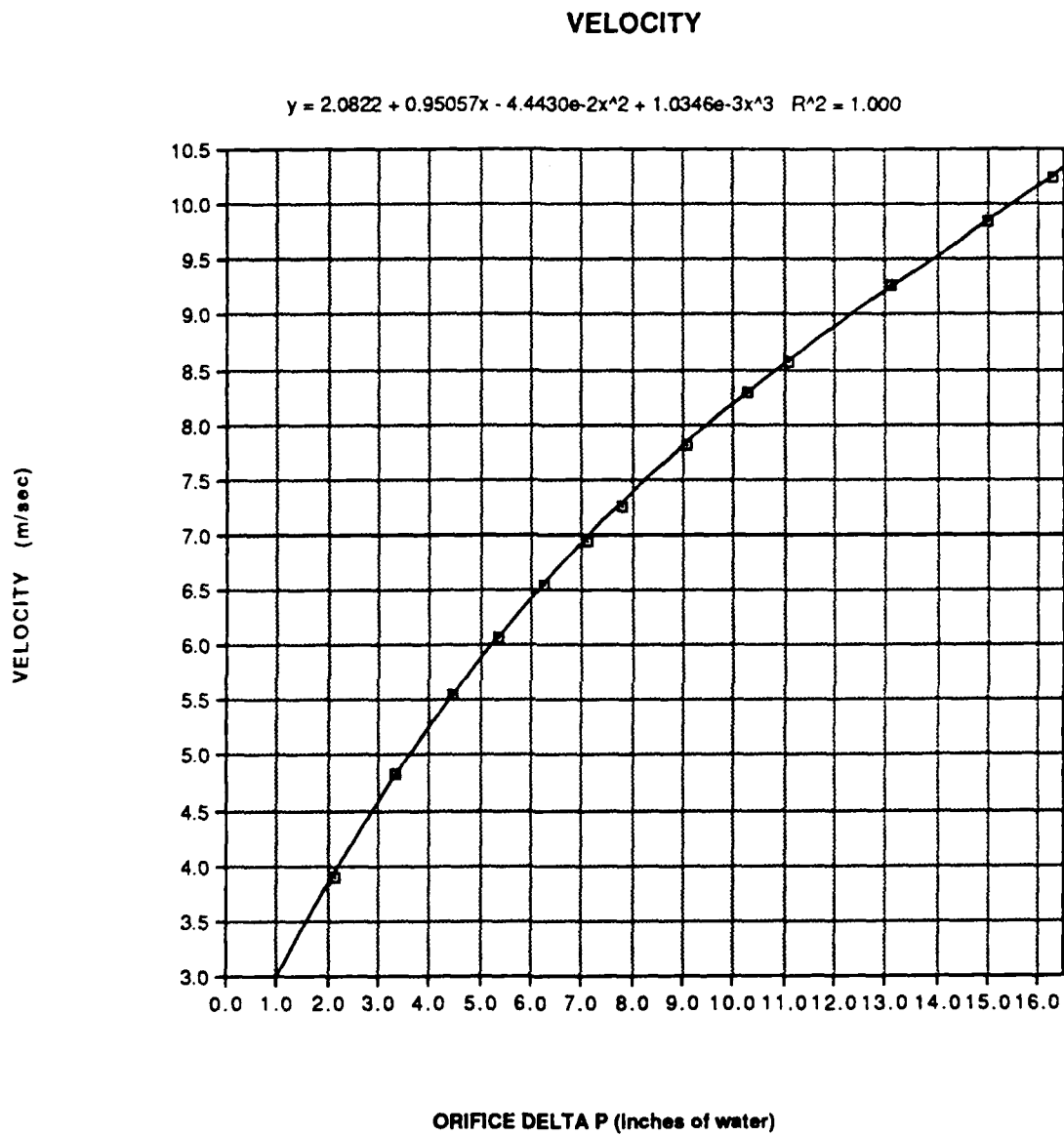


Figure 19. Velocity vs. Orifice delta P
(for delta P > 2.25 inches of water)

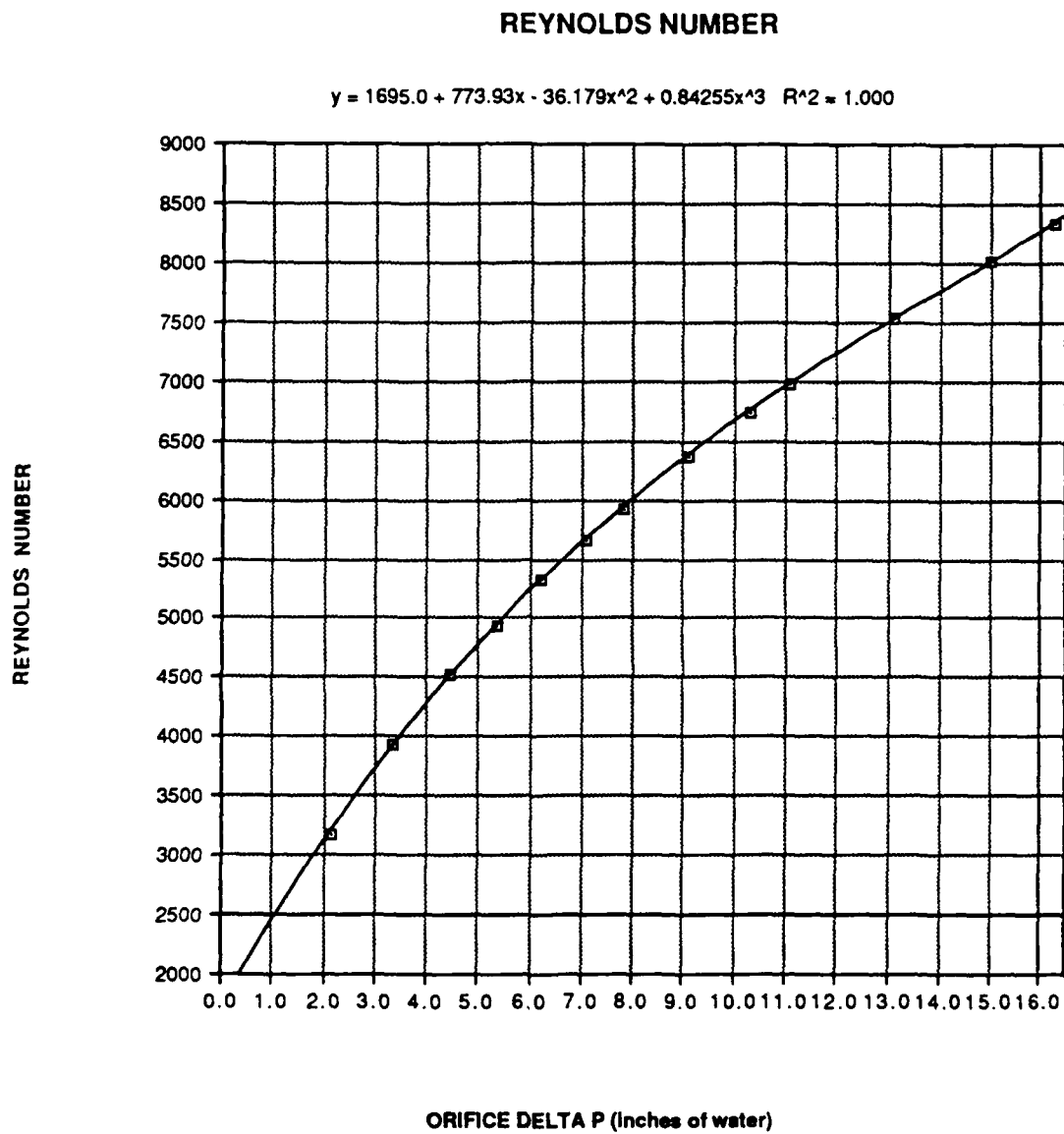


Figure 20. Reynolds Number vs. Orifice delta P
(for delta P > 2.25 inches of water)

MASS FLOW RATE

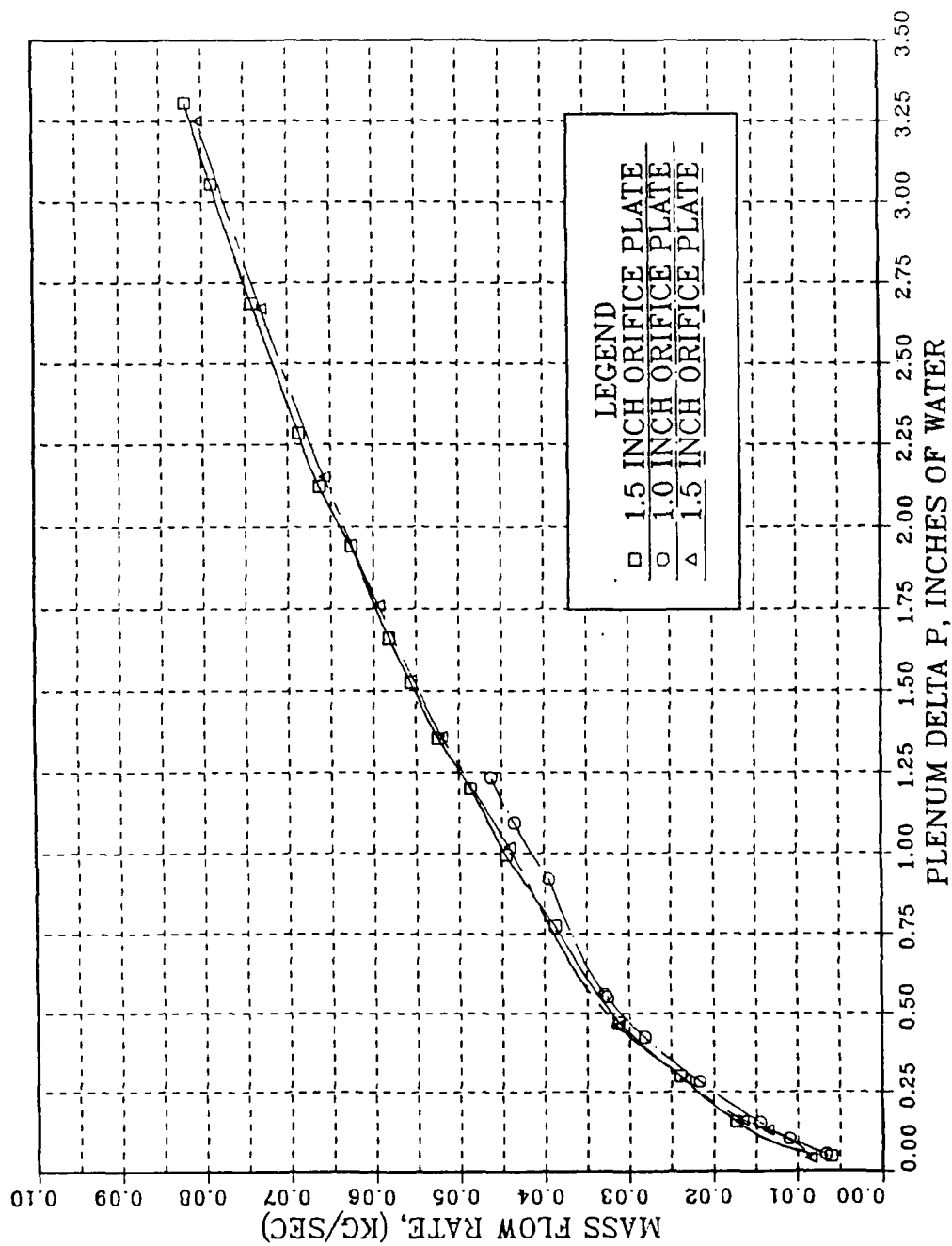


Figure 21. Mass Flow Rate vs. Plenum delta P

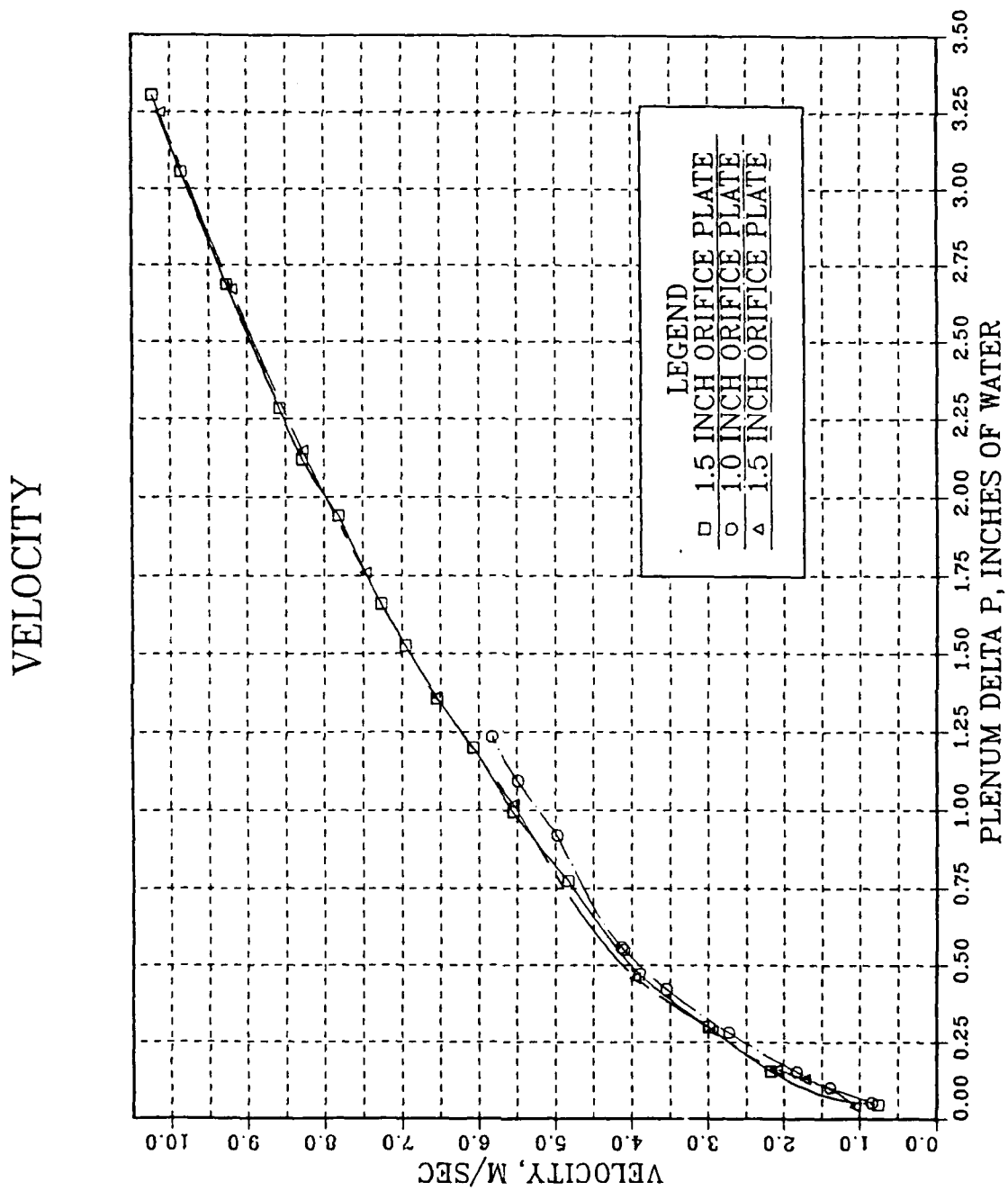


Figure 22. Velocity vs.
Plenum delta P

REYNOLDS NUMBER

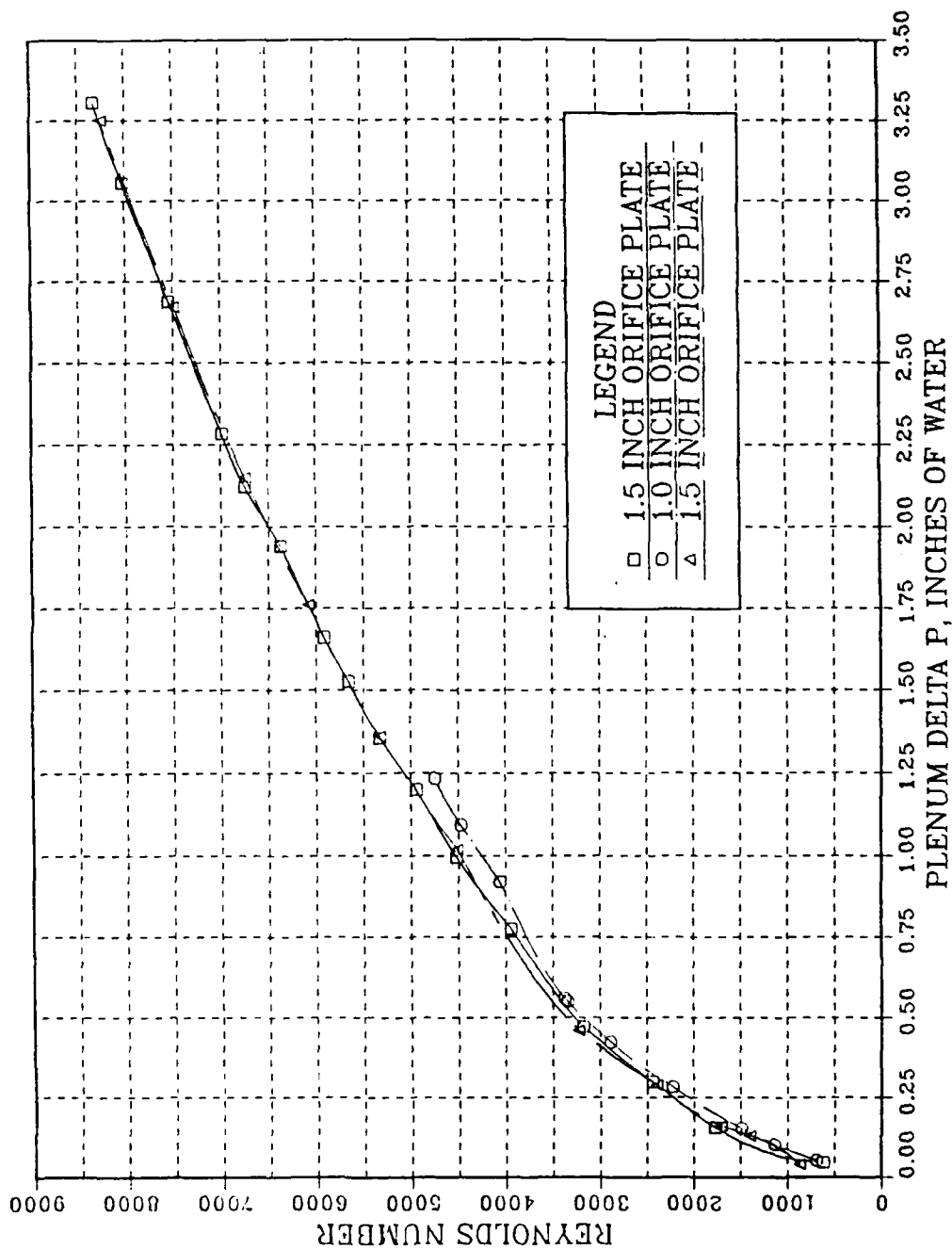


Figure 23. Reynolds Number vs. Plenum delta P

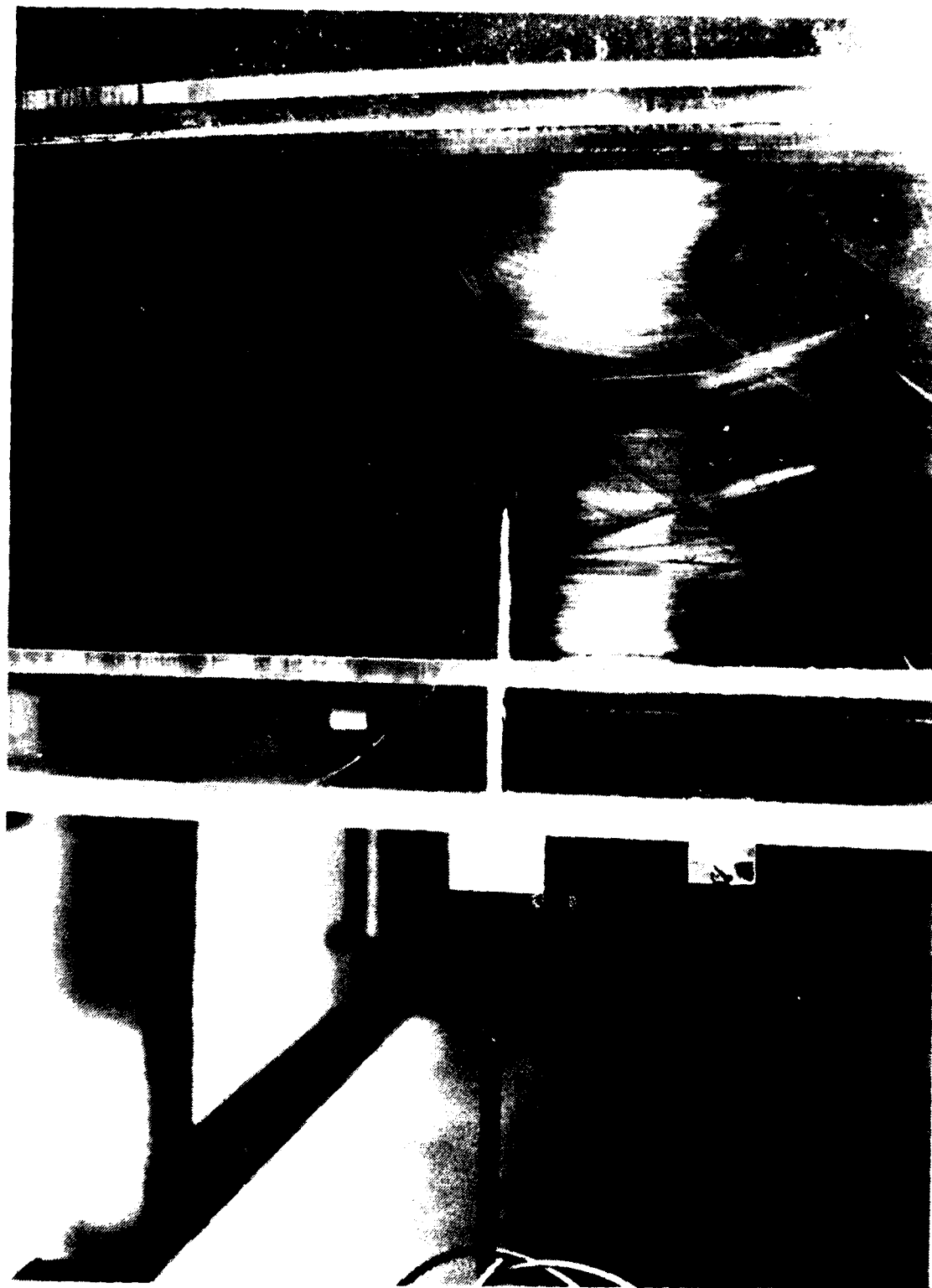


Figure 24. Hot Wire

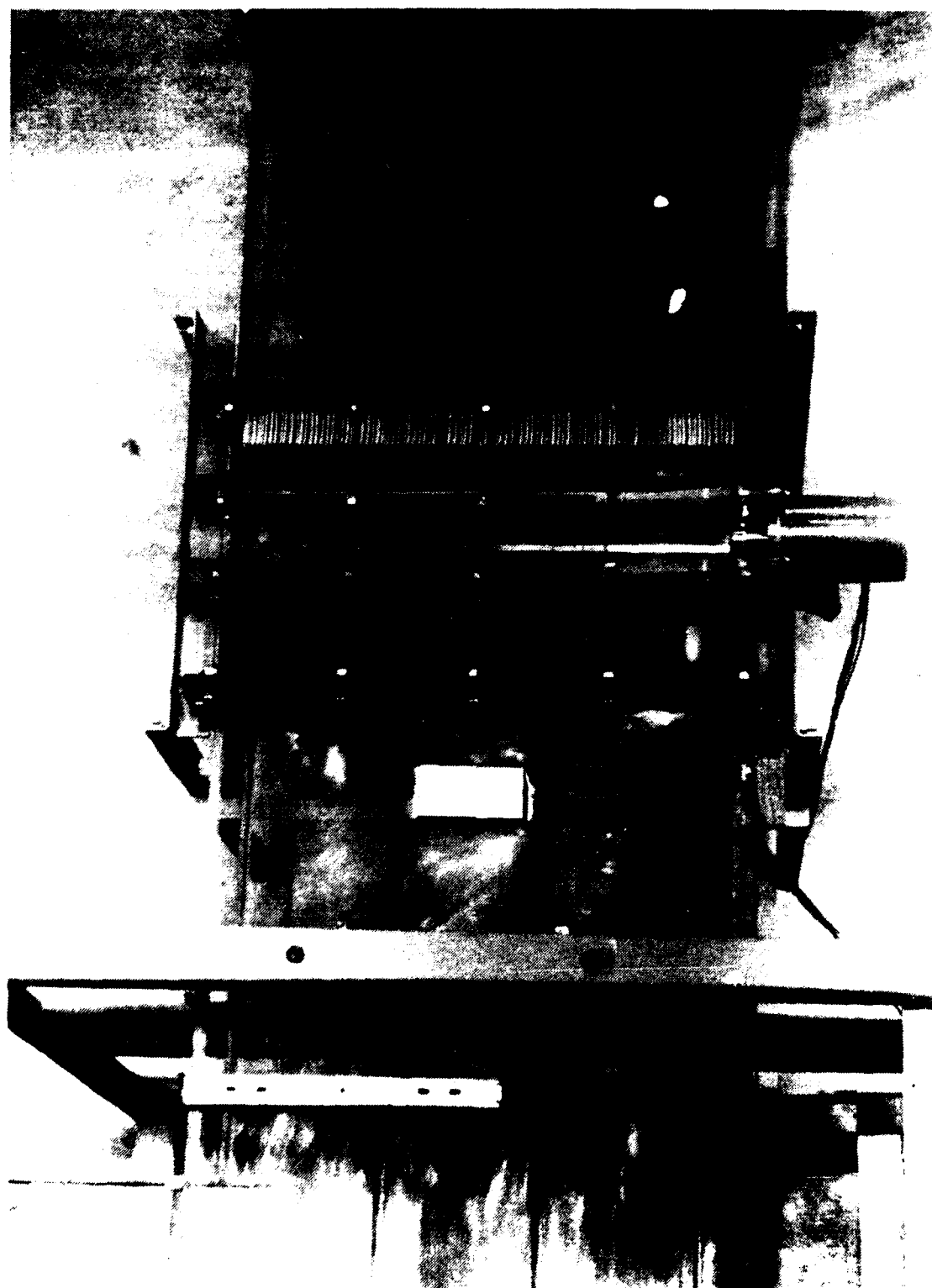


Fig. 25. Hot Wire Probe and Unsteady Device

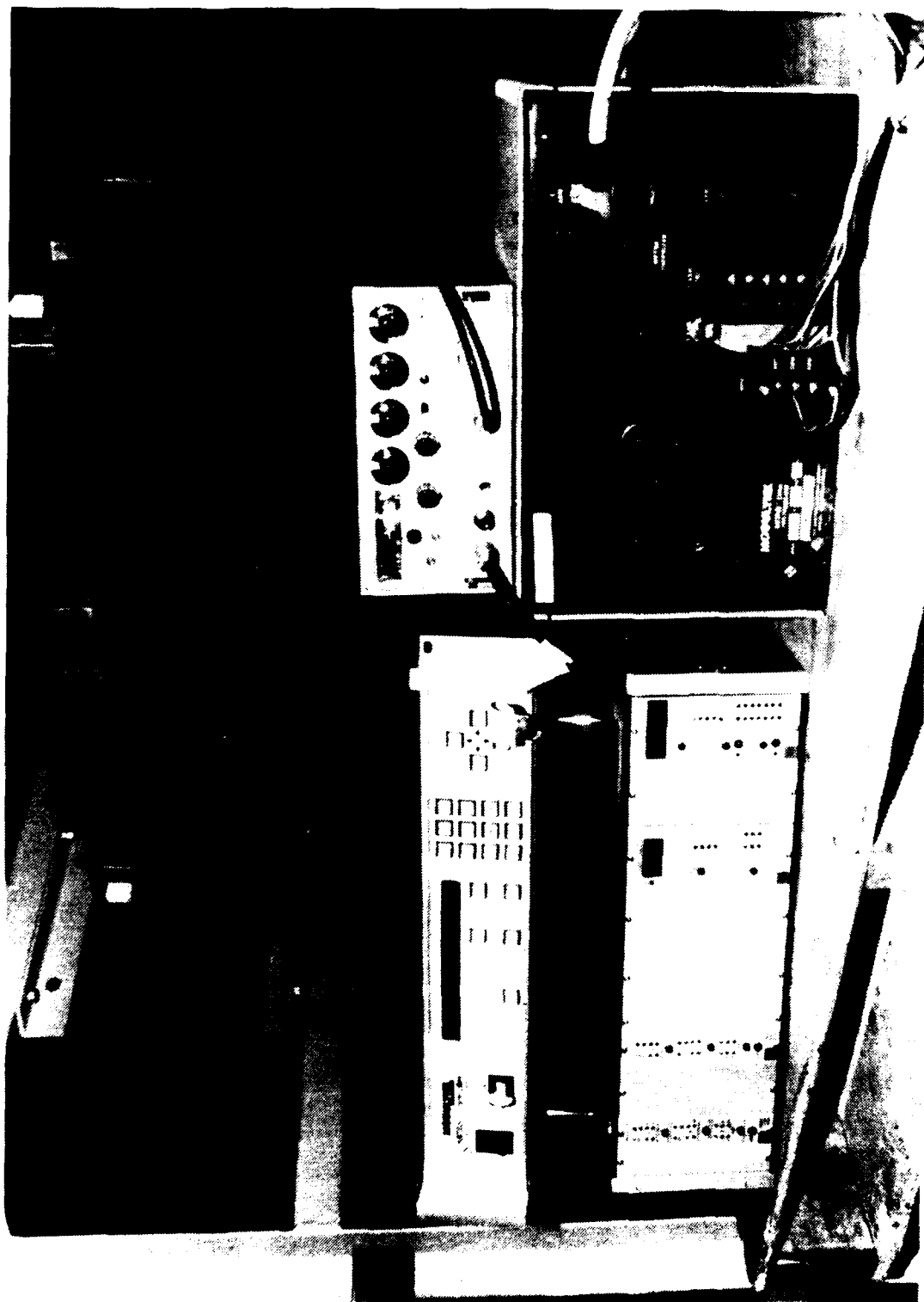


Figure 20. Constant Temperature Bridge and Signal Conditioner
with the Motor Drive and Motor Controller

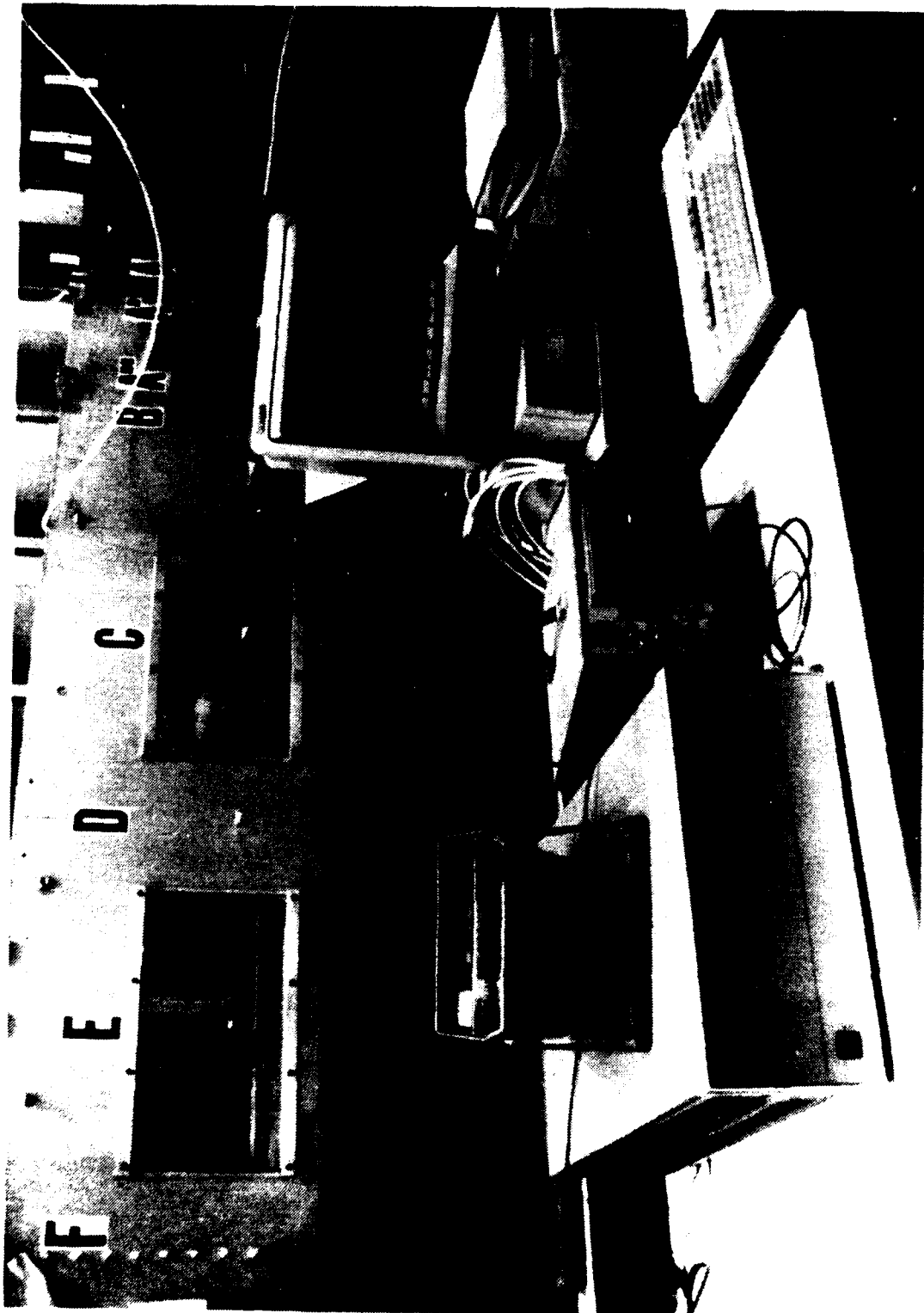


Figure 27. Data Acquisition System

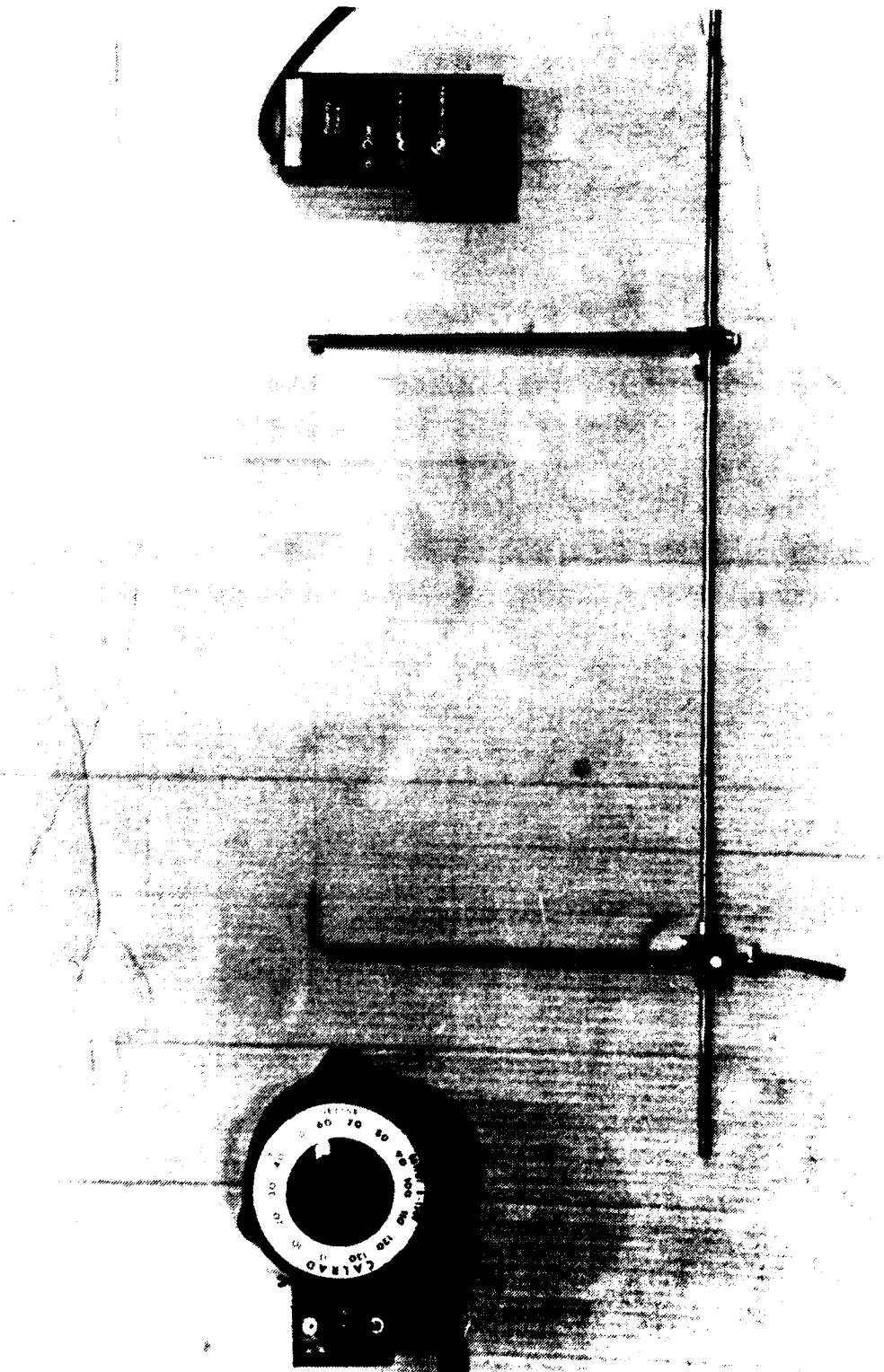
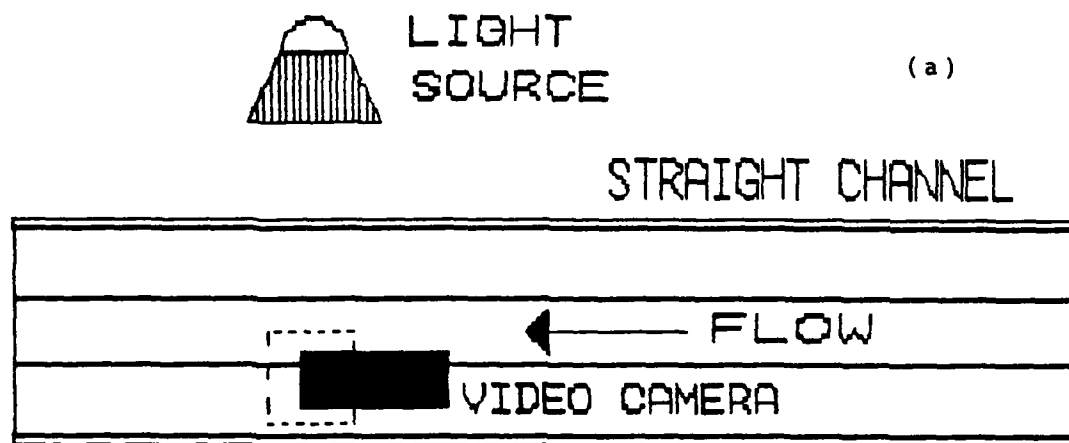
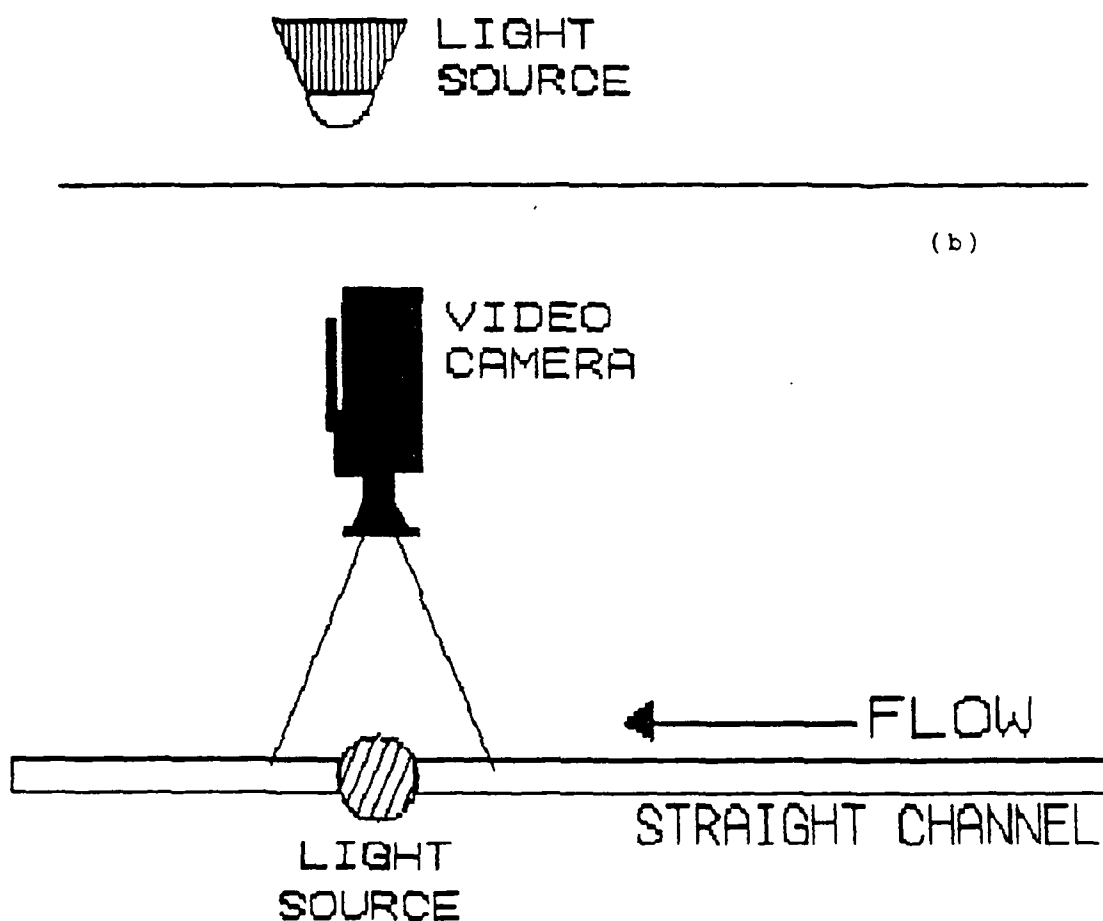


Figure 28. Smoke Wire Equipment



(a)



(b)

Figure 29. Video Camera and Light Source Set-up for Straight Channel Flow Visualization
(a) Top View (b) Side View



Figure 25. Flow Visualization at $De=75$ and
25 Degrees from Start of Curvature



Figure 21. Flow Visualization at $De=75$ and
05 Degrees from Start of Convection

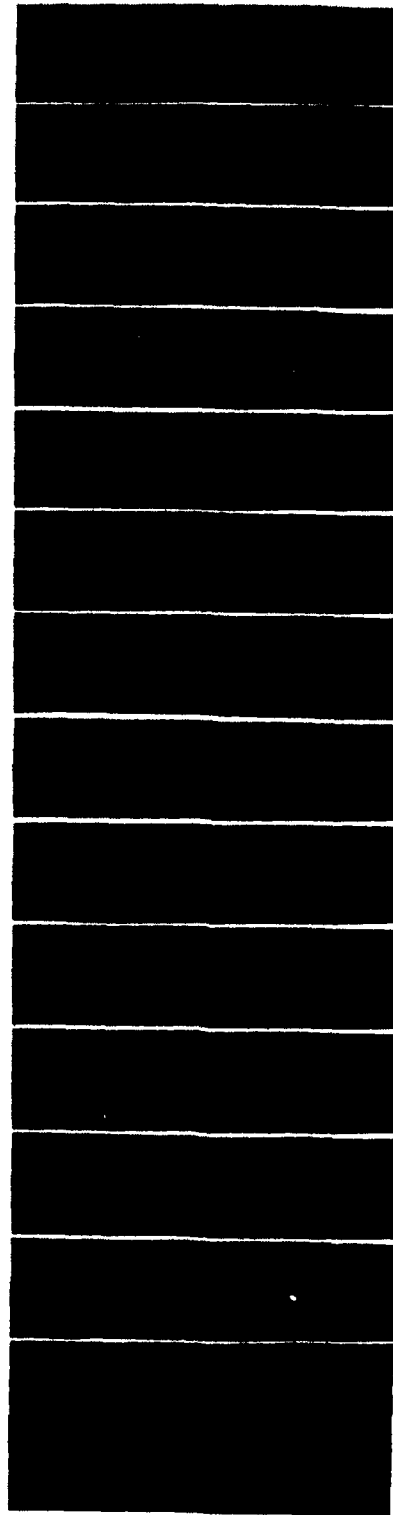


Figure 32. Flow Visualization at $\Delta\alpha=75^\circ$ and 125° Degrees from Start of Curvature (Sequence 1)

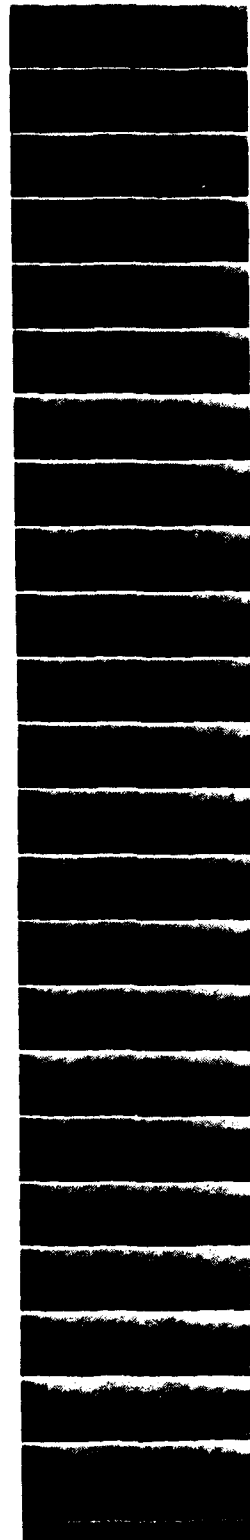


Fig. 10. 20. Flow Visualization at $\alpha = 25^\circ$ and 105° Degrees
of Angle of Circulation (Sequence 1)

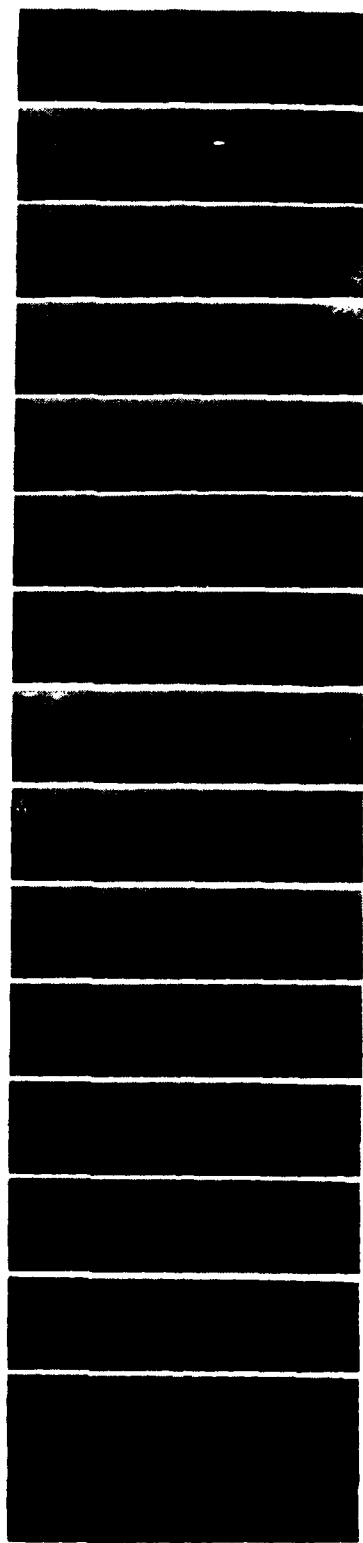


Figure 24. Flow Visualization at $\alpha = 75^\circ$ and 105° Degrees
from Start of Curvature (Sequence 2)

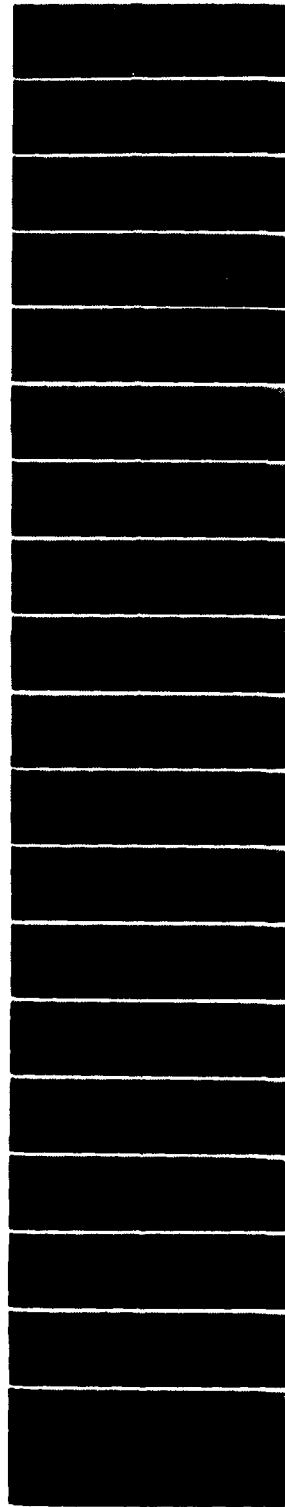


Figure 35. Flow Visualization at $\text{Re}=75$ and 105 Degrees
for Start of Curvature (Sequence 4)

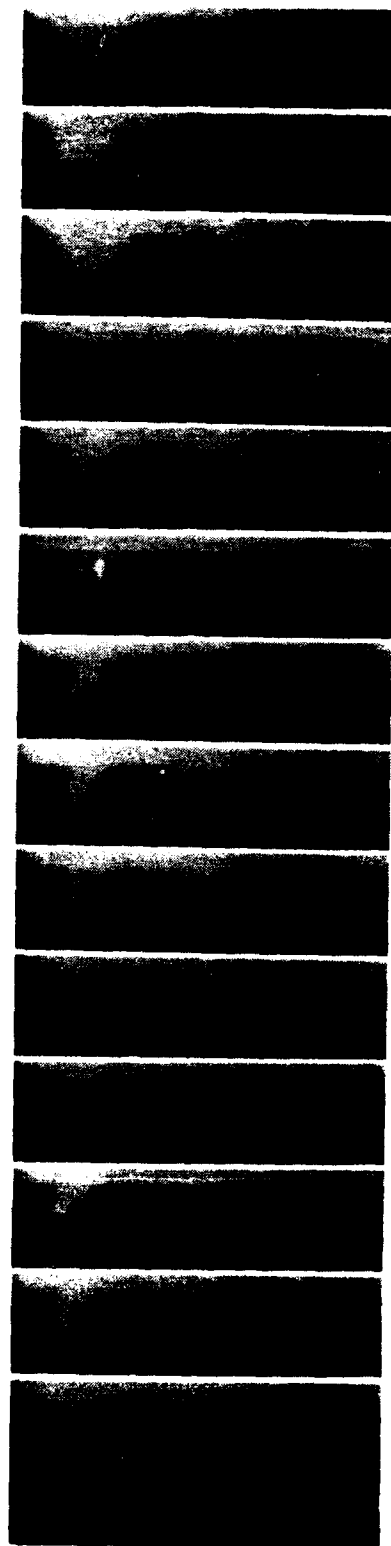


Figure 20. Flow Visualization at $\alpha=75^\circ$ and 125° Degrees
from Start of Curvature (Sequence 5)

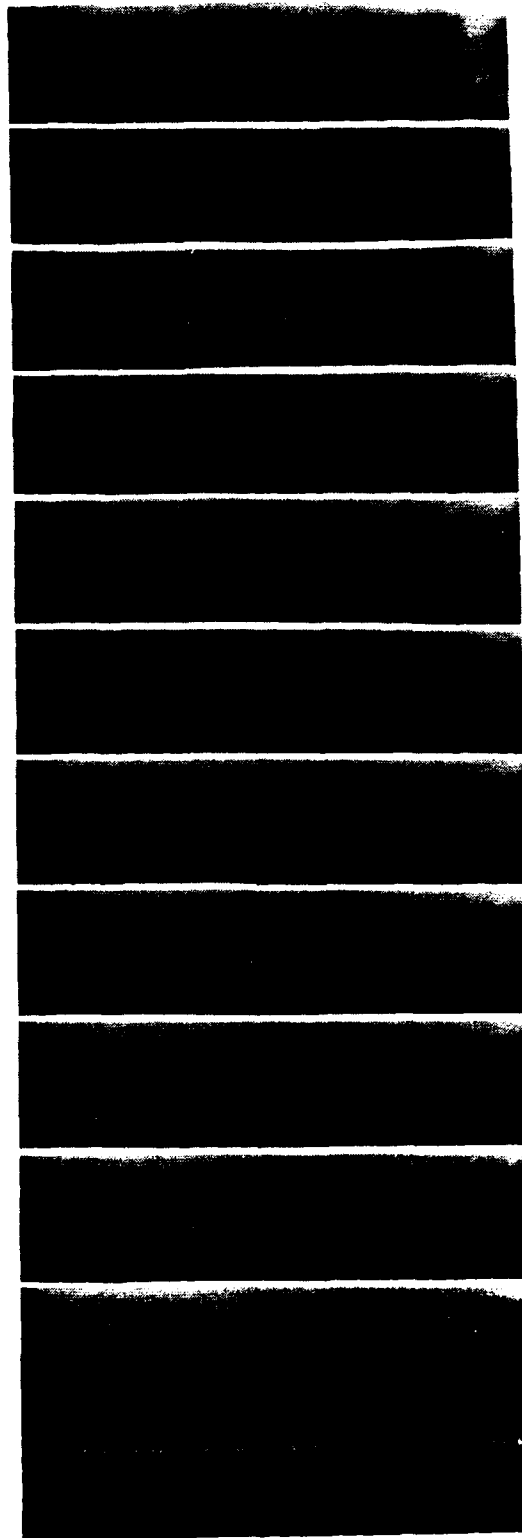


Figure 27. Flow Visualization at $\alpha=75^\circ$ and 105° Degrees from Start of Curvature (Sequence C)

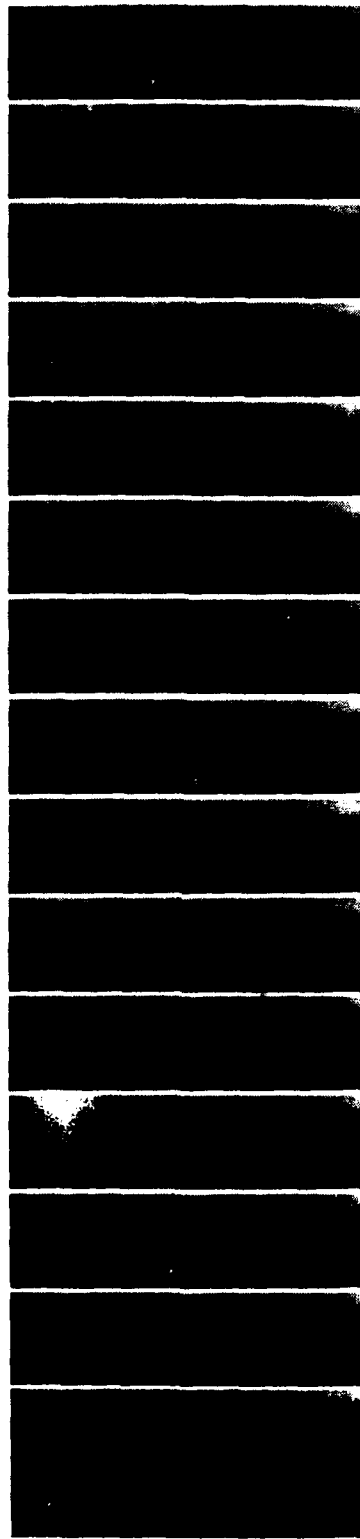


Figure 28. Flow Visualization at $\Delta\theta=75^\circ$ and 105° Degrees from Start of Curvature (Sequence 7)



FIGURE 20. Time Visualization of the 75 and 100 degree
 20 degree of curvature (Sequence 2)

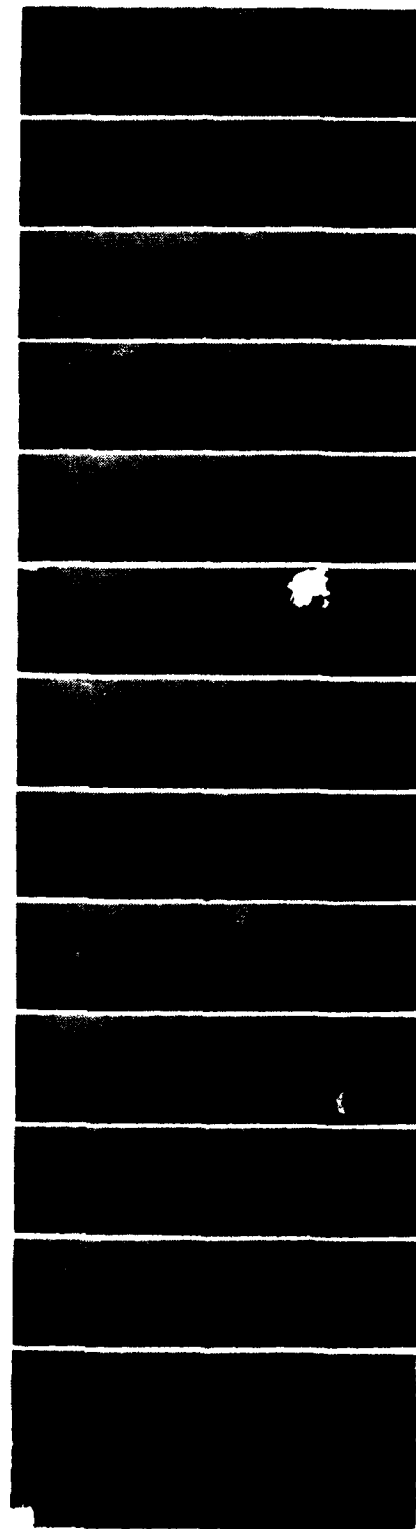


Figure 40. Flow Visualization at $\theta = 75^\circ$ and 105° Downstream from Start of Curvature (Sequence 9)

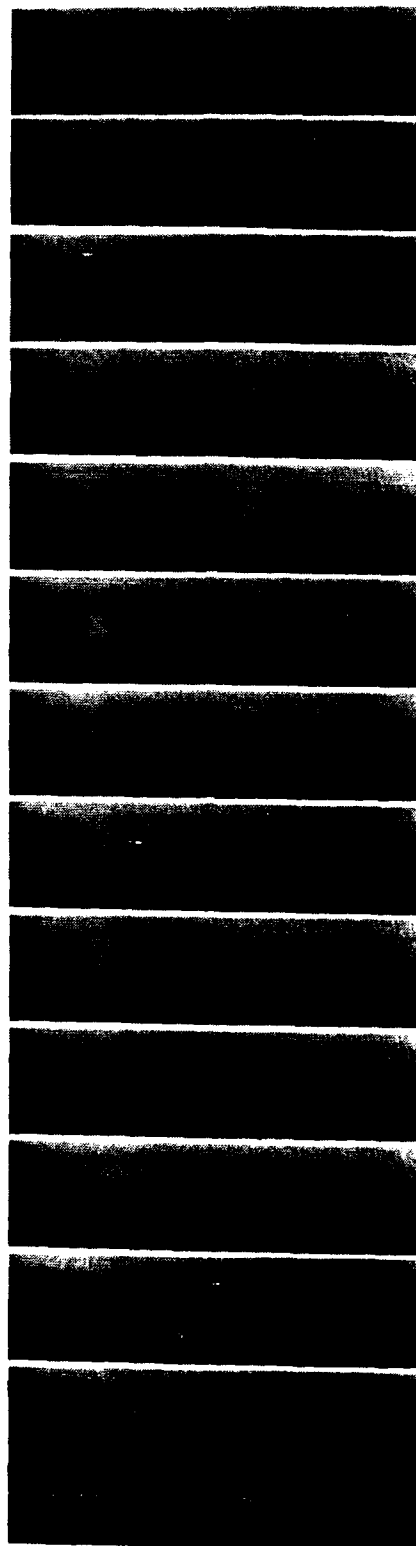


Figure 11. P11. Visualization at $\theta = 75^\circ$ and 105° degrees
for Start of Curvature (Degree = 10°)



Figure 42. Flow Visualization at $De=100$ and 95° Degree, from Start of Correlation

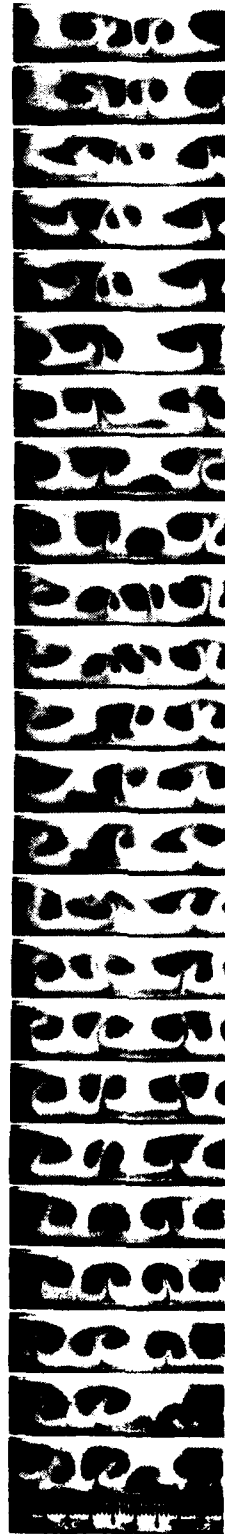


Figure 40. Flow visualization of 20-100 um/
105 Degree for Start of Collection

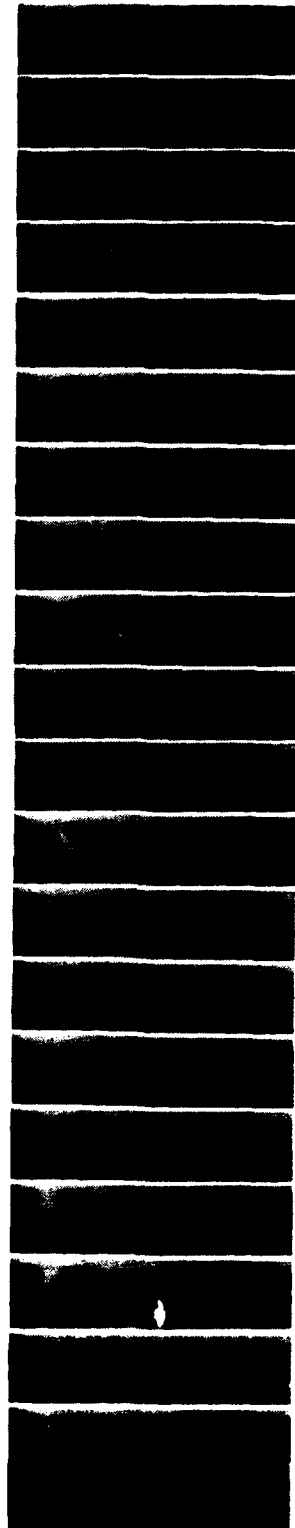


Figure 44. Flow Visualization at $\theta = 100^\circ$ and
145 Degrees from Start of Curvature



Figure 15. File Visualization at 100 and 155 Degree for Start of Clivity

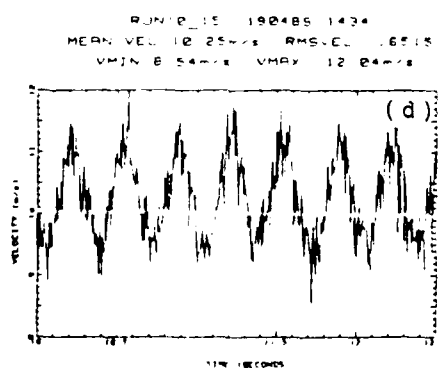
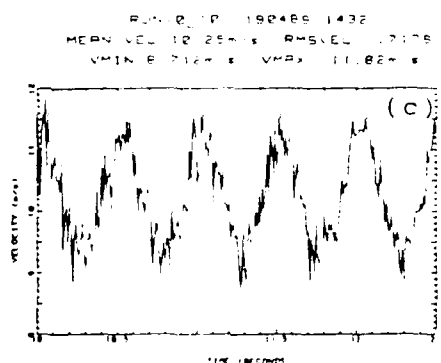
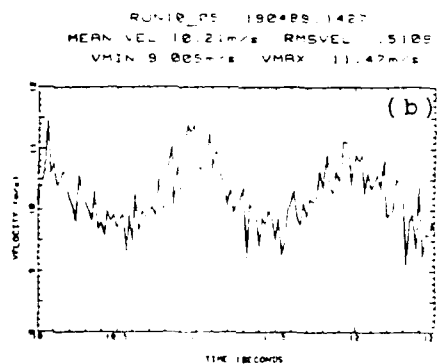
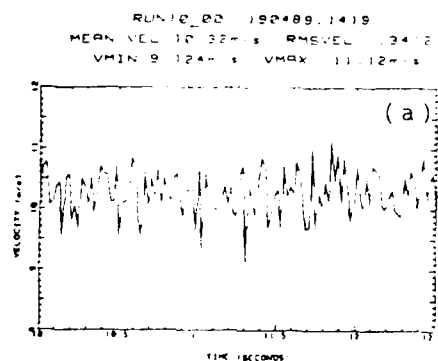
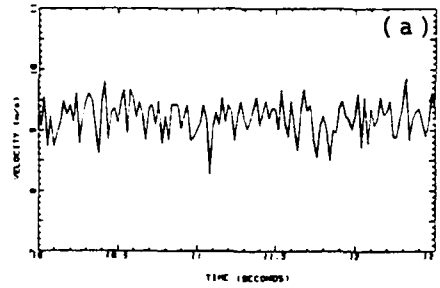
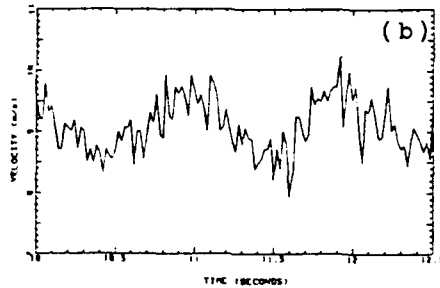


Figure 46. Instantaneous Velocity Traces ($Re=8444$)
(a) No Unsteadiness (b) $Str=0.0040$
(c) $Str=0.0080$ (d) $Str=0.0119$

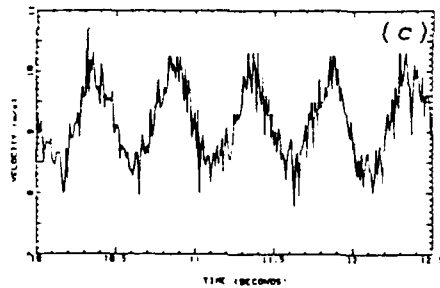
RUN09_00 190489.1436
 MEAN VEL 9.183m/s RMSVEL .3057
 VMIN 8.258m/s VMAX 9.863m/s



RUN09_05 190489.1441
 MEAN VEL 9.126m/s RMSVEL .4238
 VMIN 7.929m/s VMAX 10.25m/s



RUN09_10 190489.1444
 MEAN VEL 9.132m/s RMSVEL .5971
 VMIN 7.768m/s VMAX 12.71m/s



RUN09_15 190489.1447
 MEAN VEL 9.136m/s RMSVEL .5189
 VMIN 7.715m/s VMAX 10.38m/s

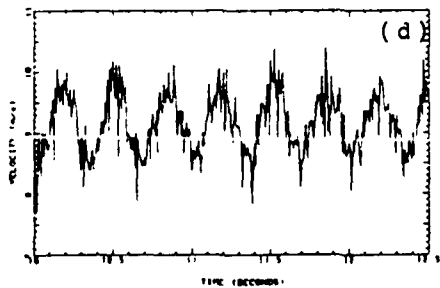


Figure 47. Instantaneous Velocity Traces ($Re=7578$)
 (a) No Unsteadiness (b) $Str=0.0044$
 (c) $Str=0.0089$ (c) $Str=0.0133$

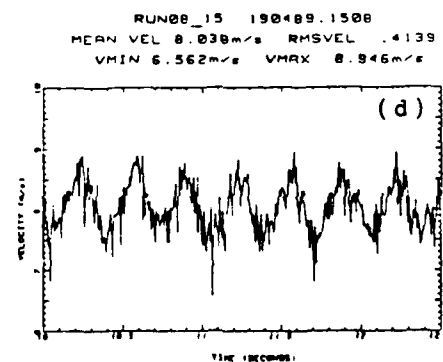
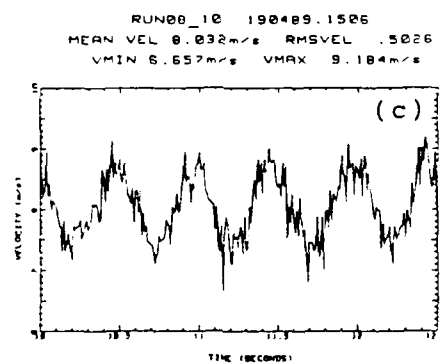
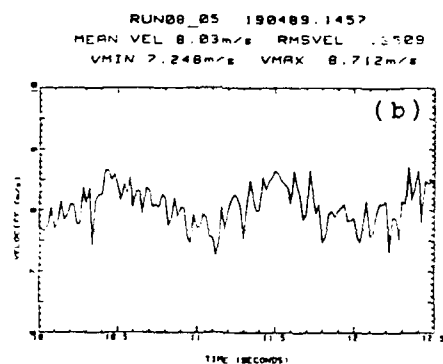
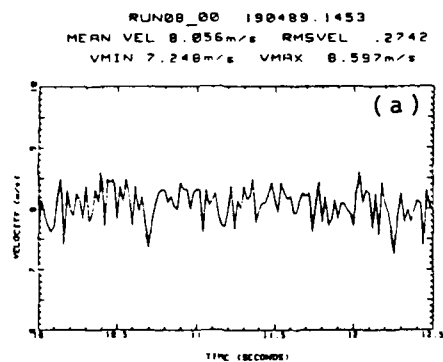


Figure 48. Instantaneous Velocity Traces ($Re=6729$)
 (a) No Unsteadiness (b) $Str=0.0050$
 (c) $Str=0.0100$ (c) $Str=0.0150$

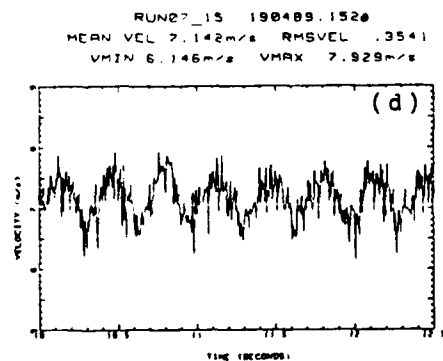
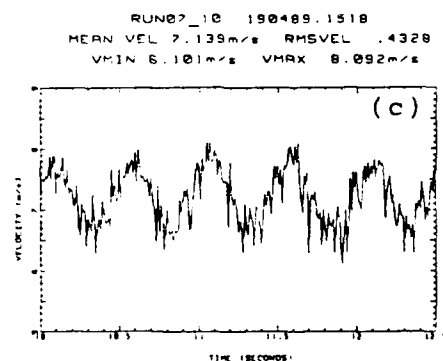
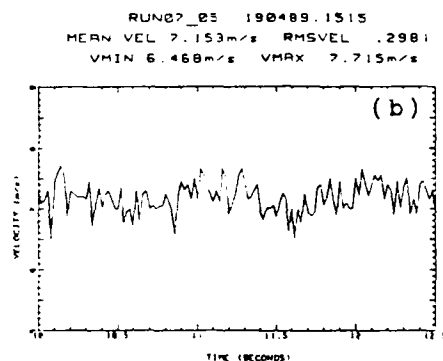
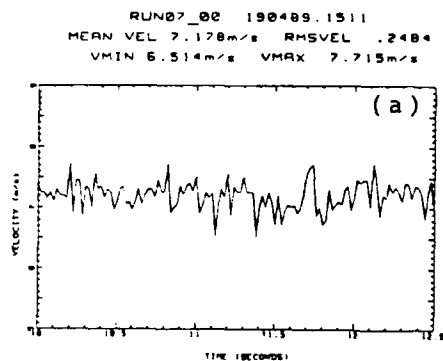


Figure 49. Instantaneous Velocity Traces ($Re=5943$)
 (a) No Unsteadiness (b) $Str=0.0057$
 (c) $Str=0.0113$ (c) $Str=0.0170$

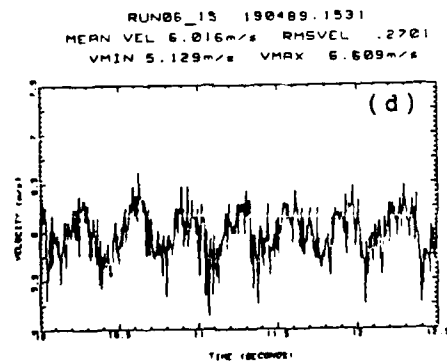
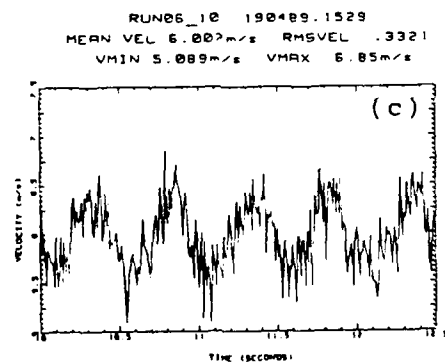
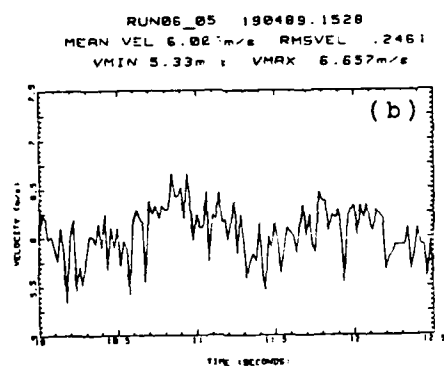
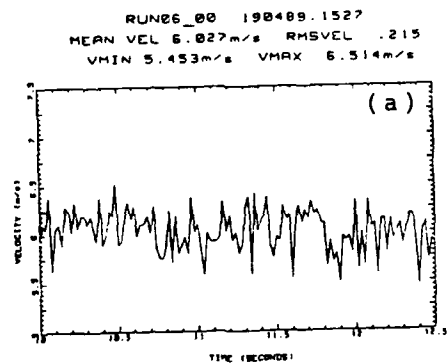


Figure 50. Instantaneous Velocity Traces ($Re=4954$)
 (a) No Unsteadiness (b) $Str=0.0068$
 (c) $Str=0.0136$ (c) $Str=0.0203$

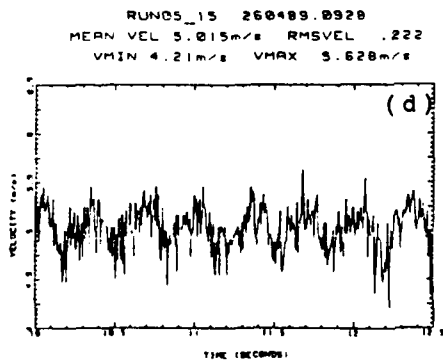
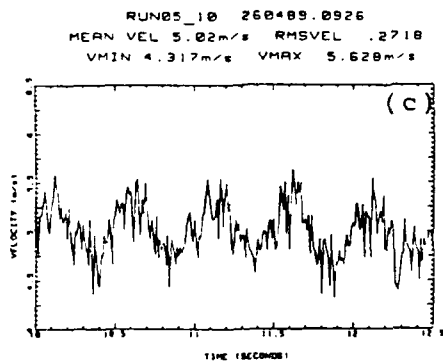
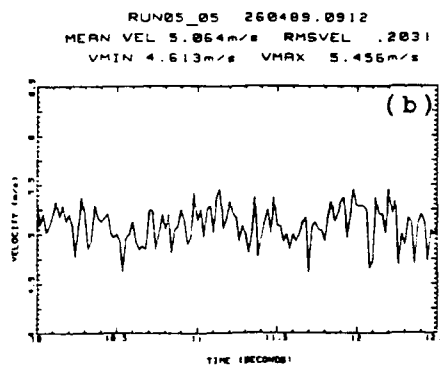
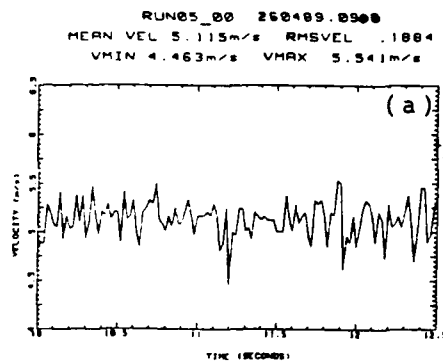


Figure 51. Instantaneous Velocity Traces ($Re=4134$)
 (a) No Unsteadiness (b) $Str=0.0081$
 (c) $Str=0.0163$ (c) $Str=0.0244$

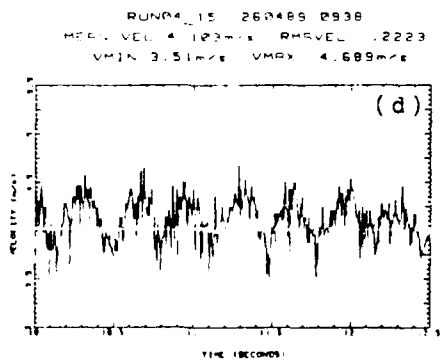
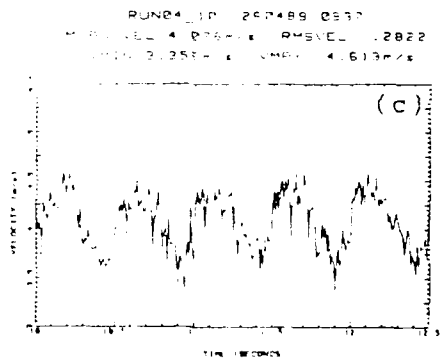
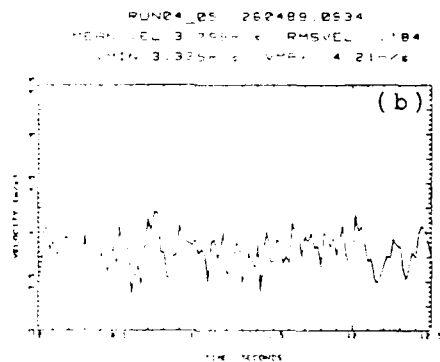
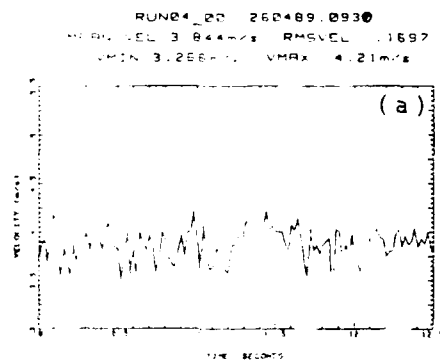


Figure 52. Instantaneous Velocity Traces ($Re=3343$)
 (a) No Unsteadiness (b) $Str=0.0101$
 (c) $Str=0.0201$ (d) $Str=0.0302$

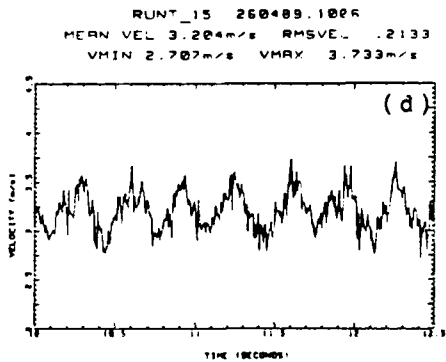
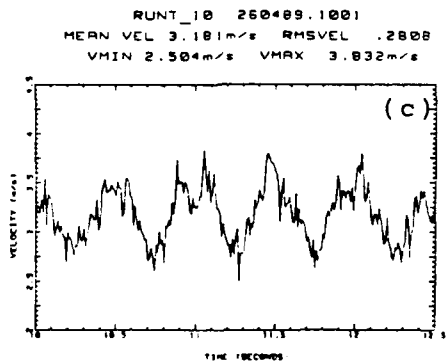
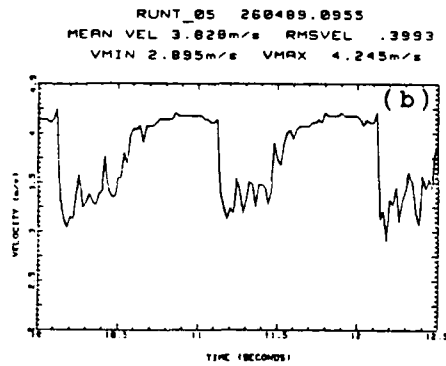
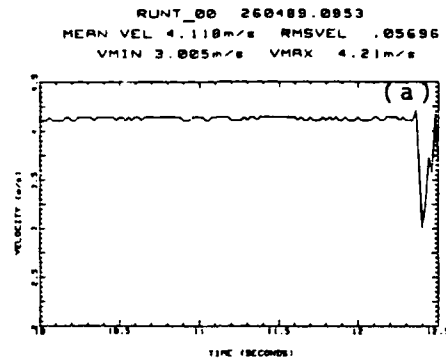


Figure 53. Instantaneous Velocity Traces ($Re=2754$)
 (a) No Unsteadiness (b) $Str=0.0122$
 (c) $Str=0.0244$ (c) $Str=0.0366$

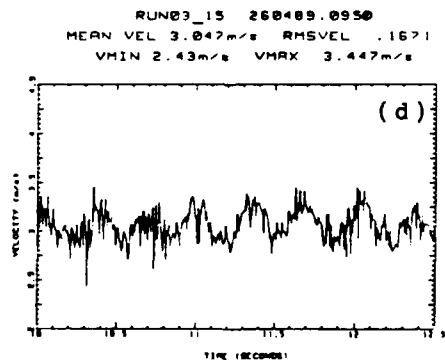
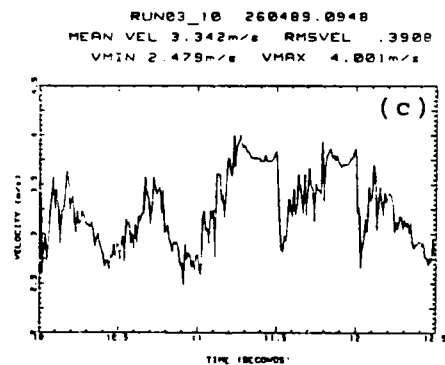
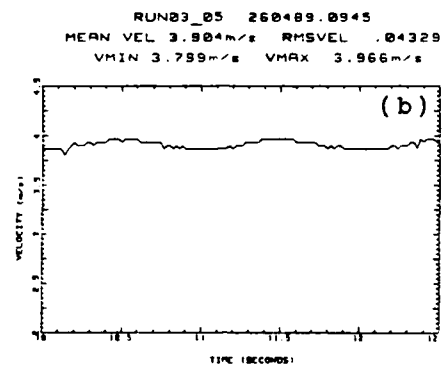
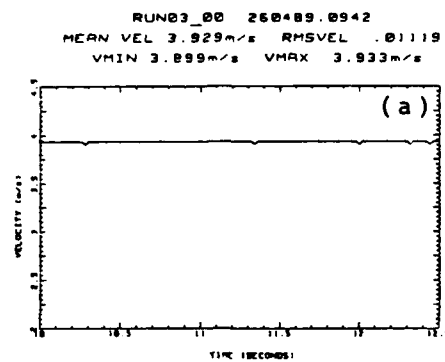


Figure 54. Instantaneous Velocity Traces ($Re=2569$)
 (a) No Unsteadiness (b) $Str=0.0131$
 (c) $Str=0.0262$ (c) $Str=0.0392$

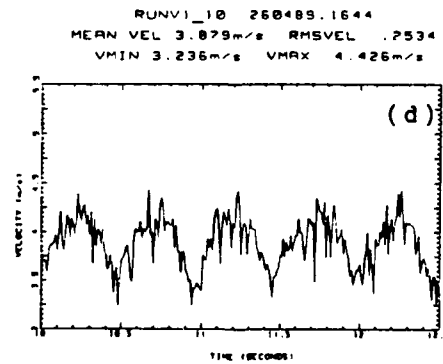
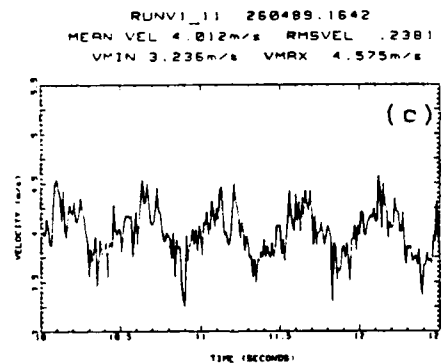
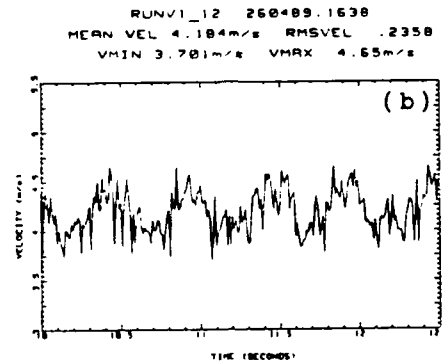
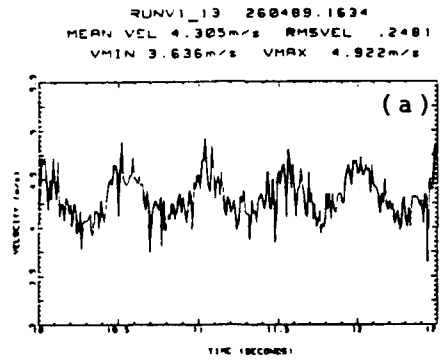


Figure 55. Instantaneous Velocity Traces
 (a) Re=3537 Str=0.0190 (b) Re=3453 Str=0.0195
 (c) Re=3284 Str=0.0205 (d) Re=3158 Str=0.0213

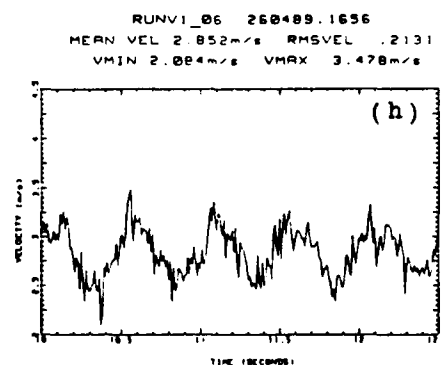
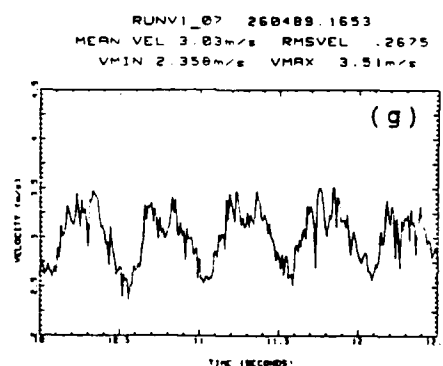
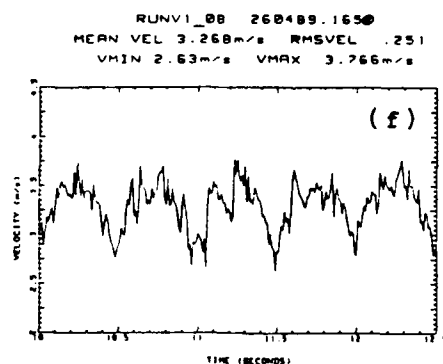
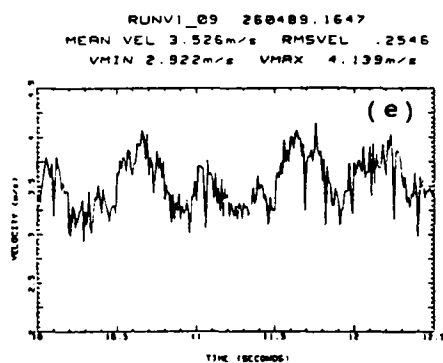


Figure 55. Instantaneous Velocity Traces
 (e) Re=2990 Str=0.0225 (f) Re=2863 Str=0.0235
 (g) Re=2611 Str=0.0257 (h) Re=2442 Str=0.0275

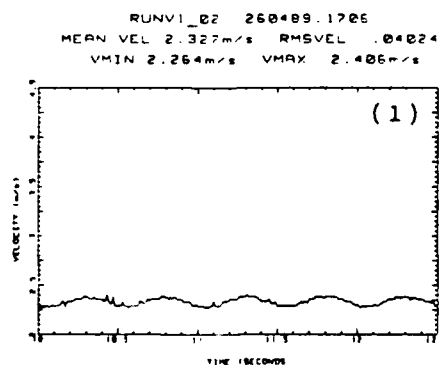
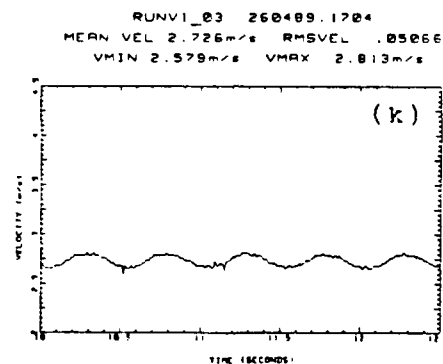
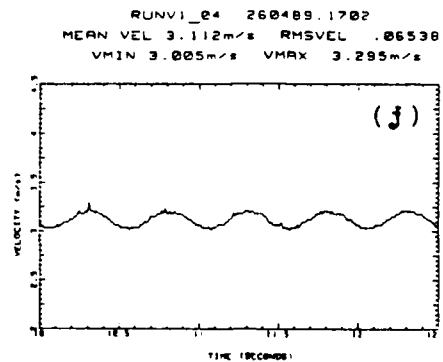
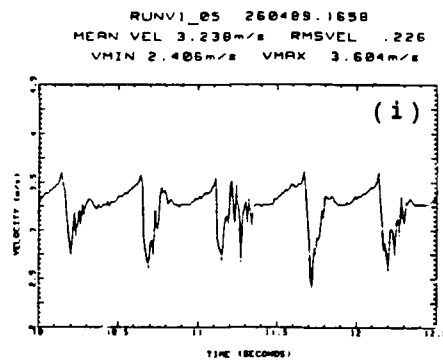


Figure 55. Instantaneous Velocity Traces
 (i) $Re=2274$ $Str=0.0296$ (j) $Re=2003$ $Str=0.0326$
 (k) $Re=1684$ $Str=0.0399$ (l) $Re=1432$ $Str=0.0469$

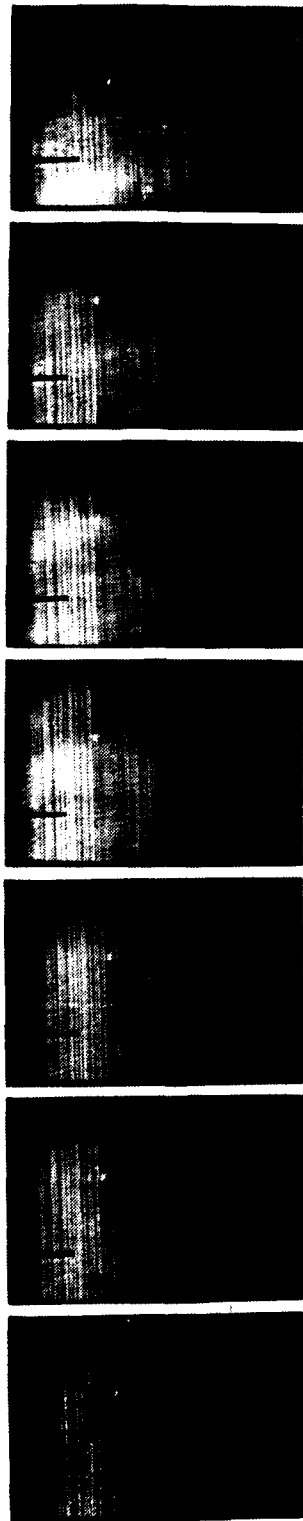


Figure 5C. Flow Visualization: $Re = 2350$, $St = 0.0295$,
 $y/d = 0.84$

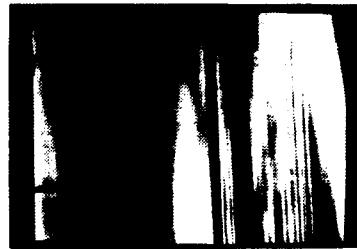
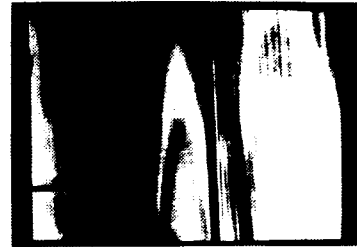
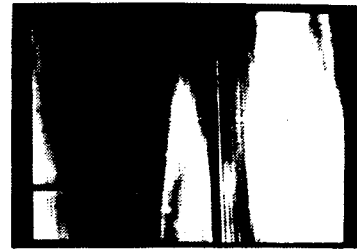
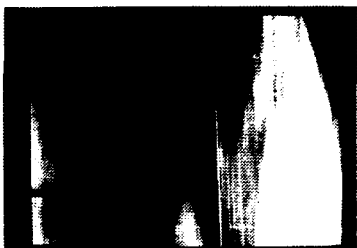
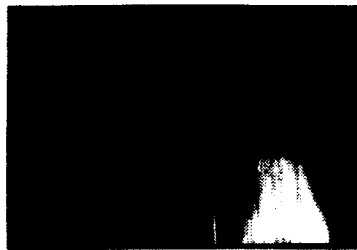


Figure 57. Flow Visualization. $Re = 2527$, $St = 0.0000$, $\gamma/d = 0.00$

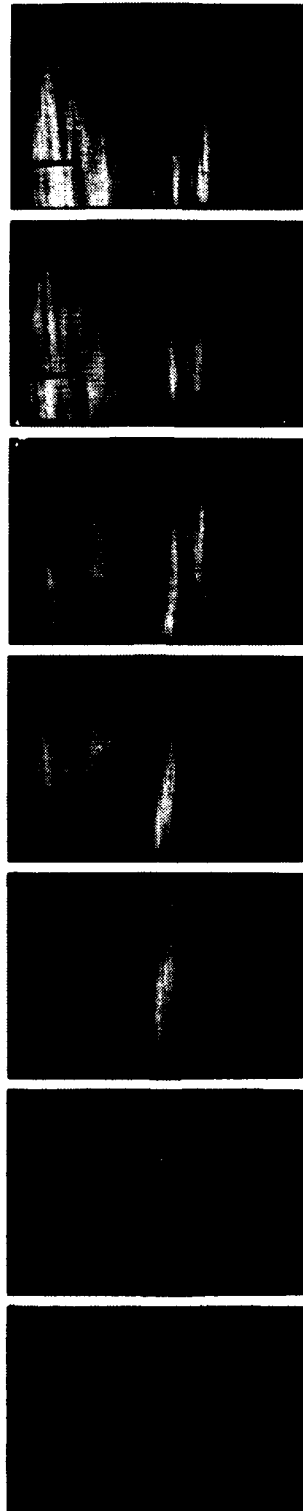


Figure 59. Flow Visualization: $Re = 2611$, $Str = 0.0257$,
 $y/d = +0.84$

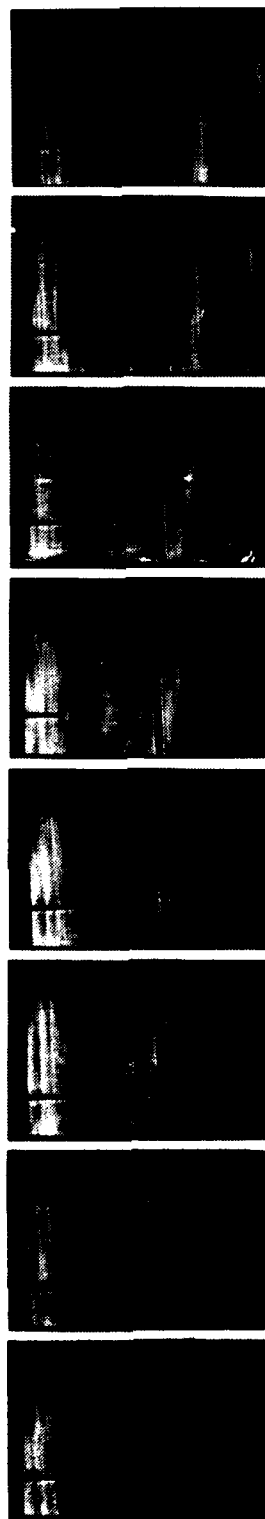


Figure 50. Flow Visualization: $Re = 2625$, $Str = 0.0240$,
 $\phi = 0.5$

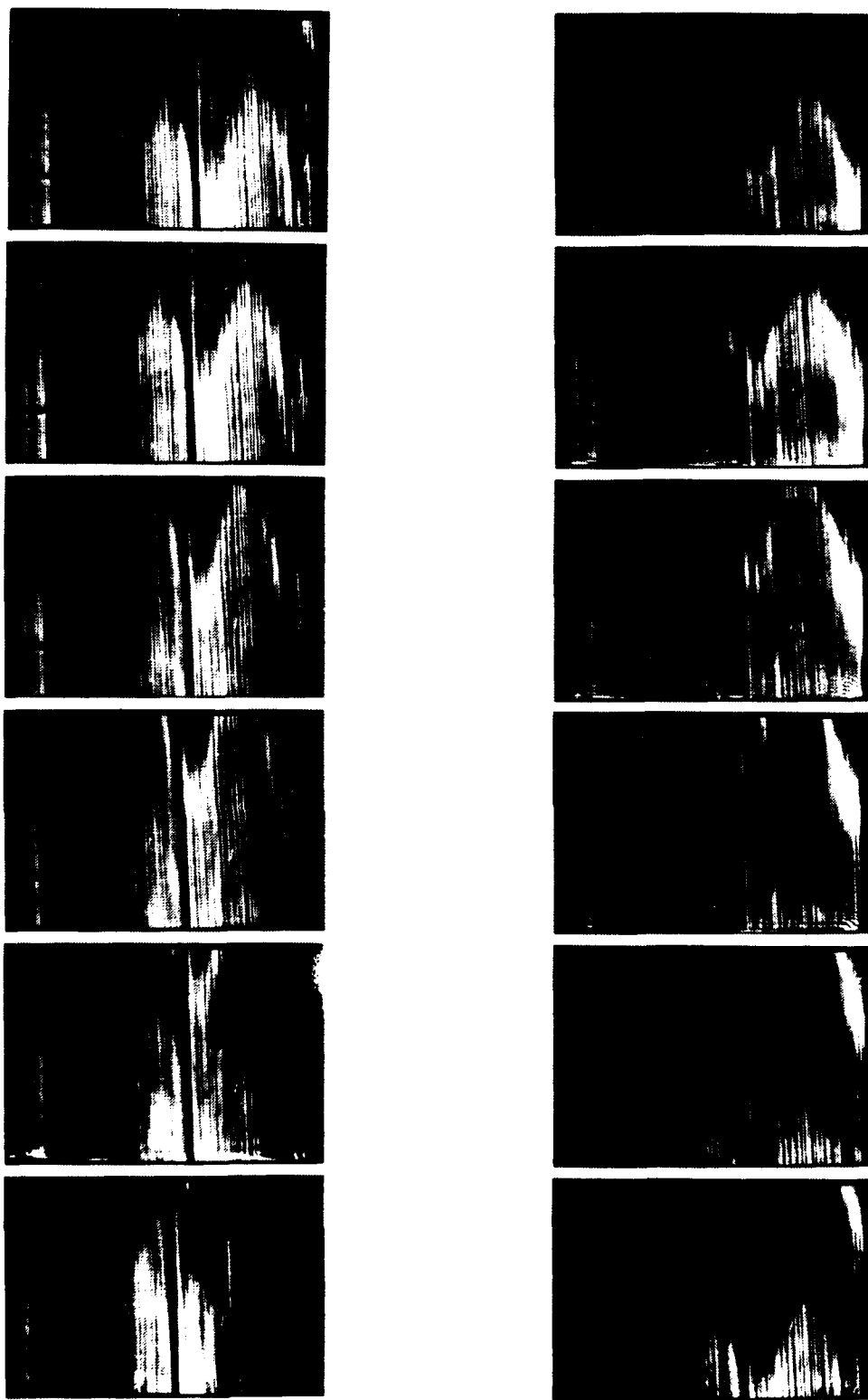


Figure 60. Flow Visualization: $Re = 2190$, $Str = 0.0400$,
 $\omega = 0.00$

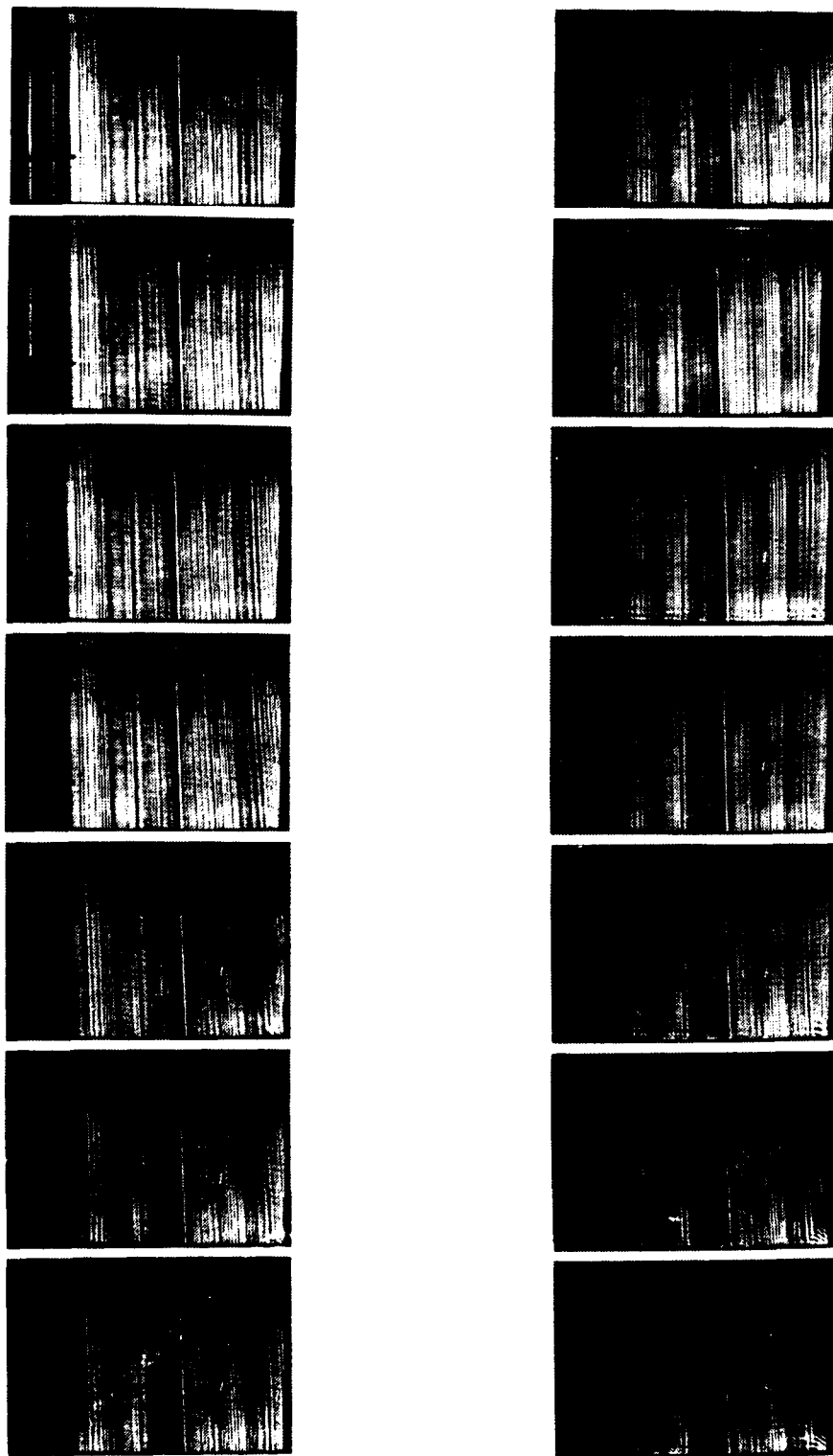


Figure 61. Flow Visualization: $Re = 2274$, $Str = 0.0443$,
 $\gamma = 10.01$

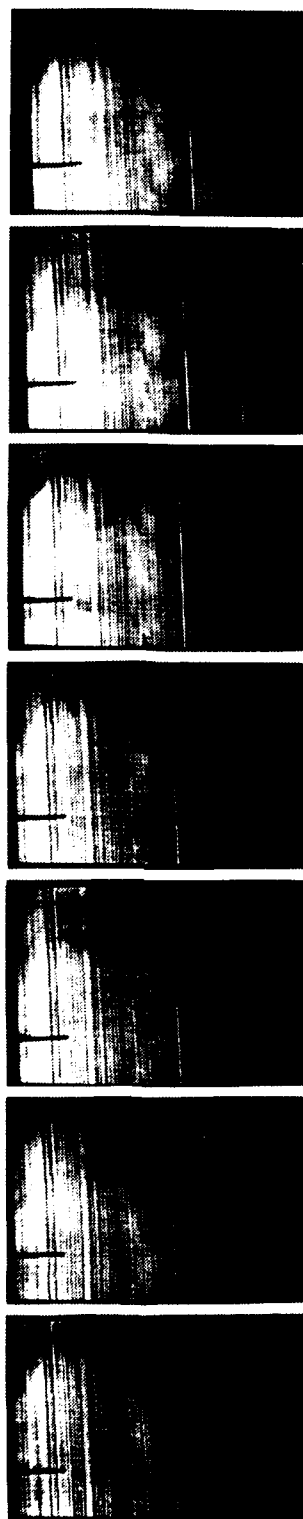


Figure 62. Flow Visualization: $Re = 2352$, $Str = 0.0427$,
 $W/D = 10.84$

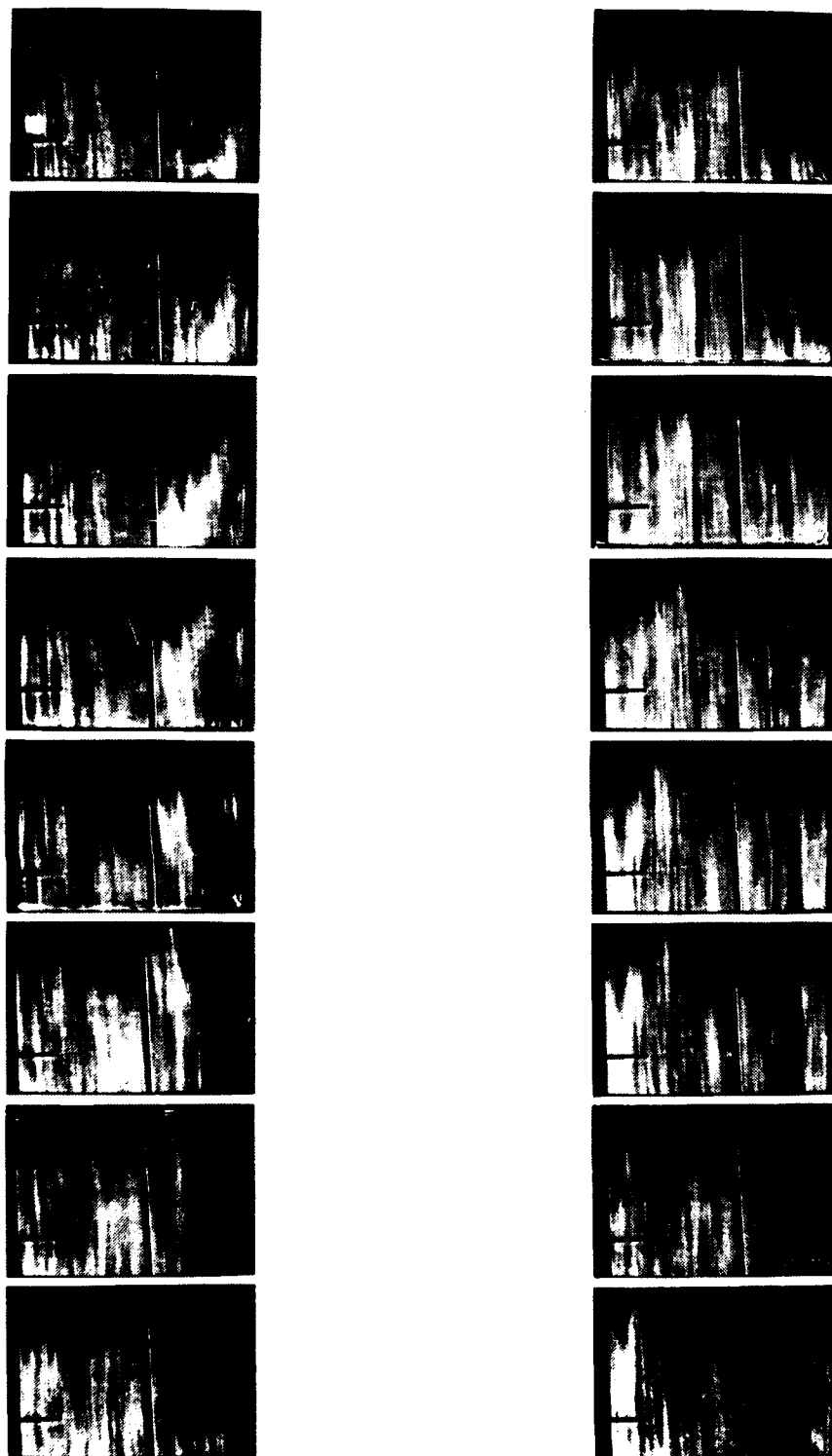


Figure 62. Flow Visualization: $Re = 2442$, $Str = 0.0413$,
 $y/d = +0.84$

APPENDIX B

SOFTWARE DIRECTORY

This Appendix gives a listing of the various programs used in this thesis. Each program listing contains a summary of how the program is used, user inputs, program outputs and additional features, if any.

I. CURVED CHANNEL

A. DEAN15

Program to sample orifice pressure drop and calculate Dean number.

user input: a) ambient pressure in inches of water.
b) ambient temperature (or temperature measured by a transducer).

program output: a) mass flow rate.
b) orifice pressure drop.
c) Reynolds number.
d) Dean number.

additional features: allows user to adjust throttle valve (flow rate) and then recalculates the Dean number.

II. STRAIGHT CHANNEL

A. DEAN15 (or DEAN10)

Same program used for the curved channel but here it is used to sample orifice pressure drop and calculate mass flow rate, velocity, and Reynolds number (DEAN15 used for 1.5 inch orifice plate, DEAN10 used for 1.0 inch orifice plate).

user input: a) ambient pressure in inches of water.

b) ambient temperature (or temperature measured by a transducer).

program output: a) mass flow rate.

b) velocity.

c) Reynolds number.

B. HOTWIRE1:

Program to sample hot-wire voltage signals using a HP6944A high speed data acquisition system.

user input: sampling frequency.

program output: data file of instantaneous voltage values.

C. HWCAL:

Program used to calculate calibration coefficients for hot-wire probes. The coefficients are used in the plotting program "O_SCOPE1".

user input: a) ambient temperature ($^{\circ}\text{C}$).
b) ambient pressure (millibars).
c) orifice delta P in inches of water.
d) measured hot-wire mean voltage with no flow.
e) hot-wire mean voltage reading from a voltmeter (with flow).
f) number of points.

program output: a) EOC (calibration coefficient).
b) B (calibration coefficient).

D. O_SCOPE1:

Program which converts hot-wire instantaneous voltages to instantaneous velocities and plots velocity vs. time.

user input: a) values of EOC and B (from HWCAL).
b) time to begin plotting (point number).
c) total time range to plot (point number determined from frequency of data acquisition).

program output: velocity vs. time plot.

LIST OF REFERENCES

1. Bella, D.W., Flow Visualization of Time-Varying Structural Characteristics of Dean Vortices in a Curved Channel, Master's Thesis, Naval Postgraduate School, Monterey, California, December 1988.
2. Niver, R. D., Structural Characteristics of Dean Vortices in a Curved Channel, Master's Thesis, Naval Postgraduate School, Monterey, California, June 1987.
3. Baun, L. R., The Development and Structural Characteristics of Dean Vortices in a Curved Rectangular Channel, Engineer's Thesis, Naval Postgraduate School, Monterey, California, September 1988.
4. Ligrani, P. M. and Subramanian, C. S., "Effects of Unsteadiness on Laminar-Turbulent Transition in Straight Channel Flow", Naval Postgraduate School Project Progress Report, Department of Mechanical Engineering, Naval Postgraduate School, Monterey, California, March 1989.
5. Thermoscience Division, Department of Mechanical Engineering, Stanford University Report TF-31, Numerical Simulation Studies of Laminar-Turbulent Transition in the Plane Channel, by R. Singer, J. H. Ferziger, H. Reed, May 1987.
6. Giedband, M. A., A Flow Visualization Study of Laminar/Turbulent Transition in a Curved Channel, Master's Thesis, Naval Postgraduate School, Monterey, California, March 1987.
7. Ligrani, P. M. and Niver, R. D., "Flow Visualization of Dean Vortices in a Curved Channel with 40 to 1 Aspect Ratio," The Physics of Fluids, v. 31, n. 12, pp. 3605-3617, December 1988.
8. Miller, J. A. and Fejer, A. A., "Transition Phenomena in Oscillating Boundary-Layer Flows," Journal of Fluid Mechanics, v. 18, pp. 438-448, 1964.
9. Morrison, C. A., On the Use of Liquid Crystal Thermography as a Technique of Flow Visualization, Master's Thesis, Naval Postgraduate School, Monterey, California, June 1984.

10. Hughes, R. E., Development and Qualification of a Curved Channel with 40 to 1 Aspect Ratio for Heat Transfer Studies, Master's Thesis, Naval Postgraduate School, Monterey, California, September, 1989.

INITIAL DISTRIBUTION LIST

	No. copies
1. Defense Technical Information Center Cameron Station Alexandria, Virginia 22304-6145	2
2. Library, Code 0142 Naval Postgraduate School Monterey, California 93943-5002	2
3. Professor P. M. Ligrani, Code 69L1 Department of Mechanical Engineering Naval Postgraduate School Monterey, California 93943-5000	10
4. Department Chairman, Code 69 Department of Mechanical Engineering Naval Postgraduate School Monterey, California 93943-5000	1
5. Mr. K. Civinekas Aerospace Engineer Computational Applications Branch Mail Stop 5-11 NASA-Lewis Research Center 21000 Brookpark Road Cleveland, Ohio 45432	10
6. Naval Engineering Curricular Officer, Code 34 Department of Mechanical Engineering Naval Postgraduate School Monterey, California 93943-5000	1
7. Professor C. S. Subramanian, Code 69Su Department of Mechanical Engineering Naval Postgraduate School Monterey, California 93943-5000	2
8. LT Jerry M. Longest 2855 Anna Lane N.W. Corydon, Indiana 47112	2